

11157

NATIONAL LIBRARY
OTTAWA



BIBLIOTHÈQUE NATIONALE
OTTAWA

NAME OF AUTHOR... SHANKAR DASS POPLI
TITLE OF THESIS... Dissolution Rate Studies
... of Powdered drugs
UNIVERSITY... University of Alberta
DEGREE FOR WHICH THESIS WAS PRESENTED... Ph.D.
YEAR THIS DEGREE GRANTED... 1972

Permission is hereby granted to THE NATIONAL LIBRARY
OF CANADA to microfilm this thesis and to lend or sell copies
of the film.

The author reserves other publication rights, and
neither the thesis nor extensive extracts from it may be
printed or otherwise reproduced without the author's
written permission.

(Signed)..... S. Popli.....

PERMANENT ADDRESS:

... College of Pharmacy
... Univ. of Michigan
... Ann Arbor, Michigan

DATED... 25... 11... 1971

U S A

THE UNIVERSITY OF ALBERTA

Dissolution Rate Studies of Powdered Drugs

by



Shankar Dass Popli

A THESIS

SUBMITTED TO THE FACULTY OF GRADUATE STUDIES AND RESEARCH
IN PARTIAL FULFILMENT OF THE REQUIREMENTS FOR THE DEGREE OF
DOCTOR OF PHILOSOPHY

FACULTY OF PHARMACY AND PHARMACEUTICAL SCIENCES

EDMONTON, ALBERTA

SPRING, 1972

UNIVERSITY OF ALBERTA
FACULTY OF GRADUATE STUDIES AND RESEARCH

The undersigned certify that they have read, and recommend to the Faculty of Graduate Studies and Research for acceptance, a thesis entitled "Dissolution Rate Studies of Powdered Drugs" submitted by Shankar Dass Popli in partial fulfilment of the requirements for the degree of Doctor of Philosophy.

J. A. Clements
Supervisor

A. G. Nuttall

James A. Rogers

Thompson

H. J. Anderson

H. S. Dufford

Date 24th November
1971

ABSTRACT

Studies were undertaken to investigate the possible existence of polymorphic forms of meprobamate. A metastable form was prepared by crystallization from a super-cooled melt.

The forms of meprobamate (designated Form I and Form II) were characterized by melting point, optical properties, infrared spectroscopy, differential thermal analysis and X-ray diffraction pattern. Quantitative heats of fusion of both the forms of meprobamate were obtained using differential thermal analysis techniques.

A procedure was developed for the quantitative determination of meprobamate in aqueous solutions by gas-liquid chromatography.

The aqueous solubility of each crystal form at several temperatures was measured. The kinetics of the dissolution of each form were examined. The solubility of the Form II was found to be approximately twice the solubility of the Form I at each temperature. The kinetics of dissolution of the Form II showed a slow reversion back to the Form I, similar to that described for several other compounds by other workers. The temperature of transition and the thermodynamic properties of the form change have been calculated from these data.

A particle sizing unit has been assembled, consisting of a Coulter counter Model B particle size analyser, a

128-channel multichannel analyser, an oscilloscope display and an X-Y plotter. This unit is capable of measuring, recording and displaying complete size distributions in much shorter times than is possible with the Coulter counter operated in the conventional (single channel) mode.

The unit was calibrated with essentially monosize particles, and the size distribution obtained was compared with those obtained with two other particle sizing methods. The unit was compared with the Coulter counter operated in the conventional mode, using powders with a wide size distribution, and good agreement was obtained between the methods.

Since data acquisition was fast using this unit, it could be used to advantage in studies on the dissolution of powdered drugs. The dissolution of sparingly soluble drugs was followed using the particle size change. The theory derived to describe the dissolution rate of particles with time in a diffusion controlled dissolution process was verified.

ACKNOWLEDGEMENTS

The author is deeply indebted to Dr. John A. Clements for the advice and guidance extended during the course of this investigation, and for his continued support and encouragement.

The author also owes a very special debt of gratitude to Mr. C. Ediss for his help with the multichannel Coulter counter assembly.

Appreciation is expressed to members of the supervisory committee who were kind enough to offer suggestions for the improvement of this work.

Sincere thanks are extended to Dr. F. Otto, for extending the facilities to work with the differential thermal analyser, and to Dr. R. Morton for X-ray diffraction analysis.

The author wishes to express his thanks to his friends for reading the manuscript.

Thanks to Miss J. Dorsey for typing the manuscript.

Financial assistance from the University of Alberta and Medical Research Council is gratefully acknowledged.

Finally the author wishes to express his appreciation and acknowledge his indebtedness to his wife, Uma, for her patience.

TABLE OF CONTENTS

	<u>Page</u>
Abstract	i
Acknowledgements	iii
Table of Contents	iv
List of Tables	vii
List of Figures	x
CHAPTER I. INTRODUCTION	1
CHAPTER II. LITERATURE SURVEY	4
A. Dissolution Mechanism	5
B. Factors Affecting Dissolution Rate	16
C. Dissolution Methods	20
1. Natural Convection Methods	21
2. Forced Convection Methods	24
D. Polymorphism	32
1. Methods Used to Study Polymorphism	33
2. Crystal Structure and Dissolution	37
3. Crystal Structure and Drug Availability	42
E. Aims and Objects of the Present Study	45
CHAPTER III. EXPERIMENTAL METHODS	46
A. Physico-Chemical Studies of Meprobamate	47
1. Preparation of Polymorphic Forms of Meprobamate	47
2. Characterization of the Polymorphic Forms	47
3. Quantitative Measurements of Heats of Fusion	50
4. Analytical Procedure for Determination of Meprobamate Contents	54
5. Solubility and Dissolution Rate Studies	58

TABLE OF CONTENTS - continued

	<u>Page</u>
B. Multichannel Coulter Counter Assembly for Dissolution Rate Studies	59
1. Assembling of 128 Multichannel Analyser with the Coulter Counter	59
2. Size Distribution Measurements of Ragweed Pollen Grains and Latex Particles Using a Microscope	62
3. Size Distribution Measurements of Ragweed Pollen Grains and Latex Particles with the Coulter Counter Using the Conventional Method .	63
4. Size Distribution Measurements of Ragweed Pollen Grains and Latex Particles Using the Multichannel Coulter Counter Assembly	65
5. Size Distribution Measurements of Micronized Hydrocortisone Acetate and Griseofulvin	67
6. Solubility Determination of Hydrocortisone Acetate and Griseofulvin	68
7. Dissolution Rate Studies	69
CHAPTER IV. RESULTS	72
A. Physico-Chemical Studies of Meprobamate	73
1. Polymorphic Forms of Meprobamate	73
2. Characterization of the Polymorphic Forms . . .	73
3. Quantitative Measurements of Heats of Fusion .	83
4. Gas-Liquid Chromatographic Procedure	85
5. Solubility and Dissolution Rate Studies	91
6. Isergonic Relationship in Polymorphic Phase Reversion and Anhydrate to Hydrate Changes . .	99
B. Multichannel Coulter Counter Assembly for Dissolution Rate Studies	101
1. Size Distribution Measurements of Ragweed Pollen Grains and Latex Particles Using a Microscope	101

TABLE OF CONTENTS - continued

	<u>Page</u>
2. Size Distribution Measurements of Ragweed Pollen Grains and Latex Particles with the Coulter Counter Using the Conventional Method	105
3. Size Distribution Measurements of Ragweed Pollen Grains and Latex Particles Using the Multichannel Coulter Counter Assembly	108
4. Size Distribution Measurements of Micronized Hydrocortisone Acetate and Griseofulvin	118
5. Solubility Determination of Hydrocortisone Acetate and Griseofulvin	127
6. Dissolution Rate Studies	131
CHAPTER V. DISCUSSION	142
A. Physico-Chemical Studies of Meprobamate	143
1. Preparation of Polymorphic Forms of Meprobamate	143
2. Characterization of the Polymorphic Forms	143
3. Analytical Procedure for Determination of Meprobamate Contents	145
4. Solubility and Dissolution Rate Studies	146
B. Multichannel Coulter Counter Assembly for Dissolution Rate Studies	151
1. Dissolution Rate Studies of Micronized Hydrocortisone Acetate	151
2. Dissolution Rate Studies of Micronized Griseofulvin	154
3. Limitations and Advantages of the Multichannel Coulter Counter Assembly	155
CHAPTER VI. SUMMARY	159
Bibliography	161

LIST OF TABLES

<u>Table</u>	<u>Page</u>
I	Heats of Fusion of the Standard Materials . . . 51
II	Elemental Analysis Data of Meprobamate 73
III	Melting Point of Meprobamate Form I and Form II 74
IV	Fusion Temperature and Calibration Coefficient of Gallium, Indium and Tin 83
V	Differential Thermal Analysis Results 86
VI	Recovery of Meprobamate from Aqueous Solutions 88
VII	Relationship of the Concentration of Mepro- bamate to Peak Area for Meprobamate/Peak Area for Internal Standard 89
VIII	Dissolution Rates in Distilled Water of Meprobamate Form I and Form II at 25°C 92
IX	Dissolution Rates in Distilled Water of Mepro- bamate Form II at 30°C, 35°C and 40°C 93
X	Solubilities in Distilled Water of Mepro- bamate Form I and Form II at 25°C, 30°C, 35°C and 40°C 93
XI	Thermodynamic Values Calculated for Mepro- bamate Form I and Form II 99
XII	Microscopic Measurement Data for Ragweed Pollen Grains 102
XIII	Size Distribution of Ragweed Pollen Grains with the Microscopic Method 103
XIV	Size Distribution of Latex Particles with the Microscopic Method 104
XV	Data for Calibration of the Coulter Counter Using Ragweed Pollen Grains 105
XVI	Coulter Counter Data and Number & Calculations 107
XVII	Size Distribution of Ragweed Pollen Grains Using the Coulter Counter 109
XVIII	Size Distribution of Latex Particles Using the Coulter Counter 110

LIST OF TABLES - continued

<u>Table</u>	<u>Page</u>
XIX	Data for Size Distribution of Latex Particles Illustrating the Calibration of Multichannel Coulter Counter Assembly 113
XX	Size Distribution of Latex Particles Using Multichannel Coulter Counter Assembly 116
XXI	Size Distribution of Ragweed Pollen Grains Using the Multichannel Coulter Counter Assembly 117
XXII	Size Distribution of Micronized Hydrocortisone Acetate Using the Coulter Counter 121
XXIII	Size Distribution of Micronized Hydrocortisone Acetate Using the Multichannel Coulter Counter Assembly 122
XXIV	Size Distribution of Micronized Griseofulvin Using the Coulter Counter 123
XXV	Size Distribution of Micronized Griseofulvin Using the Multichannel Coulter Counter Assembly 124
XXVI	Relationship of Concentration of Hydrocortisone Acetate to Absorbance at 246 nm 127
XXVII	Relationship of Concentration of Griseofulvin to Absorbance at 292 nm 128
XXVIII	Solubility of Hydrocortisone Acetate and Griseofulvin 128
XXIX	Multichannel Coulter Counter Assembly Data for Dissolution of Micronized Hydrocortisone Acetate in 0.9% Aqueous Sodium Chloride Solution 132
XXX	Multichannel Coulter Counter Assembly Data for Dissolution of Micronized Griseofulvin in 0.05% Tween 80 Solution in Normal Saline 135
XXXI	Multichannel Coulter Counter Assembly Data for Dissolution of Micronized Griseofulvin in 0.1% Tween 80 Solution in Normal Saline 136
XXXII	Dissolution of Micronized Hydrocortisone Acetate by Chemical Method 141

LIST OF TABLES - continued

<u>Table</u>		<u>Page</u>
XXXIII	Dissolution of Micronized Griseofulvin by Chemical Method	141
XXXIV	Free Energy Differences of Various Polymorphic Systems and Anhydrous-Trihydrate Ampicillin System	149

LIST OF FIGURES

<u>Figure</u>		<u>Page</u>
1	Schematic Representation of Coulter Counter, Interface, Multichannel Analyser and Display Units	61
2	Infrared Spectrum of Meprobamate Form I	76
3	Infrared Spectrum of Meprobamate Form II	77
4	X-ray Photographic Diffractions of Meprobamate Form I and Form II	78
5	X-ray Diffractogram of Meprobamate Form I	79
6	X-ray Diffractogram of Meprobamate Form II	80
7	DTA Thermogram of Meprobamate Form I	81
8	DTA Thermogram of Meprobamate Form II	82
9	Calibration Curve for the DTA Calorimeter Cell	84
10	Typical Gas Chromatogram of an Aqueous Extract Containing Meprobamate	87
11	GLC Calibration Curve for Meprobamate in Distilled Water	90
12	Dissolution Curves for Meprobamate Form I and Form II in Distilled Water at 25°C	94
13	Dissolution Curves for Meprobamate Form II in Distilled Water	95
14	The van't Hoff Type Plot for Meprobamate Form I and Form II	97
15	Isergonic Plot of the Relation Between Enthalpy and Entropy Changes in Polymorphic and Hydration Phase Transformations	100
16	Differential Frequency Distribution Obtained for Latex Particles, Using the Multichannel Coulter Counter Assembly	112
17	Plot of Cumulative Counts Obtained for Latex Particles Against the Channel Number	115
18	The Size Distributions of Latex Particles	119

LIST OF FIGURES - continued

<u>Figure</u>		<u>Page</u>
19	The Size Distributions of Ragweed Pollen Grains	120
20	The Size Distributions of Micronized Hydrocortisone Acetate	125
21	The Size Distributions of Micronized Griseofulvin	126
22	Relationship of Concentration of Hydrocortisone Acetate to Absorbance at 246 nm	129
23	Relationship of Concentration of Griseofulvin to Absorbance at 292 nm	130
24	Plots of Cumulative Counts Against Particle Radius for Micronized Hydrocortisone Acetate in Normal Saline	133
25	Plots of Cumulative Counts Against Particle (Diameter) ² for Micronized Hydrocortisone Acetate in Normal Saline	134
26	Plots of Cumulative Counts Against Particle Radius for Micronized Griseofulvin in 0.05% Tween 80 solution in Normal Saline	137
27	Plots of Cumulative Counts Against Particle (Diameter) ² for Micronized Hydrocortisone Acetate in 0.05% Tween 80 Solution in Normal Saline	138
28	Plots of Cumulative Counts Against Particle Radius for Micronized Griseofulvin in 0.1% Tween 80 Solution in Normal Saline	139
29	Plots of Cumulative Counts Against Particle (Diameter) ² for Micronized Griseofulvin in 0.1% Tween 80 Solution in Normal Saline	140

CHAPTER I. INTRODUCTION

Dissolution is the act of dissolving and the rate of dissolving a drug from the solid state is called the dissolution rate. In recent years the dissolution rates of drugs of low solubility have drawn considerable attention and many authors have also stressed the importance of crystal structure of the drugs and its effects on the dissolution behavior.

Many organic compounds are capable of existing in more than one crystalline form, having different physico-chemical properties and possessing different thermodynamic activities. The knowledge of the thermodynamic properties associated with the crystal modification can usually help in the proper selection of the crystal modification for therapeutic activity.

The popularity of meprobamate as a tranquillizer has been well established. It was of interest to investigate the possible existence of polymorphism in this drug and to study the dissolution behavior.

The Coulter counter has been extensively used for the size analysis of pharmaceutical materials during the past decade. The method has two important advantages over the classical methods of size analysis. Firstly, the time taken for size distribution is reduced, and secondly, the method is suitable for sizing particles between 0.5μ - 200μ in diameter. This size range covers most of the finely divided drugs, such as griseofulvin. One application of the Coulter counter has been in the study of the

dissolution of the solid particles in aqueous medium and investigations of this aspect have been reported.

Although the Coulter counter is a fast method of size analysis in comparison with the classical methods, the speed of data acquisition can be greatly increased by converting it from a single channel analyser to a multichannel analyser. The complete size distribution can be obtained in a single step, resulting in a much more rapid determination.

To evaluate the multichannel assembly, two standard materials, latex particles and ragweed pollen grains, were used. Another evaluation of the method was to compare the size distributions obtained with this method of materials having a wider distribution of particle sizes, with those obtained by other methods. Micronized hydrocortisone acetate and griseofulvin were used for size distribution analysis and for dissolution rate studies.

CHAPTER II. LITERATURE SURVEY

A. DISSOLUTION MECHANISM

Noyes and Whitney (1) quantitatively studied dissolution rate by rotating cylinders of benzoic acid and lead chloride in water. After analysing the solution at certain intervals, these workers derived a law which concerns the rate at which solids dissolve in their own solutions when change in the surface area of exposed solid is negligible. This law states that the rate of concentration change, dC/dt , is at any instant directly proportional to the difference between the concentration of a saturated solution, C_s , and the concentration, C , existing in the solution at this instant. The equation in its original form is written as:

$$\frac{dC}{dt} = k(C_s - C) \quad (\text{eq. 1})$$

Noyes and Whitney explained the dissolution process on the assumptions that a very thin layer of saturated solution was formed at the surface of the solid and the rate at which the solid dissolved was governed by the rate of diffusion from this saturated layer into the main body of the solution.

While Noyes and Whitney (2) later assumed that the rate would be proportional to the surface, it was Bruner and Tolloczko (3-7) who showed this dependence and also that the constant, k , depended upon temperature and rate of stirring.

Subsequently Nernst (8) advanced the concepts of the Noyes and Whitney law to include all kinds of heterogeneous

reactions and suggested that equation 1 could be written

$$\frac{dC}{dt} = \frac{DA}{V\delta} (C_s - C) \quad (\text{eq. 2})$$

where D is the diffusion coefficient, V is the volume of the solvent, A is the area of the interface, and δ is the thickness of the stagnant film of the solvent on the solid surface. Brunner (9) showed the rate dependence on the diffusion constant. Nernst and Brunner postulated that the velocity of a heterogeneous reaction was determined by the velocities of the diffusion processes that accompanied it. This included the concept that the equilibrium is set up at the boundary surface practically instantaneously compared with the rate of diffusion.

The Nernst and Brunner theory was criticized by many workers, while other workers have published data which substantiate the film theory. In formulating their theory, Nernst and Brunner assumed that the process at the surface proceeds much faster than the transport process and that a linear concentration gradient is confined to the layer of solution adhering to the solid surface. It is apparent that if the intrinsic reaction rate at the interface is not faster than the rate of the transport process, deviation would occur. Roller (10-12) raised objections to the film theory concept and stated that an activation energy for the interfacial reaction should be required since all collisions of the solvent could not be expected to result in the release of molecules from the solid surface. Van

Name and Hill (13, 14) and also King (15) criticized the film theory and reported that the theoretical thickness of the film was larger than the physically acceptable value. Nernst and Brunner while calculating the film thickness proposed that diffusion was the only mode of transport and the boundary film remained stationary. The work of Van Name and Hill led them to postulate that the fluid motion component perpendicular to the surface becomes smaller and thus does not materially affect the transport rate.

Wilderman (16) and Zdanovskii (17-19) were the other workers who subjected the entire Nernst-Brunner diffusion theory to severe analysis and experimental study. Wilderman threw considerable doubt upon it as an explanation of the nature of the solution process. Zdanovskii, after experimentation with the dissolution of inorganic salts, reported that when the rate determining step is the surface or interface process, the rate of dissolution is given by:

$$\frac{dW}{dt} = \alpha S(C_s - C_y) \quad (\text{eq. 3})$$

When the process is diffusion controlled, the rate of dissolution is given by

$$\frac{dW}{dt} = \left(\frac{D}{h}\right) S(C_y - C_x) \quad (\text{eq. 4})$$

where dW/dt is the rate of dissolution, α is the rate constant of the interface process, h is the thickness of the diffusion layer, S is the surface area, C_s is the

concentration at saturation, C_x is the concentration in the bulk solution, and C_y is the concentration in the boundary diffusion layer.

Higuchi and co-workers (20), showed where the Nernst-Brunner theory would be expected to fail. Using the Nernst-Brunner model and assuming non-linear concentration gradients in a single diffusion layer, these authors derived an equation which offered satisfactory explanation for the rate of dissolution of weak acids and bases in various solutions and buffers. King and Brodie (21) and Hixson and Baum (22) studied the dissolution rates of benzoic acid in dilute aqueous sodium and potassium hydroxide solutions. They explained their data on the basis of the Nernst-Brunner film model of diffusion controlled kinetics. This theory assumes linear concentration gradients in the diffusion layer.

In many dissolution studies conditions are chosen so that that the term, $DA/V\delta$, remains essentially constant during the experiment. This is accomplished by using single large particles or compressed tablets. The fraction of the particle which dissolves is very small so that the surface can be assumed constant as long as the particle remains intact. The thickness of the Nernst-Brunner layer is kept constant by maintaining the position of the particle with respect to the stirrer. When dissolution from powder is studied these conditions may not be obtained. Thus the surface area of the particles may be expected to change during an

experiment.

Hixson and Crowell (23) derived a general expression for reaction rate in terms of variable surface area and concentration. They wrote an excellent review of the theory of the dissolution of the solids and derived a new law, known as cube root law, in which the velocity of dissolution of a solid in a liquid is expressed as a function of the surface area and concentration. They assumed that dissolution takes place normal to the surface of the dissolving solid, the same effect of agitation is observed on all areas of the solid surface, no stagnation of the liquid takes place in any region and the solid particles remain intact throughout dissolution.

Hixson and Crowell pointed out that the surface area of a particle was proportional to its weight raised to the two-thirds power, the proportionality constant being composed of density and volume shape factor. If the shape factor remains constant as the particle dissolves, the substitution of $(W)^{2/3}$ for A in Nernst equation can be made. Then under the condition that $C_s \gg C$ and D, V and h are constant, the equation can be integrated to give:

$$W_0^{1/3} - W_t^{1/3} = kt \quad (\text{eq. 5})$$

where W_0 is the initial weight of the undissolved solid, W_t is the weight of the undissolved solid at time t , and k is a constant.

Niebergall and co-workers (24) working with various

sizes of powders stated that the Hixson-Crowell cube root law did not describe their data. However, the data was described by an equation derived by making the assumption that the thickness of the diffusion layer in the Nernst-Brunner equation was proportional to the square root of the mean volume diameter. Niebergall and Goyan (25) extended this law to apply it to a multiparticulate system. The usefulness of the above equation has been shown by many workers including Parrott and co-workers (26), Goldberg and co-workers (27, 28), and Clements and Stanski (29).

Danckwerts' (30) model derived for dissolution of a gas in a liquid assumes that transport of solute away from the solid surface is achieved by means of macroscopic packets of solvents which attach themselves to the surface. It is proposed further that free diffusion takes place into each of the packets during the short period of time in which the packet is in contact with the surface. The rationality of such a model is supported strongly by the work of Fage and Townend (31), who found evidence of turbulent flow in a tube as close as 0.6μ from the interface. The validity of the model has been discussed by Dankwerts (30) and Hanratty (32). Johnson and Huang (33) demonstrated the applicability of the model for the dissolution from a flat surface into turbulent liquid. Goyan (34) using this model derived equations for the dissolution of solids in a multiparticulate system. The equations obtained are capable of explaining the deviations from linearity of

cube root plots.

Higuchi (35) has discussed the dissolution rate laws predicted by the different mechanisms in an extensive review of the drug release rate processes. Wurster and Taylor (36) and Wagner (37) have also discussed the subject and Wagner also related it to the biological availability. Wurster and Taylor (38) in their studies of the dissolution rate behaviour of prednisolone employed a diffusion layer model equation as well as the double-barrier model which was obtained by combining the interfacial barrier concept with the diffusion layer concept. These investigators suggested that double barrier mechanism better described their data on the influence of agitation upon the dissolution rates.

Higuchi and Hiestand (39) derived a mathematical equation which describes the dissolution rates of fine particles in a diffusion controlled dissolution process. They stated that particle size distribution effects may be taken into account by selecting a particle size distribution function that is time dependent.

Several assumptions have been made in describing the dissolution of single particles. These include the following: (i) the dissolution rate is diffusion controlled; (ii) the diffusion layer thickness is the same for all particles of the same size; (iii) the concentration change of dissolved solid in the bulk solution is negligible at all times; and (iv) the effective particle shape approximates a sphere.

From the Fick's law of diffusion (40)

$$\frac{dm}{dt} = D4\pi r^2 \frac{dC}{dr} \quad (\text{eq. 6})$$

where m is the weight of the solid particle, D is the diffusion rate constant, C is the concentration of the dissolved solid, t is the time and r is the radius of a sphere through which the diffusion occurs. If a is the radius of a particle at time t , then by the steady state equation we get:

$$\frac{dm}{dt} = -4\pi Da\Delta C \quad (\text{eq. 7})$$

where $\Delta C = C_s - C_o$. Since it has been assumed that ΔC is independent of time, particle size, a , is the only variable with time. From the volume of the particle, v , and density, p :

$$\frac{dm}{dt} = \frac{d(vp)}{dt} = 4\pi pa^2 \frac{da}{dt} \quad (\text{eq. 8})$$

From equations 7 and 8:

$$ap \frac{da}{dt} = -D\Delta C \quad (\text{eq. 9})$$

Setting $a = a_o$ at $t = 0$, then integration of equation 9 gives:

$$a^2 = a_o^2 - \frac{2D\Delta Ct}{p} \quad (\text{eq. 10})$$

Equation 10 provides a means of calculating any particle diameter at time t , if its radius at zero time is known.

The total dissolution rate of a powder with log normal

distribution is expressed as a function of the number of particles and the mass mean radius of the particles in the distribution. For the general case of a micronized powder with the distribution of particle sizes, the following equation was derived (39):

$$Q = \frac{\int_{a_{0t}}^{a_{10}} (a_0^2 - \frac{2DAc_t}{p})^{3/2} n(a_0) da_0}{\int_{a_{S_0}}^{a_{10}} a_0^3 n(a_0) da_0} \quad (\text{eq. 11})$$

where Q is the fraction of powder not dissolved at time t , a_{10} is the radius of the largest particle at time zero and a_{S_0} is the radius of the smallest particle at time zero, a_0 is the radius of a particle at time zero and the other symbols have already been defined.

Later on, Higuchi and co-workers (41) tested the theory using micronized methylprednisolone, and a reasonably good agreement was obtained. The differences were believed to be due to the combined effects of agitation, sedimentation, particle shapes, and the variation of the solubility with particle size. This suggested to them that a much better test of the equation could be provided by using emulsion droplets. Higuchi used the Coulter counter to follow the time change in the number distribution of an emulsion of a slightly miscible liquid (dibutylphthalate) in aqueous medium (42).

Edmundson and Lees (43) followed the change in particle size of hydrocortisone acetate in suspension by means of a Coulter counter. They made the assumption that the

solution is an etching process in which a given surface recedes in depth to an extent proportional to time. The dissolution rate was expressed as diameter loss per unit time. By neglecting the complicated factors, such as the increasing concentration of the solution, particle shape and higher solubility of the smaller particles, and by standardizing the variables such as temperature and degree of agitation, it can be assumed that diameter will decrease linearly with time and that the diameter of any particle at any time will be in conformity with the equation

$$d_t = d_o - k_2 t \quad (\text{eq. 12})$$

where d_t is the diameter at time t , d_o is the initial diameter and k_2 is a constant.

Dissolution Involving Simultaneous Phase Changes

There are a number of reports in the literature (44, 45) where the formation of a new surface phase was noted during the dissolution of the drug. Physical models (20) involving the use of simultaneous diffusion and rapid equilibria have been successful in describing diffusion controlled kinetics of dissolution in reactive media. The model involving a new phase precipitation has now been employed in a number of instances (46-49). Recently Higuchi and co-workers (50) examined the dissolution rate behaviour of polymorphs of methylprednisolone. They proposed a theory assuming that a simultaneous surface reversion of polymorph II to polymorph I occurs during the dissolution of polymorph II. The theory states that as dissolution of the drug begins from

an initially uniform mixture of polymorphs, by diffusion across the effective liquid diffusion layer of thickness, h , only Form II dissolves initially because the solution concentration at the solid-liquid interface is still greater than the solubility of Form I. Thus at time zero, the solution concentration at the solid-liquid interface is equal to the solubility of Form II. At later times the solution concentration at the solid-liquid interface is in between the solubility of Form II and Form I. Finally in the steady state, the concentration at the solid-liquid interface is approximately equal to the solubility of Form I, and both Forms I and II dissolve at a rate proportional to their percentages in the original mixture.

This theory also explains why the dissolution rates for both Forms I and II are indistinguishable, at high stirring rates, as reported by many workers (38, 51, 52).

Higuchi and co-workers (53) investigated the theory for the dissolution rate of polyphase mixtures and applied it to benzoic acid-salicylic acid, the benzocaine-caffeine,¹ and the benzoic acid-trisodium phosphate mixtures.

B. FACTORS AFFECTING DISSOLUTION RATE

The physico-chemical factors which affect the dissolution rate may be deduced from the dissolution mechanism. A modified Noyes-Whitney equation is:

$$\frac{dC}{dt} = KS(C_s - C) \quad (\text{eq. 13})$$

where S is the surface area and the other symbols have the same meaning as in equation 1. By an examination of the equation, it is apparent that the rate of dissolution is directly proportional to the surface area, S , and the concentration difference ($C_s - C$). In intrinsic dissolution rate studies, the variables which must be controlled include surface area, agitation intensity, temperature of the system and the volume of the dissolution medium.

Surface Area:

The dissolution rate is directly proportional to the area exposed to the solvent under uniform agitation and constant shape. Alexander (54) found a linear relationship between the logarithm of the solubility and the surface area. Wurster and Seitz (55) used compressed tablets containing large pores to follow dissolution in distilled water. Studies indicated that the surface area was not completely exposed to the solvent due to occlusion of air. An increase in dissolution rate was obtained from dissolution media with a lower surface tension than water.

The mechanism of solution involves surface action and a given solute will dissolve more rapidly (56) if the surface

area is increased. Several investigators (57-62) reported an enhanced dissolution and biological availability of water insoluble drugs when the particle size of these drugs was reduced. The usefulness of the solid state dispersion of drugs has been demonstrated in a number of recent publications (63-68). The increase in dissolution rate appears to be due to the reduction of particle size, thus increasing the surface area for dissolution. The relationship between the particle size, dissolution and drug availability is well recognized and many articles have been published (69-71).

Agitation Intensity:

From the earlier discussion on the dissolution mechanism, it becomes apparent that agitation conditions will affect diffusion controlled dissolution. An increase in the rate of stirring should be accompanied by a decrease in the diffusion layer thickness, δ , in the Nernst-Brunner equation. Several authors (23, 38, 72-75) have reviewed the literature concerning the effect of agitation speed on the velocity of heterogeneous reactions and the kinetics of dissolution and many of them have expressed their results in a power relation of the form,

$$K = (N)^a$$

where K is the reaction rate, N is the agitation or stirring rate, and a is a constant. When the reaction is diffusion controlled the value of 'a' has been found to be approximately equal to 1. The value of the exponent, a, varies with the

type of agitation used, as pointed out by Hixson and Baum (76, 77). Their study together with the observations of Garner and Hoffman (78) showed that the value of the exponent also depends on the characteristics of the fluid motion in the boundary layer. Levy and co-workers (79, 80) have pointed out the need for ascertaining the correct agitation rate so as to achieve correlation between in vivo and in vitro data. Hamlin and co-workers (51) determined the in vitro dissolution rate of two methylprednisolone polymorphs which were shown to have significantly different in vivo dissolution rates when implanted as pellets in rats. These workers, using the pellet method for dissolution study which has a very low degree of agitation, observed a difference in the in vitro dissolution of the two polymorphs. No significant differences in the dissolution rates were observed when other methods having higher degree of agitation were employed. Levy and Procknal (52) developed the concept of "rotating disk equivalent" or RDE, in which the intrinsic dissolution data for methylprednisolone obtained using the rotating disk method over a wide range of stirring was used as a standard.

From the assumption of Nernst that δ is a function of the rate and type of stirring, K should be proportional to the coefficient of diffusion of the solute and hence inversely proportional to the viscosity of the solution. Results in agreement with these views have been obtained (15, 81). Several equations have been derived that show

the dissolution rate to be a function of viscosity raised to some power (12, 82, 83).

There are several other factors affecting the rate of dissolution of drugs. These include the following: the concentration gradient, that is, the difference in concentration between the solubility of the drug in the dissolution medium and the average concentration in the bulk fluid. Any means whereby the solubility of the drug can be increased or the concentration in the bulk fluid can be reduced, will cause a corresponding increase in the dissolution rate. Considerable evidence has been presented to show that the initial rate of dissolution is directly proportional to the solubility of the compound in the dissolution medium (84).

The saturation solubility of weakly acidic and basic drugs will vary with the pH of the dissolution medium. The dissolution rates of several weak acids and their sodium salts in aqueous solutions having pH values close to those of the gastrointestinal fluids were reported by Nelson (85). The effect of pH was reported for the dissolution of commercial warfarin tablets by O'Reilly and co-workers (86).

Parrott and co-workers (26) studied the dissolution rates of benzoic acid in the presence of unreactive additives in the solvent phase. Surface active agents, at concentrations in excess of critical micelle concentration have been used and enhanced dissolution rates have been observed by

many investigators (87-89).

It has been reported (90) that if a heterogeneous reaction is diffusion controlled, the 10°C temperature coefficient will be close to 1.3.

C. DISSOLUTION METHODS

The dissolution apparatus suitable for both research and quality control should be economically practical. It must be capable of giving reproducible intensities of agitation and should also be flexible in effective degree of agitation. Cook (91) has stressed the need for a suitable dissolution apparatus for pharmaceutical control.

In order to get a suitable dissolution apparatus for a particular study, almost every team of scientists working in this field have devised their own dissolution apparatus and method.

Hersey (92) in 1969 has attempted to classify the dissolution methods on the basis of whether dissolution process occurs under sink or non-sink conditions, and on the type

of agitation. The dissolution methods discussed below are based upon whether convection is natural or forced.

1. Natural Convection Methods

Solvometer Method:

In 1932, Klein (93) determined the dissolution rate of a compressed tablet. One year later, Elliott (94) used Klein's apparatus which Elliott called a "Solvometer". It consisted essentially of a "boat" immersed in the dissolution medium. The tablet was placed in the boat, and as it dissolved, the loss in weight was continuously read directly on a scale. The technique does not require an assay method and modifications of the technique were subsequently made.

Hanging Pellet Method:

The hanging pellet method was first described by Nelson (85). The method consisted of attaching a compressed flat faced disk of the drug under study to an aluminum strip by means of wax so that only the upper circular face of the disk was exposed. The strip was suspended from one arm of a balance so that the strip and the pellet were completely immersed in the dissolution medium. The dissolution was followed by recording the weight loss of the pellet over a period of time. It was possible to show significant differences between the dissolution rates of weak acids and their sodium salts.

Nelson (95) used this technique to study the enhancement of the dissolution of the weak acids when formulated as

mixtures with tribasic sodium phosphate.

Using the hanging plate method, Morozowich and co-workers (45) were able to demonstrate a relationship between the in vitro dissolution rate of certain salts of benzphetamine and eryptamine and the median lethal time of death in mice. Hamlin and co-workers (51), using this method, were able to distinguish between the two polymorphic forms of methylprednisolone that had significantly different in vivo dissolution rates when implanted in rats.

Nelson (62) used the hanging pellet method and showed a direct relationship between the excretion rates of several tetracyclines administered as pellets and their in vitro dissolution rate.

Static Disk Method:

Wagner (96) gave an equation to describe the average rate of dissolution per unit surface area from a rectangular surface suspended vertically in dissolution medium under static condition.

$$R'_n = 0.726 D C_s \left(\frac{g \cdot \Delta \rho}{H D \eta \rho_o} \right)^{1/4} \quad (\text{eq. 14})$$

where R'_n is the mean rate of dissolution per unit surface area, H is the height of the rectangular plate, η is the viscosity of the diffusion layer, $\Delta \rho$ is the difference in the density between the diffusion layer and the bulk solution, g is the gravitational constant, ρ_o is the density of the dissolution medium, D is the diffusion coefficient of

the solute, and C_s is the concentration of a saturated solution of the solute in the dissolution medium. Wagner verified the equation by determining weight loss of thin plates of rock salt suspended vertically in unstirred water on a spring balance by means of a silver wire. It was concluded that under such conditions diffusion and natural convections due to the density difference between a saturated solution and the pure water are the rate determining factors.

The static disk method developed by Levy (75) is closely related to the hanging plate method. Levy described the procedure and used a non-disintegrating disk or tablet. The method has also been used by Gibaldi and co-workers (97). Jouhar and co-workers (98) used an adaptation of the static disk method for slow release tablets of potassium chloride.

Sintered Filter Method:

Cook (99) used a medium porosity sintered filter funnel filled with 500 ml of gastric fluid. The tablet was introduced so as to rest in the centre of the sintered glass surface. The dissolution medium moves past the dosage form in the filter funnel under gravity, without any externally applied agitation. Cook and co-workers (100) compared the sintered funnel method and the stationary basket method using five samples of hydrochlorthiazide tablets. They obtained a slower dissolution rate with former method.

2. Forced Convection Methods

Rotating Disk Method:

This method, described by Levy and Sahli (101), requires a 0.5 inch diameter plane faced tablet to be mounted in a plexiglas holder with paraffin wax so that one plane surface is exposed to the dissolution medium. The holder is attached to a metal shaft driven by a constant speed motor. The constant speed motor turns the tablet in a fluid at a known angular velocity.

Levich (102) in 1962, assuming laminar flow and diffusion controlled process, derived an equation called the Levich equation for the rotating disk.

$$J = 0.62 D^{2/3} \nu^{-1/6} \omega^{1/2} C_s \quad (\text{eq. 15})$$

where J is the rate of dissolution, D is the diffusion coefficient, ν is the kinematic viscosity, ω is the angular rotation and C_s is the solubility of the compound in the dissolution medium. Gregory and Riddiford (103) derived the following equation.

$$J = 1.61 \left(\frac{D}{\nu}\right)^{1/3} \sqrt{\frac{\nu}{\omega}} [1 + 0.35 \left(\frac{D}{\nu}\right)^{0.36}] C_s \quad (\text{eq. 16})$$

where the symbols have the same meaning as described above.

Because of the variations of the dissolution rate with the rotation rate of the tablet, a precision apparatus was developed by Levy and Tanski (104). Wood and co-workers (105) later described a compression assembly which also served as a tablet holder. Paikoff and Drumm (106) described a stirrer suitable for holding a capsule during

dissolution.

Several investigators (52, 75, 97, 107-109) used the rotating disk method to study the intrinsic rate of dissolution of drugs in a variety of media.

Simonelli and co-workers (110), in 1969, used the reverse rotating disk method or static disk with an external agitation method. In this case the solution is stirred while the holder remains stationary. The same apparatus was used by Higuchi and co-workers (53) in an investigation of the dissolution rate of drugs in polyphase mixtures. Desai and co-workers (111) and also Lapidus and Lordi (112) reported other dissolution systems in which dissolution medium flows over one surface of the disk or tablet.

Rotating Bottle Method:

Souder and Ellenbogen (113) devised the rotating bottle method to follow the release of dextroamphetamine sulphate from sustained release pellets. Samples of the pellets were placed in 90 ml bottles containing 60 ml of a suitable dissolution medium. The bottles were turned end over end at 40 r.p.m., by placing them in a rack at 37°C in a constant temperature water bath. Other workers (114, 115) have used the method with different sizes of containers and rates of rotation.

Over the years there have been several critics of the rotating bottle method. Hamlin and co-workers (51) claimed that the intensity of agitation may be too great, thereby

obliterating any in vitro differences that one might expect if in vivo differences were shown between the products.

Rosen and Swintosky (116) used radio-isotope tracers to follow the in vitro dissolution of drugs from sustained release dosage forms. Similar approaches were made by Rosen (117), and Montgomery and co-workers (118), for finding the in vitro release characteristics of radio-labeled drugs.

The National Formulary XII (2nd supplement) (119) included the rotating bottle method as an in vitro test procedure for timed release tablets or capsules.

Higuchi and co-workers (41) used a similar technique to study the dissolution of micronized methylprednisolone in order to confirm their theoretical model proposed for dissolution of finely powdered drugs.

Ferrari and Khoury (120) and other workers (121) reported some modifications of the rotating bottle method.

Beaker Method:

The beaker method was originally used by Parrott and co-workers (26) for the dissolution of pure benzoic acid, and later by Nelson (95, 122).

However, in its present form as used for tablets, the procedure may be credited to Levy and Hayes (123). A 400 ml beaker containing 250 ml of dissolution medium at 37°C was used. The agitation was provided by means of a three blade polyethylene stirrer. The tablet is normally allowed to disintegrate and total dissolution rate determined. By

mounting a hard pellet of the drug on a glass slide so that only one surface is exposed, the method may also be used for intrinsic dissolution rate measurements (95, 122, 124).

The method is one of the simplest and most widely used techniques for carrying out dissolution rate studies. The method has been used by Levy and co-workers (125-127) in obtaining dissolution data on a wide range of materials. The method with some modifications has been used by many workers (128-131).

Oscillating Tube Method:

The oscillating tube for dissolution rate studies is a modification of the official Gershberg-Stoll (132) apparatus used for disintegration test. Broadhead and co-workers (133) used the disintegration apparatus of the British Pharmacopeia (134) for dissolution studies. The method with various modifications has been used by many investigators (135-142). The National Formulary XIII (143) describes a dissolution test based on the Gershberg-Stoll apparatus.

Rotating Basket and Stationary Basket Methods:

Searl and Pernarowski (144) described a rotating basket apparatus which is based on the beaker method of Levy and Hayes (123). The rotating basket assembly is included in the National Formulary XIII (143) as one of the two official dissolution methods, and is the official method of the United States Pharmacopeia XVIII (145).

A stationary basket method was described by Cook and

co-workers (100) and was employed by Middleton and co-workers (146) in studying the in vitro dissolution rates of the formulations of para-amino salicylic acid.

Tape Method:

This method was first described by Goldberg and co-workers (147). The dissolution apparatus consisted of a 600 ml beaker with two stainless steel sliders. A pressure sensitive tape was fastened to a wire frame and this was mounted into the sliders in the beaker. A constant speed motor attached to a laboratory jack allowed the motor to be raised and lowered and to position the stirrer paddle in the dissolution medium. Dissolution of particles of benzoic acid and salicylamide scattered on the surface of the tape was followed in 400 ml water maintained at 37°C. Goldberg and co-workers used the method in further studies (27, 28, 65).

Clements and Stanski (29) used this method for dissolution studies of phenobarbitone polymorphs, maintaining essentially sink conditions.

Direct Particle Size Measurement:

Edmundson and Lees (43) developed a direct method for determining the solution rates of fine particles that did not require the particles to be of specified size, shape or uniformity. The Coulter counter described by Coulter (148) was used for determining the solution rate.

The Coulter counter has been used extensively for size analysis of a wide variety of particulate materials in

suspension (149-154). Higuchi and Saad (155, 156) used the Coulter counter to determine the solubility and dissolution rate of cholesterol in aqueous medium. The Coulter counter was employed to follow the particle size distribution within an undersaturated cholesterol suspension system. Later, Higuchi (42) used the Coulter counter to measure the diameter of emulsion droplets in the micron range, in order to verify the theory developed to explain the effect of the distribution of the particle size upon a diffusion controlled dissolution process.

Recently Piccolo and Tawashi (157) used the Coulter counter to study the dissolution rate of poorly water soluble drugs in the presence of water soluble dye.

Miscellaneous Methods:

Wurster and Polli (158) described a method which was identical to that of Parrott and co-workers (26) but used charcoal or bentonite in the dissolution medium to adsorb dissolved benzoic acid.

Marlowe and Shangraw (159) used a dialysis cell similar to that reported by Patel and Foss (160) to determine the effect of additives on the dissolution from sodium salicylate tablets. Broadhead and co-workers (133) described the use of "metabolic shaker" as a convenient means of agitation, for dissolution studies. Macdonald and co-workers (161) employed a V-shaped transparent plastic cylinder to follow the in vitro dissolution of various tetracycline tablets.

Tawashi (162) has described a method in which a single large crystal is suspended in solution, and the decrease in size of the crystal is measured by an optical system. Piccolo and Tawashi (163) employed this method to investigate the effect on the dissolution of single crystals of sulfathiazole, phenobarbitone, thymol and sulfaguanidine.

Automatic Methods:

Automatic dissolution procedure involves a circulation of the dissolution medium through a cell, filter and a suitable measuring device. The circulation fluid generally provides the necessary agitation. The first flow-through dissolution cell was probably that of Wiley, as reported by Myers (164). The apparatus consisted of a stoppered cylindrical tube with a glass wool filter above the bottom outlet and an outlet for returning the fluid to the reservoir. The apparatus was immersed in a water bath at 37°C. A pump was used to circulate the fluid. A modification of this apparatus was reported by Baun and Walker (165).

By modifications of the basic method of Levy and Hayes (123), Niebergall and Goyan (25) developed an automatic recording apparatus for use with the beaker method. Using this apparatus Neibergall and co-workers (24) obtained dissolution data on drug particles of different size fractions. Richter and co-workers (166) described an automatic beaker method, operating under sink conditions.

Pernarowski and co-workers (167) reported an automated version of the rotating basket method assembly in which a

variable speed pump was used to take the test fluids directly to a collection container or through a flow cell in a spectrophotometer.

Automatic dissolution systems based on the official disintegration apparatus have been described by Schroeter and Wagner (168) and Schroeter and Hamlin (169).

Barzilay and Hersey (170) developed an automatic dialysis method. With this method the disadvantages inherent in the manual discontinuous operation of dialysis method of Marlowe and Shangraw (159) were overcome.

Tingstad and Riegelman (171) described an apparatus for the study of dissolution rate under continuous flow. The effects of particle size, surfactant concentration and flow rate on the dissolution behavior of prednisolone powder and prednisolone tablets were observed.

Ullah and Cadwallader (172) developed a three compartmental apparatus for dissolution studies of slightly soluble powders under sink conditions. The apparatus was designed to include an organic phase in which the drug is very soluble, thus producing a sink condition. A barrier in the dissolution medium was also included in the apparatus, which prevented floating powders from entering and dissolving directly in the sink phase.

McClintock and co-workers (173) described a continuous method for radio-isotope labeled materials, using techniques earlier applied by Rosen and Swintosky (116).

Many workers (174-176) described vertical column apparatus

for dissolution rate studies. Lerk and Zuurman (176) investigated the influence of pulsation on the dissolution rate measurement in column type apparatus and suggested that momentum pumps should be used instead of displacement pumps so that results found at different times in different laboratories can be compared.

D. POLYMORPHISM

The discovery of polymorphism (177) dates back to 1798, when Klaproth observed that calcium carbonate crystallizes both as calcite and aragonite. Humphrey Davy in 1809 pointed out that diamond and graphite are both carbon and differ only in their arrangement of carbon atoms in the solid phase. Mitscherlich (178) in 1822 first used the term polymorphism during his work on the isomorphous sulfates of iron (ferrous), cobalt, nickel, magnesium, copper, zinc and manganese.

Many authors have systematically studied different classes of compounds exhibiting polymorphisms. It has been

stated that organic molecules readily exhibit polymorphism due to their complex molecular and structural arrangement (179, 180). Each polymorphic structure of a substance generally possesses a different molecular arrangement, melting point and solubility. Mesley and co-workers extensively studied the polymorphism of steroids (181, 182), barbiturates (183, 184) and sulphonamides (185). Brandstätter-Kuhnert and co-workers reported on the polymorphisms of steroids (186-188), antihistamines (189) and barbiturates (190-192). Huang (193) prepared four forms of phenobarbitone by microsublimation procedure, and two more forms by crystallization from super-cooled melt (194). In 1959 Cleverly and Williams (195) reported on the polymorphism exhibited by twenty barbituric acid derivatives.

Among the steroids, spectral evidence of polymorphisms of cortisone acetate (196, 197), oestradiol (198), ethinyl-oestradiol (199, 200), methylprednisolone (201) and several other compounds, have been shown (202, 203). Shell (204) in 1955 reported that there was no evidence of polymorphism in hydrocortisone acetate. However, an unstable solvate crystallized from dimethylformamide solutions. In 1965, Brandstätter-Kuhnert (205) reported that polymorphism was observed in 16 of 40 sulfonamides, in 63% of 38 barbiturates and in 67% of the 48 steroids studied.

1. Methods Used to Study Polymorphism

A number of techniques have been used to identify different polymorphic phases of a compound. Although each

of these techniques is capable of successfully identifying each crystalline modification, a combination of several techniques has usually been used.

Melting Point Determination:

This method is probably the least reliable for identification of the various polymorphic structures because of the possible presence of impurities in the sample, or the effect of elevated temperatures on the crystalline structure of the compound. In capillary-tube melting point determinations polymorphic transitions may not be detected.

Optical Microscopy:

Different polymorphs of a crystal may belong to one of the two classes, isotropic and anisotropic, depending on the effect of transmission of light in different directions through the crystals. Different polymorphs do have different sets of refractive indices (206). Trivedi and co-workers (207) have reported the optical crystallographic properties of ouabain hydrates. Optical crystallographic properties were determined for National Formulary X drugs exhibiting polymorphism (208). Witt and Poe and co-workers (209-213) found the optical crystallographic properties of organic compounds of pharmaceutical interest. Reffner and McCrone (214) tested a number of compounds for their optical crystallographic properties and found polymorphism to be prevalent with some of the compounds tested. Rose and Van Camp studied the optical crystallographic properties of rauwolfia alkaloids (215-219), antibiotics (220, 221) and other

compounds of pharmaceutical interest. Optical crystallographic properties have been used to aid in predicting molecular orientations in the solid state (222, 223).

Hot stage microscopy became a very useful tool for investigating polymorphism. By the use of the polarizing microscope fitted with a hot stage, it is possible to detect polymorphism and often to obtain the transition temperature and the melting point. The "thermomicromethod" studies of polymorphic modifications of organic compounds was reported by Kofler (224). With this method Brandstätter-Kuhnert and Kofler (225) noted that 11 of the 16 hormones studied were polymorphic and 3 were present in commercial products in the unstable modification.

Infrared Spectroscopy:

Many authors (182, 183, 195, 226-229) have used infrared spectroscopy to study polymorphism. The technique is claimed to be rapid as well as qualitative and quantitative (226). It has generally been reported that care must be taken in preparing potassium bromide disk for infrared analysis to avoid excessive grinding (230).

X-ray Powder Diffraction:

X-ray powder diffraction is one of the most widely used techniques after optical microscopy. X-rays are a form of electromagnetic radiation with wave lengths intermediate between ultraviolet rays and gamma rays. X-rays are diffracted by the crystal just as visible light is dispersed into a color spectrum by a ruled grating. Each

powder pattern of the crystal lattice is characteristic for a given polymorph. This technique has the advantage over the other identification techniques in that the sample is examined as presented and as the method is non destructive, the sample can be recovered. Several investigators (231, 232) have used this technique to identify the polymorphs of medicinal substances.

Differential Thermal Analysis (DTA):

Ever since its inception, the method of differential thermal analysis (DTA) has been used extensively for qualitative and quantitative study of processes involving heat changes (233). The enthalpic changes observed in DTA are caused by phase transitions and may be either exothermic or endothermic. For example fusion, boiling and solid-solid transition produce endothermic effects, whereas crystallization produces an exothermic effect (234). Many workers (229, 235) have used this technique, in combination with the other techniques, to determine the thermodynamic transition from one polymorph to another. Using DTA, Guillory (236) obtained the heats of transition of methylprednisolone and sulfathiazole polymorphs. Verma (237) determined the heats of fusion for a group of organic compounds. Sakurai and Yabe (238) have calculated the heat absorbed in the solid phase transition and fusion of n-hexadecanamide. Guillory and co-workers (239) have used DTA for detection of possible interactions between pharmaceutical compounds. Other quantitative applications have been reviewed by

Murphy (240).

Other common identification techniques for polymorphs include: dilatometry, proton magnetic resonance (PMR) spectroscopy, nuclear magnetic resonance (NMR) spectroscopy, solubility and dissolution rate.

Ravin and Higuchi (241) used dilatometry to follow the melting behavior of theobroma oil. The PMR spectra of the crystal modifications of chloramphenicol palmitate were recently reported by Borka (242). Rudman and Post (243), using NMR spectroscopy technique, found that cyclooctanone exists in three distinct crystalline phases.

2. Crystal Structure and Dissolution

It has been demonstrated that the absorption and therapeutic efficacy of various drugs can be influenced by the solubility and the dissolution rate (244-246). Recent reports stress the effect of crystal forms on drug availability (247, 248). McCrone (249) has reported that the thermal stability of a drug depends on the polymorphic form and that "often the performance of a given compound can be improved through change to a different polymorphic form". Many investigators have used solubility determinations to characterize the different modifications of medicinal compounds. Using this method, thermodynamic values for transitions from one form to the other form were also calculated (250).

Each polymorphic form of a substance possesses a different molecular arrangement and solubility, and therefore generally has a different in vivo availability. The free

energy of a metastable polymorphic form exceeds that of the stable form and with this is associated the higher solubility of the metastable form.

The influence of the crystalline form on the dissolution rate was first observed by Wilderman (16) and later by Gross (251). The rate of solution and solubility of calcium sulfate in both the anhydrous and hydrated forms was measured by Roller (10, 11). He found that the anhydrous form exhibited a solubility of about 1.5 times the solubility of the hydrated form. The relative rate of release at the interface of the crystalline forms was suggested as the reason for this difference in solubility. Taylor and Henderson (252) and Hill (253) reported the physico-chemical properties of the crystalline forms of calcium nitrate and calcium sulphate.

More recently, studies have been made of the organic compounds in the anhydrous and hydrated forms. The anhydrous form of phenobarbitone and two of its hydrates were examined by Eriksson (254) for apparent solubility in water as a function of time. Shefter and Higuchi (255) examined quantitatively the relative dissolution rates of some solvated and non-solvated organic medicinal compounds using a fine multiparticulate system. From the study they observed a definite difference in the dissolution rates of the crystal forms. However, it would be impossible to quantitate these differences because of the uncontrolled surface area and rapid dissolution rate of these materials.

These workers also determined the thermodynamic properties of several of these crystal forms.

Poole and Bahal (256, 257) reported the dissolution and solubility behavior of the anhydrous and trihydrate forms of ampicillin and also of the anhydrous and dihydrate forms of WY-4508, an aminoalicyclic penicillin.

Hamlin and co-workers (51) studied the dissolution rate of two polymorphic forms of methylprednisolone. They reported that the differences in the dissolution rates of methylprednisolone polymorph I and II observed at low agitation intensities disappeared at higher agitation intensities.

Levy and Procknal (52) suggested that the results obtained by Hamlin and co-workers (51) could be due to loss of sensitivity encountered with the apparatus and methodology used or to an intrinsic property of the polymorphs. Using the rotating disk method, these workers also determined the dissolution rates of methylprednisolone polymorphs I and II, as a function of the rate of rotation. Their experimental data confirmed the observations made by Hamlin and co-workers that differences in the dissolution rate of methylprednisolone polymorphs diminish at higher agitation intensities and are due to an intrinsic property of the drug and are not caused by a particular apparatus or methodology.

Wurster and Taylor (38) reported the dissolution rate of three crystalline forms of prednisolone. By determining

the relative dissolution rates of these crystal forms under different agitation intensities, it was suggested that the dissolution process could be described by consecutive processes which involve reaction at the interface and transport away from the interface.

Higuchi and co-workers (50) later proposed the answer to the "anomalous" dissolution rate behavior observed with different agitation conditions. Working with polymorphic forms of sulfathiazole and methylprednisolone, the authors proposed a theory to account for dissolution from a mixture of two polymorphs. The theory was the extension of that discussed by the authors for the dissolution behavior of polyphase mixture (53).

Milosovich (250) employed dissolution rate measurements to determine the solubility of metastable sulfathiazole polymorph. Thermodynamic data for both the forms of sulfathiazole were obtained.

Nogami and co-workers (258) proposed a model to describe the dissolution phenomena using p-hydroxy benzoic acid and phenobarbitone which change to their respective hydrates during dissolution. Using this model they obtained the solubility of anhydrous forms. The thermodynamic functions of the transition from anhydrate to hydrate form were determined. Nogami and co-workers (259) also determined the dissolution rate constants of barbitone polymorphs in water using the rotating disk method. Examining the rate constants, it was found that the dissolution of phase I

does not accord with Levich's equation (102). They concluded that the phenomena may not be fully interpreted by the diffusion process mechanism only. By combining the Levich equation and the concept of consecutive process, the authors calculated the diffusion coefficient and the rate constant of interfacial chemical reaction and that of transport process.

Clements and Stanski (29) found the dissolution rate of four polymorphs of phenobarbitone, using the tape method for dissolution studies, and observed a higher dissolution rate for two of the metastable forms.

Aguiar and Zelmer (246) measured the relative rates of dissolution and solubilities of three polymorphic forms of chloramphenicol palmitate and two polymorphs of mefenamic acid. The thermodynamic relationships involving the transition of the metastable form to the stable one were reported.

Mitchell and Saville (124) reported the variation in the intrinsic dissolution rates of commercial aspirin, and later suggested that polymorphism was a possible cause (260). During the determination of the solubility of aspirin, a pattern of dissolution was observed, which suggested that aspirin undergoes phase changes. Griffiths and Mitchell (261) reported this solvent-mediated phase change when aspirin crystals are dissolved in aqueous medium. It is suggested that phase change is caused by the crystallization of a less soluble form on crystal surfaces during

dissolution.

3. Crystal Structure and Drug Availability

While investigating the physico-chemical analysis of percutaneous absorption from creams and ointments, Higuchi (262) found that the maximum penetration rate of a drug is obtained by using the crystal form with the highest thermodynamic potential. It was suggested that the use of a more energetic metastable form is advantageous. Ballard and Nelson (263) demonstrated the influence of polymorphism on the solubility of methylprednisolone and found that the metastable form (Form II) has 1.2 times the solubility of the stable form (Form I). They implanted pellets of two polymorphic forms of methylprednisolone in rats and found that form II was absorbed 1.7 times faster than Form I. Ballard and Biles (264) studied the in vivo absorption rates of hydrocortisone tert-butyl acetate and prednisolone tert-butyl acetate and their solvates by the pellet implantation technique. Solvates of these compounds gave different solid drug absorption rates.

Aguiar and co-workers (248) reported the existence of three crystalline polymorphs of chloramphenicol palmitate. They investigated the in vivo absorption of polymorphs A and B, and found a higher in vivo absorption rate with form B. Their experimental data also demonstrated that absorption is influenced by the type and concentration of the polymorph present. Anderson (265) had previously examined several commercial preparations and powders of

chloramphenicol palmitate. It was found that the therapeutic inactive preparations contained polymorph A, the inactive form.

The biological availability of ampicillin after oral administration to laboratory animals and human subjects appears to correlate with the physico-chemical characterization of the solubility and the dissolution rate noted for the anhydrous and trihydrate forms. As suggested, the higher aqueous solubility of anhydrous form is probably the major factor responsible for the enhanced in vivo availability noted for this form of the drug (247).

Hamlin and co-workers (51) determined the in vitro and in vivo dissolution rates of two forms of methylprednisolone. The in vivo results showed a higher dissolution rate for the metastable form than for the thermodynamically more stable form.

Haleblian and Biles (266) compared the physical properties and biological activities of some of the crystalline phases of fluprednisolone and found that the ratio of in vitro dissolution rate for the highest and the lowest energetic phases was 2.24. The ratio between the highest and the lowest energetic phases for in vivo dissolution rate was found to be 1.61.

It has been also suggested that polymorphism in aspirin may be involved in differences in in vivo availability (267). Tawashi (162) has reported that Form II dissolves 50% faster than Form I.

When a drug can exist in either the crystalline and/or the amorphous form, the in vitro and in vivo dissolution rate of both the forms generally differ. Mullins and Macek (268) found that the stable crystalline form of novobiocin did not yield adequate blood levels on oral administration. However, when administered as a metastable amorphous form, novobiocin was better available for gastrointestinal absorption. The differences in availability were thought to be due to the differences in the water solubility of the two forms.

It is reported that the crystalline form of chloramphenicol stearate and chloramphenicol palmitate are therapeutically inactive and only the amorphous forms of these two compounds are hydrolysed in the gastrointestinal tract to chloramphenicol (269). Glazko and co-workers (270) pointed out that the rate of hydrolysis of chloramphenicol palmitate is an essential factor in controlling the rate of absorption of the free alcohol.

E. AIMS AND OBJECTS OF THE PRESENT STUDY

The particular aim of this study was to investigate the dissolution characteristics of powdered drugs. Specifically, the study was undertaken to show the effect of crystal modifications on the dissolution behavior of meprobamate, and to make use of multichannel Coulter counter assembly for the rapid size distribution of pharmaceutical materials and for determining the dissolution rate of powdered drugs.

Physico-chemical evaluation of meprobamate was made and included the identification of the two crystalline forms. Studies were conducted to investigate the relative dissolution behavior of the two forms in distilled water.

It was also the purpose of the study to develop a sensitive analytical procedure for the determination of meprobamate in aqueous solutions for its dissolution rate studies.

A 128 multichannel Coulter counter assembly was evaluated with materials having a narrow size range and also with materials having a wide size range. With the multichannel Coulter counter assembly, the speed of data acquisition was greatly increased over the conventional Coulter counter method, which suggested its use for studies of the dissolution of powdered drugs by following the change in the particle size distribution of the materials.

CHAPTER III. EXPERIMENTAL METHODS

A. PHYSICO-CHEMICAL STUDIES OF MEPROBAMATE

1. Preparation of Polymorphic Forms of Meprobamate

The meprobamate^a was dissolved in hot water and filtered immediately. The deposited crystals, after cooling the solution, were collected and dried under vacuum. This was designated as Form I. A second form was prepared from Form I, by crystallization from a super-cooled melt.

Form I of meprobamate was fused in a china crucible placed in a temperature controlled oven at 110°C. When the substance was completely fused, it was poured immediately onto a cold petri glass plate. This was left overnight at room temperature to solidify. The solidified mass was carefully crushed with a spatula. The crushed powder was screened to obtain the desired sieve fraction.

Elemental Analysis:

Elemental analysis was performed on both the forms of meprobamate. The instruments used were the Coleman Carbon-Hydrogen Analyser^b and the Coleman Nitrogen Analyser^b.

2. Characterization of the Polymorphic Forms

Several methods were used to distinguish the two crystal forms. These were:

- (a) melting point determination;
- (b) infrared spectroscopy;
- (c) X-ray diffraction pattern;
- (d) differential thermal analysis;

^aFrank W. Horner Ltd., Montreal, Canada

^bFisher Scientific Co., Ltd., Toronto, Canada.

- (e) solubility determination;
- (f) dissolution rate determination.

Melting Point Determination:

Capillary tube melting point determinations were made using a Hoover^a melting point apparatus.

Melting point determinations were also made using a hot stage microscope. A Leitz microscope^b with a hot stage was used. A small amount of sample was placed between a slide and a cover slip, and the slide was placed on the hot stage. The sample was observed through the microscope as it was heated at a constant rate up to the fusion point.

Infrared Spectroscopy:

Infrared spectra of Form I and Form II of meprobamate were recorded as potassium bromide disks. The disks were prepared using a Beckman potassium bromide die and Carver Laboratory Press^c, Model B, at a pressure of 60,000 PSig. The sample-potassium bromide ratio employed was 1.5 to 200.

A Beckman IR-10 spectrophotometer^d was employed for recording spectra. The instrument employs two precision replica gratings in a single monochromater. The first grating operates from 4000 to 600 cm^{-1} , and the second from 650 to 300 cm^{-1} . For calibration of the wave length axis, polystyrene film was used.

^aA.H. Thomas Co., Philadelphia, U.S.A.

^bLeitz and Co., Ltd., Germany

^cFred S. Carver Inc., Summit, New Jersey, U.S.A.

^dBeckman Instrument, Inc., Fullerton, California, U.S.A.

X-ray Diffraction Pattern:

Crystalline materials in the powder form give characteristic X-ray diffraction patterns. From the 2θ values of these peaks can be calculated the distance, d , for the different planes of the crystal, using the Bragg equation, $n\lambda = 2d \sin \theta$, where the wave length of the X-ray source is known. Each powder pattern of the crystal lattice is characteristic of a given polymorphic form.

Powder photography and powder diffractometry were used for this study. The nickel filtered $\text{CuK}\alpha$ radiation was employed.

For obtaining powder photography a sample of powder passing through a 400 mesh sieve, for both the polymorphic forms, was separately loaded into a pyrex glass capillary tube of 0.4 mm o.d., having a very thin wall (0.01 mm). The capillary tube was filled up to one cm depth. The glass capillary was then mounted on the axis of a 57.3 mm radius Debye-Scheerer powder camera^a. The sample was then exposed to $\text{CuK}\alpha$ radiation for 2 hours.

For powder diffractometry, a Norelco diffractometer^a was employed. The powder sample was packed into a planchet having a depression 1 mm depth, 10 mm width and 20 mm length. The flat side of the spatula was used to pack the powder and to smooth it so that a uniform level surface was presented to the X-ray beam. The instrument variables of the

^aNorelco Philips Electronic Inc., South Fulton, New York,

diffractometer were set as follows:

- (a) 1° beam slit and 4° detector slit; and
- (b) CuK α radiation, 35 kv., 15 ma., Ni filtered.

Differential Thermal Analysis:

In differential thermal analysis (DTA) heat loss or gain resulting from physical or chemical changes occurring in a sample is recorded as a function of temperature or of time as the substance is heated at a uniform rate.

The Du Pont 900 differential thermal analyser^a (DTA), equipped with a standard cell, was employed to detect polymorphic transitions and melting of both polymorphic forms of meprobamate. The micro sample glass tube was filled with the test substance to a depth of approximately 2 mm. The junctions of the thermocouples were embedded in the sample. A second differential thermocouple was placed into an inert reference, consisting of glass beads. The tubes were placed in a heating block. After replacing the cell assembly the block was heated. In each case the sample was heated from room temperature to a temperature several degrees above fusion, at a uniform rate of 10°C min⁻¹. Thermograms were obtained for each polymorph.

3. Quantitative Measurements of Heats of Fusion

Although primarily a tool for qualitative analysis, use has been made of DTA in estimating heats of reaction, fusion and transition. These thermodynamic properties can be

^aDu Pont De Nemours, E.I., and Co., Inc., Wilmington, Delaware, U.S.A.

determined by integrating the endothermic or exothermic peak produced as the sample reacts, melts or undergoes a solid state transition.

The value of the heat of fusion may be determined from the area under the peak of thermogram. For quantitative measurements of heat of fusion, the Du Pont 900 differential thermal analyser equipped with a calorimeter cell was used. In the calorimeter cell, silver holders or cups for sample or reference are located in separate air cavities in a heating block. Chromel-alumel thermocouples contact the bottom of the holders. A resistance heating element is wound around the block, and gives high resistance to the transfer of heat from the sample to the block. When the sample undergoes transition, the heat developed is retained by the sample and its holders.

Calibration of the Calorimeter Cell:

Determination of Calibration Coefficient:

A curve of the calibration coefficient, E, for the calorimeter cell was determined by using materials with known heats of fusion. Gallium, indium and tin samples were used for this purpose. The heats of fusion of these elements are given in Table I.

Table I

Heats of Fusion of the Standard Materials (236)

Material	Heat of fusion (Cal gm ⁻¹)
Tin	14.20
Indium	6.79
Gallium	19.90

Procedure using tin:

Approximately 6 mg of tin was accurately weighed into an aluminum sample liner on a Sartorius Selecta semi-micro balance^a to the nearest 0.01 mg. The sample and the liner were placed in the sample holder of the calorimeter cell. The heating block cover and the insulation lid were placed into position, followed by the bell jar. The temperature of the cell was brought rapidly to approximately 100°C below the temperature of fusion. Then the heating rate control was set to provide a heating rate of 10°C min⁻¹. The Y-axis sensitivity was set at 0.5°C in⁻¹. X-axis sensitivity was set at 50°C in⁻¹. After fusion, the heating was allowed to continue for a further 30°C. At this point the run was ended. Six replicate runs were made.

Procedure using indium:

Six replicate runs were made using accurately weighed quantities of indium, using the method described for tin, except that the thermogram recording was started from room temperature.

Procedure using gallium:

The gallium sample supplied was in super-cooled condition. It was cooled well below zero degree centigrade to ensure that the sample is in the solid state rather than the super-cooled phase. Liquid nitrogen was used to cool the sample to -70°C. After weighing accurately, the sample and the liner were placed in the sample holder. After replacing the

^aSartorius-Werke, GmbH, Göttingen, Germany.

heating block cover, the cooling attachment was placed in contact with it and the liquid nitrogen added. When the temperature had fallen to -70°C , the cooling attachment was removed and the insulating lid and bell jar replaced. The run was made as for tin. Thermogram recording in this case was started from -70°C . Six replicate runs were made.

Determination of the Area of the Thermograms:

The areas of these endothermic peaks were determined by cutting out the peak areas and weighing to ± 0.01 mg. The reference weights were obtained by cutting out four square inches of the graph paper from each of the graphs and weighing. The area to be weighed was found by drawing a line from the point where the thermogram first departed from the base line to the point where the base line was resumed following fusion.

Measurements of Heats of Fusion:

After calibration, the accuracy of calibration was checked, by measuring the heat of fusion of sulfathiazole^a. The heat of fusion of Form II of sulfathiazole has recently been determined using Du Pont 900 differential thermal analyzer (236). Form II of sulfathiazole was prepared by the method of Milosovich (250).

About 2 gm of sulfathiazole was crystallized at room temperature from warm alcoholic solution. The product obtained consisted of hexagonal plates. This was heated at 180°C in a china crucible kept in a temperature-controlled

^aMallinckrodt Chemical Works Ltd., Montreal, Canada.

oven to produce Form II.

Four samples of sulfathiazole Form II were weighed into sample liners. Samples of about 3.0 mg were used in measuring the heat of fusion of sulfathiazole. These were weighed on a balance to the nearest 0.01 mg. The liner, together with the sample, was fitted into the silver sample holder of the calorimeter cell so as to obtain a good contact with the bottom of the sample holder. An aluminum liner was used in the reference cup. The thermograms were obtained as in the case of calibration of the calorimeter cell.

When the heat of fusion of Form II of sulfathiazole was computed, it was found to be in fair agreement to the values reported by Guillory (236).

For measuring heats of fusion of both the forms of meprobamate, six samples of each of the polymorphic forms were weighed into sample liners. The thermograms were obtained as for sulfathiazole. The weights of each sample used were as 2.5 mg (Form I) or 3.0 mg (Form II).

4. Analytical Procedure for Determination of Meprobamate

Contents

Quantitative analysis of meprobamate in aqueous solutions has previously been performed by colorimetric method (271, 272), thin layer chromatography (273) and gas-liquid chromatography (274-276). In the present study a gas-liquid chromatographic method was selected as the quantitative analytical method of choice for the determination of meprobamate in aqueous solutions.

Gas-liquid Chromatography Procedure:Instrumentation:

A Perkin-Elmer model 990 gas chromatograph^a equipped with a dual flame ionization detector and a 0-10 Speedomax W recorder with integrator^b was used. A chart speed of 0.5 in min⁻¹ was employed for this study throughout the experimental work. All samples were injected with a 10 μ l Hamilton gas chromatographic syringe^c.

The Chromatographic Column:

The chromatographic column was a coiled glass column (6 feet x 1/4 inch), packed with 3% weight OV-1^d on chrom-sorb G-AW-DMCS^e. Prior to use the column was conditioned at 220°C for 24 hours to minimize column bleeding.

Operating Conditions:

The oven temperature used was 200°C. The sample injection temperature was maintained at 230°C, and manifold temperature at 240°C. Helium was used as the carrier gas and was maintained at 50 psig. The hydrogen flame detector was operated with hydrogen and air both at 25 psig. All the determinations were made with attenuator settings from 100 x 2 to 100 x 4.

The optimum air pressure (25 psig) and hydrogen pressure

^aPerkin-Elmer Norwalk, Connecticut, U.S.A.

^bLeeds and Northrup Co., Inc., Philadelphia, U.S.A.

^cHamilton No. 701 Syringe, Whittier, California, U.S.A.

^dDimethylsilicone Gum

^eDiatomaceous Silica aggregate

(25 psig) were selected for the maximum response of meprobamate and internal standard, by measuring peak heights at different gas pressures.

Extraction Procedure:

One ml of the sample was pipetted into a 15 ml glass stoppered centrifuge tube. To the tube was then added 5 ml of reagent grade diethyl ether. The tube was tightly stoppered and shaken for 10 minutes on a shaker followed by centrifugation at 2000 r.p.m. for 5 minutes. The upper ethereal layer was then transferred to a 15 ml glass stoppered tube containing 1 ml of a 0.1% solution of dibutylphthalate (internal standard)^a in diethyl ether. Further 3 ml portions (2 times) of diethyl ether were added to the centrifuge tube, and the procedure of shaking, centrifuging and transferring of the ethereal layer was repeated. To the mixed ethereal extract and internal standard was then added about 500 mg of anhydrous sodium sulphate^a. The tube was stoppered and shaken for 10 minutes and then centrifuged. The ethereal layer was then transferred to a clean tube. The combined ethereal extracts and internal standard were concentrated to a small volume (about 100 to 500 μ l) by evaporation of the extract in a centrifuge tube placed in a water bath at about 35°C. Boiling was promoted by the addition of a boiling stick in the tube. Then about 0.2 μ l of the concentrate was injected on to the gas liquid chromatographic column.

^aThe British Drug Houses (Canada) Ltd., Toronto, Canada

A blank extraction was done by following exactly the same procedure, using one ml of water.

The absolute recovery of meprobamate was determined by comparing peak ratios of the ether extract for a known amount of the drug dissolved in water to that obtained for an equal amount of the drug dissolved in ether and estimated by the gas-liquid chromatographic procedure.

The reproducibility of the extraction procedure was determined by extracting eight aqueous solution samples, each containing 0.2 mg ml^{-1} of meprobamate, and assaying by the gas-liquid chromatographic procedure.

To investigate the extent of decomposition of meprobamate in water, an aqueous solution containing a known amount of drug was left at 25°C for one week and analysed at selected time intervals. A second sample of solution was also kept at 40°C for three days and analysed.

A calibration curve was prepared from aqueous solutions containing known amount of meprobamate, as follows:

Stock solutions containing known amounts of meprobamate in distilled water were prepared. From these, aqueous solutions containing $50\text{-}400 \text{ mcg ml}^{-1}$ meprobamate were assayed. The peak areas of meprobamate and dibutylphthalate were obtained. A calibration curve was then constructed by plotting the ratio of the peak areas of meprobamate to dibutylphthalate against the concentration of meprobamate in water. The calibration curve was repeated at intervals of two months.

5. Solubility and Dissolution Rate Studies

The same procedure was used to study the dissolution properties of both the forms of meprobamate. For dissolution studies at a particular temperature the same weight of each crystalline modification was used. The sample of solid used was approximately twice the concentration necessary to saturate the solution. The material which passed through a 60 mesh sieve but was retained on an 80 mesh sieve was used for solubility and dissolution rate studies.

A weighed sample of the polymorph was rapidly added to 15 ml of distilled water. The distilled water used was previously filtered through a 0.45 μ Millipore filter membrane and was equilibrated to the desired temperature. The bottle was rotated at a constant speed of 23 r.p.m. in a constant temperature water bath maintained at the appropriate temperature. Using a pipette fitted with washed glass wool filter plug, one ml of the sample, free of all solid materials, was withdrawn at predetermined time intervals and immediately diluted with distilled water to a known volume, to avoid precipitation of the meprobamate crystals in the filtered sample as the sample cooled. The meprobamate in the solution was determined by the gas-liquid chromatography method. Three replicate runs were made for each polymorphic form at each temperature.

Confirmation of the Complete Reversion of the Form II to Form I:

From the solubility and the dissolution behavior at

various temperatures, it was noted that the solubility of Form II falls essentially to that of Form I at a particular temperature.

About 180 mg of meprobamate Form II powder was added to 15 ml of distilled water in a 25 ml bottle. The bottle was rotated at 23 r.p.m. in a constant temperature water bath maintained at 40°C. After 20 minutes the solution was immediately filtered through a 0.45 μ Millipore filter membrane and the filtrate placed into a clean bottle. This was then rotated for a further 28 hours. After this period, precipitated crystals were observed, presumably of the Form I. These crystals were filtered and dried under vacuum and were examined by X-ray diffraction analysis.

B. MULTICHANNEL COULTER COUNTER ASSEMBLY FOR DISSOLUTION RATE STUDIES

1. Assembling of 128 Multichannel Analyser with the Coulter Counter

Although the Coulter counter is a fast method of size analysis in comparison with the classical methods, the speed of data acquisition can be greatly increased by converting it from a single-channel analyser to a multichannel data

analyser. In this way all the voltage pulses produced by the amplifier of the Coulter counter are monitored, with the exception of a small percentage lost by coincidence arrival at the multichannel analyser. This system has been previously described by Ho and Higuchi (277).

The relatively slow (40 microseconds) pulse from the amplifier of the Coulter counter was not suitable for use as a direct input to a multichannel analyser since the latter required a pulse with a fast leading edge. To provide a suitable input signal, interface circuitry was introduced between the Coulter counter Model B^a and the ND-555 Multichannel Analyser^b. This is shown in Figure 1. The output from the amplifier of the Coulter counter was fed into the linear gate and also into a differentiator. The differentiator output is a full single-wave pulse. This pulse is fed to a zero strobe which detects the point at which the voltage is zero and at the same instant produces a small positive square wave as output. This square-wave pulse is generated at precisely the same instant in time as the original pulse has reached its peak value. The square-wave input to the linear gate opens the gate to the original signal, so that the output from the linear gate is a voltage pulse with a fast leading edge, proportional in amplitude to the original signal. The gain of the interface circuit was adjusted so that pulse in the range of the oscilloscope

^aCoulter Electronics, Inc., Hialeah, Florida, U.S.A.

^bNuclear Data, Inc., Palatine, Illinois, U.S.A.

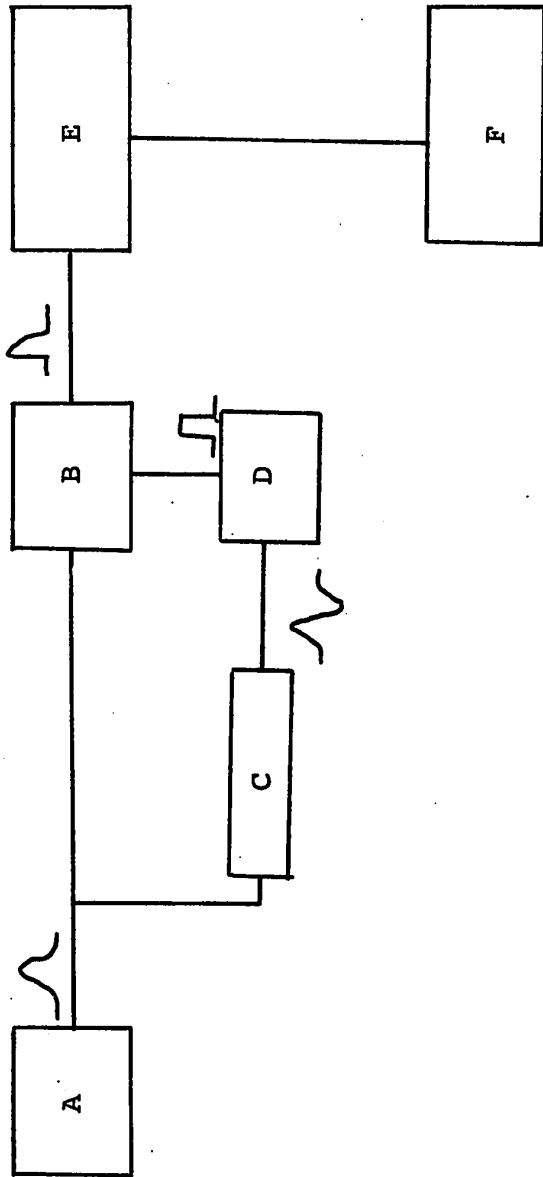


Figure 1. Schematic Representation of Coulter Counter, Interface, Multichannel Analyser and Display Units
 A - Coulter Counter; B - Linear Gate; C - Differentiator;
 D - Zero Strobe; E - Multichannel Analyser; F - Oscilloscope Display or Plotter.

of the Coulter counter was also in a suitable range for the multichannel analyser. The output from the multichannel analyser was fed to an oscilloscope^a, for immediate display, or to the input of the X-Y plotter^b, which plots the full differential frequency distribution.

Prior to use for studies of dissolution of solid particles, calibration of the multichannel Coulter counter assembly was carried out. For this purpose latex particles^c and ragweed pollen grains^c were used. The three methods used for the size analysis of these materials were: microscopic measurement; Coulter counter, using the conventional method; and multichannel Coulter counter assembly.

2. Size Distribution Measurements of Ragweed Pollen Grains and Latex Particles Using a Microscope

Microscopic Measurement of Ragweed Pollen Grains:

In order to prepare a suitable slide for examination under a microscope, a few milligrams of the sample were suspended in a few drops of 0.9% sodium chloride solution. The resulting slurry was thoroughly mixed by a stainless steel micro spatula. A small portion was then transferred on to a microscope slide using a micro spatula. Care was taken to disperse all the aggregates, without crushing the

^aAllen B. Dumont Laboratories Inc., Clifton, New Jersey,

U.S.A.

^bHewlett Packard Moseley Division, Pasadena, California,

U.S.A.

^cCoulter Diagnostics Inc., Miami Springs, Florida, U.S.A.

pollen grains. The diameter of the four hundred particles was measured individually using a Leitz microscope equipped with an eyepiece micrometer previously calibrated against a stage micrometer.

The median diameter of the particles was calculated. The corresponding volume frequency distribution was calculated assuming sphericity of the particles.

Microscopic Measurements of the Latex Particles:

A standard suspension of the latex particles was used. The sample in a tube was kept in a laboratory ultrasonic bath for 40 to 50 seconds to disperse the latex particles. Two drops of this suspension were then mixed with a few drops of glycerine. A drop of this mixture was then mounted on a microscope slide. The diameter of four hundred particles was measured individually using a Leitz microscope equipped with a calibrated eyepiece micrometer. The corresponding volume frequency distribution was calculated, assuming sphericity of the particles.

3. Size Distribution Measurements of Ragweed Pollen Grains and Latex Particles with the Coulter Counter Using the Conventional Method

Preparation of Electrolyte:

An aqueous solution of sodium chloride (0.9%) was used as an electrolyte. This was freshly prepared before use and was filtered through a 0.22 μ Millipore filter membrane, by applying suction.

Before particle size can be measured by the Coulter

counter, it is necessary to calibrate the instrument. The purpose of the calibration is to define the relationship between the volume and the electrical pulse amplitude of the particle for each aperture size.

Calibration can be carried out using any "monosized" particulate material provided that the diameter of the particle is within the range of 2% to 40% of the aperture diameter and the median volume of the particulate material is known. "Monosized" ragweed pollen grains and latex particles were employed for calibration. The diameter and the volume frequency distributions of these standard materials were determined from the microscopic measurements. For the ragweed pollen grains the 100 μ aperture tube was used with a sample volume of 500 μ l. A 50 μ aperture tube and a sample volume of 50 μ l were used for the latex particles.

Preparation of the Suspension:

Approximately 2 mg of ragweed pollen grains were mixed on a watch glass with a small drop of "Isoterge"^a or Tween 80^b. The suspension was transferred to a beaker using electrolyte solution. For latex particles, two drops of a suspension were mixed with 50 ml of electrolyte solution in a beaker. The beaker was kept in a laboratory ultrasonic bath for 40 seconds. This was then diluted to about 200 ml with electrolyte solution.

^aCoulter Diagnostics Inc., Miami Springs, Florida, U.S.A.

^bAtlas Powder Company Canada Ltd., Brantford, Canada

The concentration of the suspension was checked by setting the amplification and aperture current switches on the Model B Coulter counter so that most of the pulses reach between one third and two thirds of the maximum height of the oscilloscope screen. The upper threshold level was set to a value that excluded the doublets and triplets. At these settings, most of the particles in the sample were counted. The mean of four counts was taken. Then the counts were taken at convenient successively larger settings of the lower threshold. The setting of the lower threshold value that gave half the total number of particles in the sample of suspension was used to calculate the calibration constant.

The complete size distributions of the ragweed pollen grains and the latex particles were measured. The mode selector of the Coulter counter was left in the "separate" position. The settings of the upper and the lower threshold levels were adjusted to 70 and 28 respectively for ragweed pollen grains and 27 and 25 respectively for latex particles, and the counts were then obtained at successively lower settings of the threshold dials.

4. Size Distribution Measurements of Ragweed Pollen Grains and Latex Particles Using the Multichannel Coulter Counter Assembly

Using the multichannel Coulter counter assembly, the complete volume frequency distribution of each material was recorded in a single step. Using both the aperture current

and amplification settings on the Coulter counter at 1/2, for the latex particles, the voltage pulses were fed to the multichannel Coulter counter assembly, by having the mercury in the manometer in the "vacuum" position, thus activating the "start" switch. With the "mode" switch on the multichannel analyser set to "acquire", accumulation of counts in the channels commenced. After a suitable time interval (between 5 seconds and 25 seconds) to provide a satisfactory count, the "mode" switch was set to "stop" and then to "output".

With the mode switch on the multichannel analyser set in the "output" position the data were either displayed on an oscilloscope screen and recorded on photographic film or plotted directly on the X-Y plotter. The analyser was adjusted so that channel number one corresponded to particle volume of approximately zero by setting the lower level discriminator on multichannel analyser to exclude noise signals. For ragweed pollen grains, the aperture current and amplification settings on the Coulter counter were set at 1 and 16 respectively.

The coincidence loss of pulses arriving at the multichannel was indicated on the dead-time meter of the analyser and coincidence correction of the count in each channel gave the true count of electrical pulses arriving at the multichannel analyser. Correction of each count for primary coincidence and background count then gave the true particle count in each channel.

For each method of size analysis, the cumulative percentage of oversize particles was plotted on the probit scale against the particle volume.

5. Size Distribution Measurements of Micronized Hydrocortisone Acetate and Griseofulvin

To test the method with materials having a wider distribution of particle sizes, micronized powders of hydrocortisone acetate^a and griseofulvin^b were used.

A sample of aqueous sodium chloride solution (0.9%) was saturated with the material under study by the addition of approximately 10 times the quantity required to saturate the solution at 25°C, and stirring the solution for 5-7 days with a magnet stirrer. Just prior to use, the solution was decanted and filtered through a 0.22 μ Millipore filter membrane.

For the measurement of the size distribution, a small quantity of the powder was mixed on a watch glass with a drop of Tween 80. This was diluted with the presaturated solution to about 50 ml, subjected to ultrasonic irradiation for 40 seconds and then diluted to about 200 ml.

Size analysis of the suspension was then carried out as rapidly as possible using the multichannel Coulter counter assembly first and then using Coulter counter in the conventional manner. A 50 μ aperture tube was used for size analysis.

^aSchering Corporation, Bloomfield, New Jersey, U.S.A.

^bSchering Corporation Ltd., Pointe Claire, P.Q., Canada

6. Solubility Determination of Hydrocortisone Acetate and Griseofulvin

A calibration curve was prepared for the spectroscopic assay of hydrocortisone acetate, as follows:

Twenty mg of hydrocortisone acetate was accurately weighed and dissolved in methanol (10 ml). The volume was adjusted to 100 ml with distilled water in a volumetric flask. When the material was completely dissolved, aliquots of the solution were diluted with 10% v/v methanol in water, to obtain solutions containing 1, 2, 4, 8, 12 and 16 mcg of hydrocortisone acetate per ml of the solution. The absorbance of each of the dilutions was measured at 246 nm on a D.B. recording spectrophotometer^a, using a 1 cm path length cell. The Beer's Law relationship was verified by plotting the absorbance against concentration of hydrocortisone acetate in solution.

A calibration curve for griseofulvin was prepared by dissolving 20 mg, accurately weighed, griseofulvin in 100 ml of 60% v/v methanol in water. When the material was completely dissolved, aliquots of the solution were diluted to obtain the dilutions containing 1, 2, 4, 6, 8 and 12 mcg of griseofulvin per ml of the solution. The absorbance of each of the dilutions was measured at 292 nm on D.B. recording spectrophotometer using a 1 cm path length cell. Beer's Law relationship was verified by plotting the absorbance against concentration of griseofulvin in solution.

^aBeckman Instrument Inc., Fullerton, California, U.S.A.

Solubility of each material was determined in water at 25°C by the use of a quantity in excess of the solubility. One hundred milligrams of the solid was separately transferred to 50 ml glass bottles and 20 ml water was added to each. The caps were then screwed on tightly and the bottles were then rotated at 25°C in a constant temperature water bath for 7 days. After this period the bottles were placed upright for about an hour and an aliquot from each bottle was withdrawn using a glass syringe and filtered through a 0.45 μ Millipore filter membrane. The filtered solution was diluted appropriately with 10% v/v aqueous methanol for hydrocortisone acetate and 60% v/v aqueous methanol for griseofulvin. The absorbance of each solution was measured and the solubility of the substance was determined from the calibration curve. Three separate replicate runs were made for each substance.

Using this procedure the solubility of hydrocortisone acetate in 0.9% aqueous sodium chloride solution was determined. The solubility of griseofulvin was determined in 0.9% sodium chloride solution, and in 0.05% and 0.1% Tween 80 in 0.9% sodium chloride solution.

7. Dissolution Rate Studies

The dissolution of micronized hydrocortisone acetate in 0.9% aqueous sodium chloride solution was followed by observing the change in particle count at each particle volume with time. For this purpose the multichannel Coulter counter assembly was used.

An accurately weighed quantity of hydrocortisone acetate powder (2 mg) was triturated rapidly with 2 ml of filtered 0.9% aqueous sodium chloride solution. Using a one ml graduated pipette, 0.2 ml of this suspension was quantitatively transferred to a beaker containing 200 ml of filtered 0.9% aqueous sodium chloride solution. The quantity of the solid used corresponded to 10% of that required for saturation so that dissolution took place essentially under "sink" condition. The suspension in the beaker was stirred by a glass stirrer rotated at approximately 150 r.p.m. This speed was sufficient to keep the particles in suspension without introducing air bubbles in it.

Particle counts were taken over a 25 seconds interval and the stored data were immediately plotted on the X-Y plotter. After clearing the analyser by the erase push button, it was ready to accept fresh data. In this way the size distribution could be measured after approximately every 100 seconds. After making correction for background counts, the number of oversize particles was plotted against the particle radius and against (diameter)².

It was not possible to measure the dissolution rate of micronized griseofulvin powder in normal saline because it is a very hydrophobic powder. The particles floated on the surface of the dissolution media giving irregular counts. However, the rate of dissolution of micronized griseofulvin in 0.9% aqueous sodium chloride solution containing Tween 80

was determined. The quantity of micronized griseofulvin used corresponded to 10% of that required to saturate the dissolution medium.

Particle counts were taken over time intervals using the procedure as described for hydrocortisone acetate. After making corrections for background counts, the number of oversize particles was plotted against particle radius and against (diameter)².

The dissolution rates of micronized hydrocortisone acetate and griseofulvin in the electrolyte dissolution media were also followed by chemical analysis of samples of each solution using the D.B. recording spectrophotometer.

CHAPTER IV. RESULTS

A. PHYSICO-CHEMICAL STUDIES OF MEPROBAMATE1. Polymorphic Forms of Meprobamate

Two different polymorphic forms of meprobamate were obtained. These polymorphic forms were found to differ in crystal structure, heat of formation and other physical properties.

The C, H, N contents were estimated by elemental analysis of the meprobamate Form I and Form II, and are shown in Table II.

Table II

Elemental Analysis Data of Meprobamate ($C_9H_{18}N_2O_4$)

Polymorph	% Calculated			% Found ^a		
	C	H	N	C	H	N
Form I	49.53	8.31	12.84	49.74	8.30	12.71
Form II	49.53	8.31	12.84	49.61	8.33	13.08

a Mean of 2 runs

2. Characterization of the Polymorphic FormsMelting Point Determinations:

The different modifications of the crystal differed in their melting point. The melting points of meprobamate Form I and Form II, obtained using different methods of measurements, are shown in Table III.

Infrared Spectroscopy:

Figures 2 and 3 show the infrared spectra of meprobamate Form I and Form II respectively. A comparison of the infrared spectra of the two crystal forms as potassium

Table III

Melting Point of Meprobamate Form I and Form II

Form	Melting Point (°C)		
	a	b	c
I	103-106	102-105	103
II	94-96	94-96	94

a Capillary tube method

b Hot stage microscopic method

c Fusion temperature obtained by differential thermal analysis method

bromide disks reveals the presence of an extra peak at 1450 cm^{-1} for Form II.

X-ray Diffraction Pattern:

Figure 4 shows the powder X-ray photographic pattern for meprobamate Form I and Form II.

The X-ray diffraction patterns for meprobamate Form I and Form II are shown in Figures 5 and 6 respectively.

The different diffraction lines in X-ray photographic pattern for both the forms of meprobamate are evident from Figure 4. Figures 5 and 6 show different positions of the diffraction peaks for Form I and Form II. One of the distinguishing features in the X-ray diffraction pattern of ~~both~~ the ^{two} forms is the absence of a peak in Form I at a value corresponding to 2θ degrees at 21° .

Differential Thermal Analysis:

Figures 7 and 8 show the thermograms of meprobamate

Form I and Form II respectively. In each case a graph of differential temperature as a function of reference temperature gave an essentially straight base line, with a single endothermic peak corresponding to fusion.

Hill and Roy (278) mentioned that the best estimate of the transition temperature is obtained by using the temperature at which the curve leaves the base line. As this is often difficult to determine, they used the intersection of the extension of the base line and the extension of the straight part of the adjacent side of the peak as the transition temperature.

Guillory (236) in his study of heats of transition of methylprednisolone and sulfathiazole by differential thermal analysis technique, determined the fusion or transition temperature as the extrapolated onset temperature of the endothermic peak. In the present study this method was employed for determining the fusion temperature. The low temperature side of the peak was extrapolated to the pre-fusion base line. The fusion temperatures computed from the thermograms of meprobamate Form I and Form II are shown in Table III.

As the temperature response of the chromel-alumel thermocouples employed in the calorimeter cell is non-linear, a small temperature correction is made in the chart.

The heating rate of 10°C per minute was found to be the optimum heating rate. A sample size of about 2 to 3 mg was found to give a sharp peak suitable for area determination.

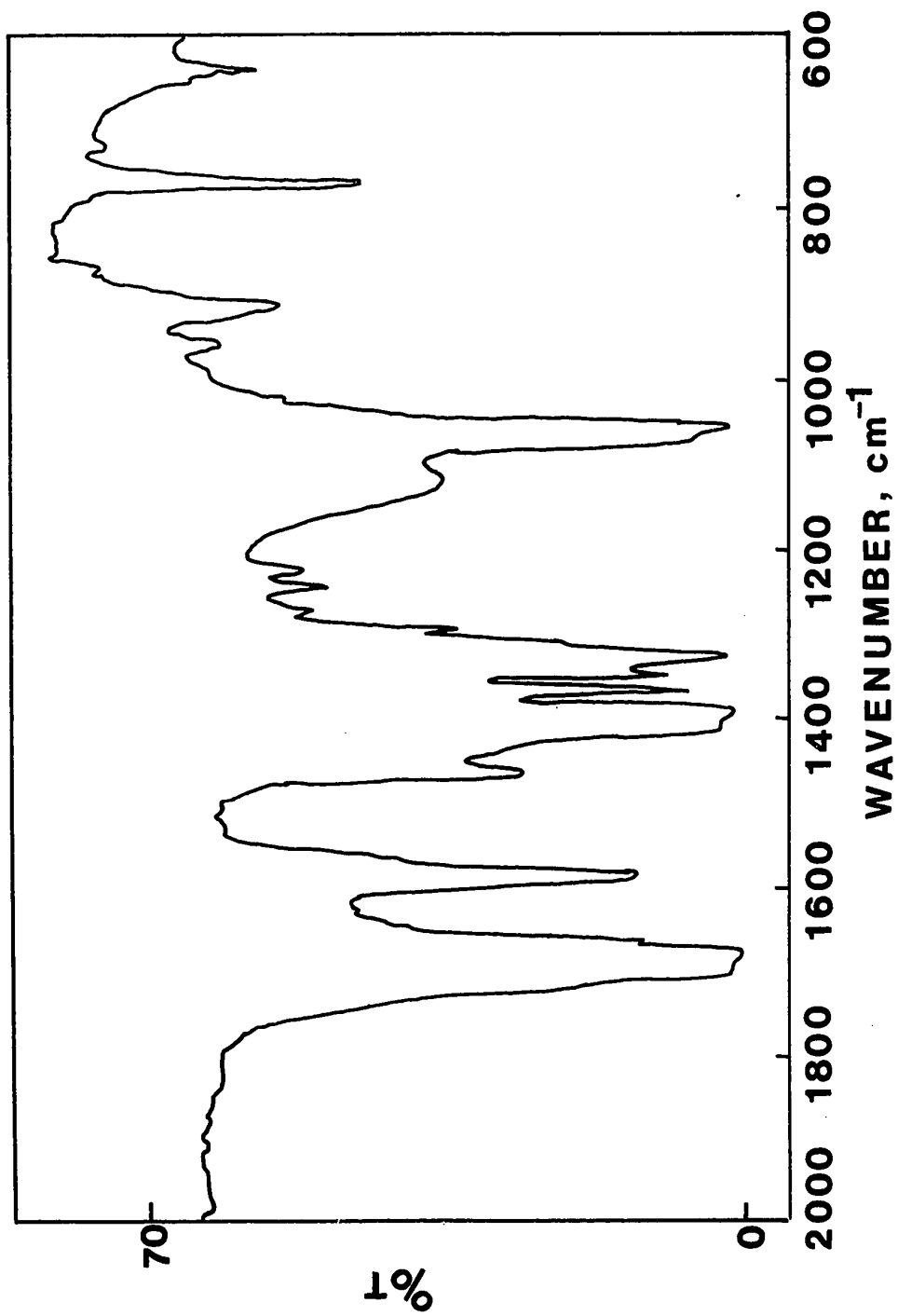


Figure 2. Infrared Spectrum of Meprobamate Form I

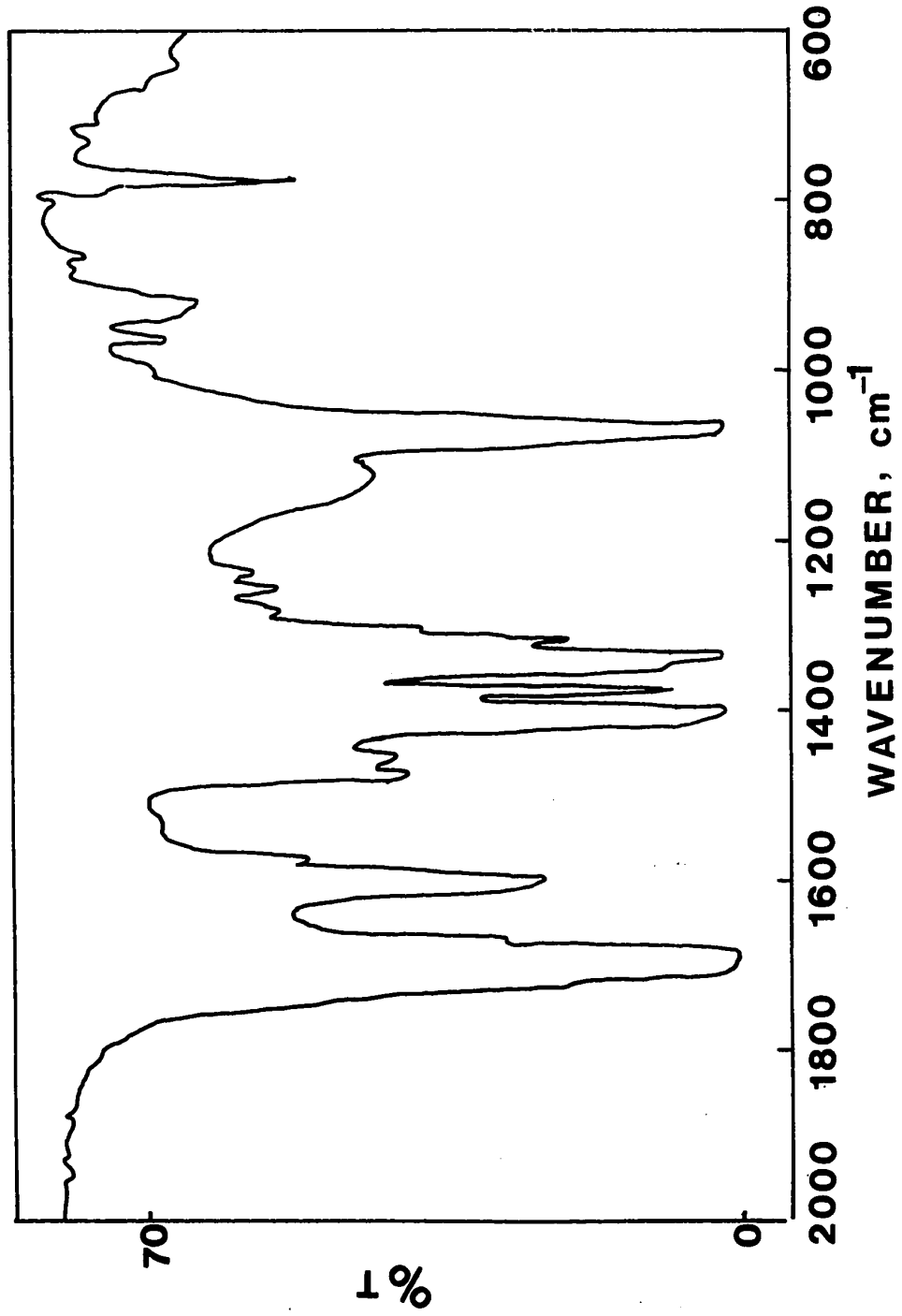
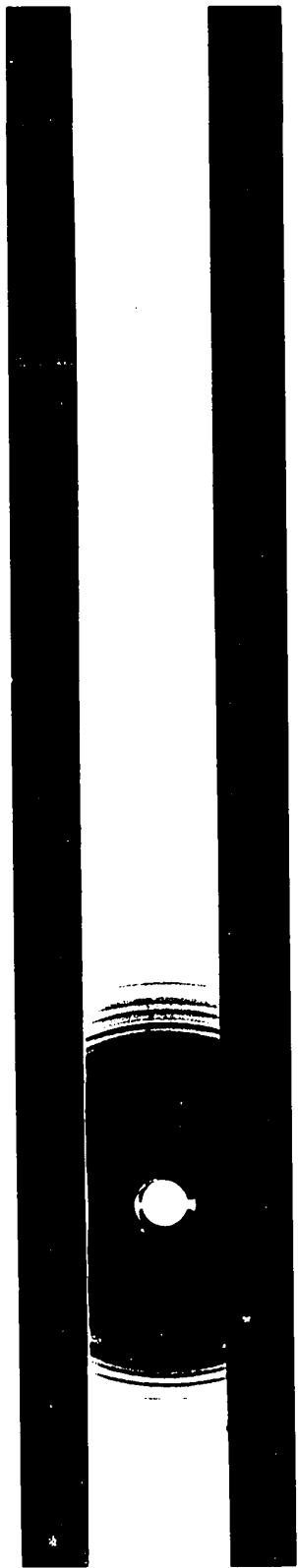
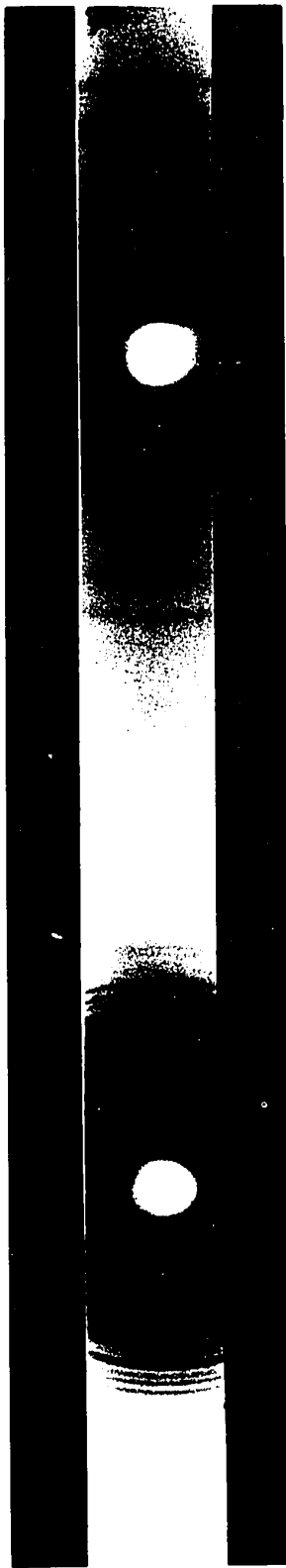


Figure 3. Infrared Spectrum of Meprobamate Form II



Form II



Form I

Figure 4. X-Ray Photographic Diffractions of Meprobamate Form I and Form II

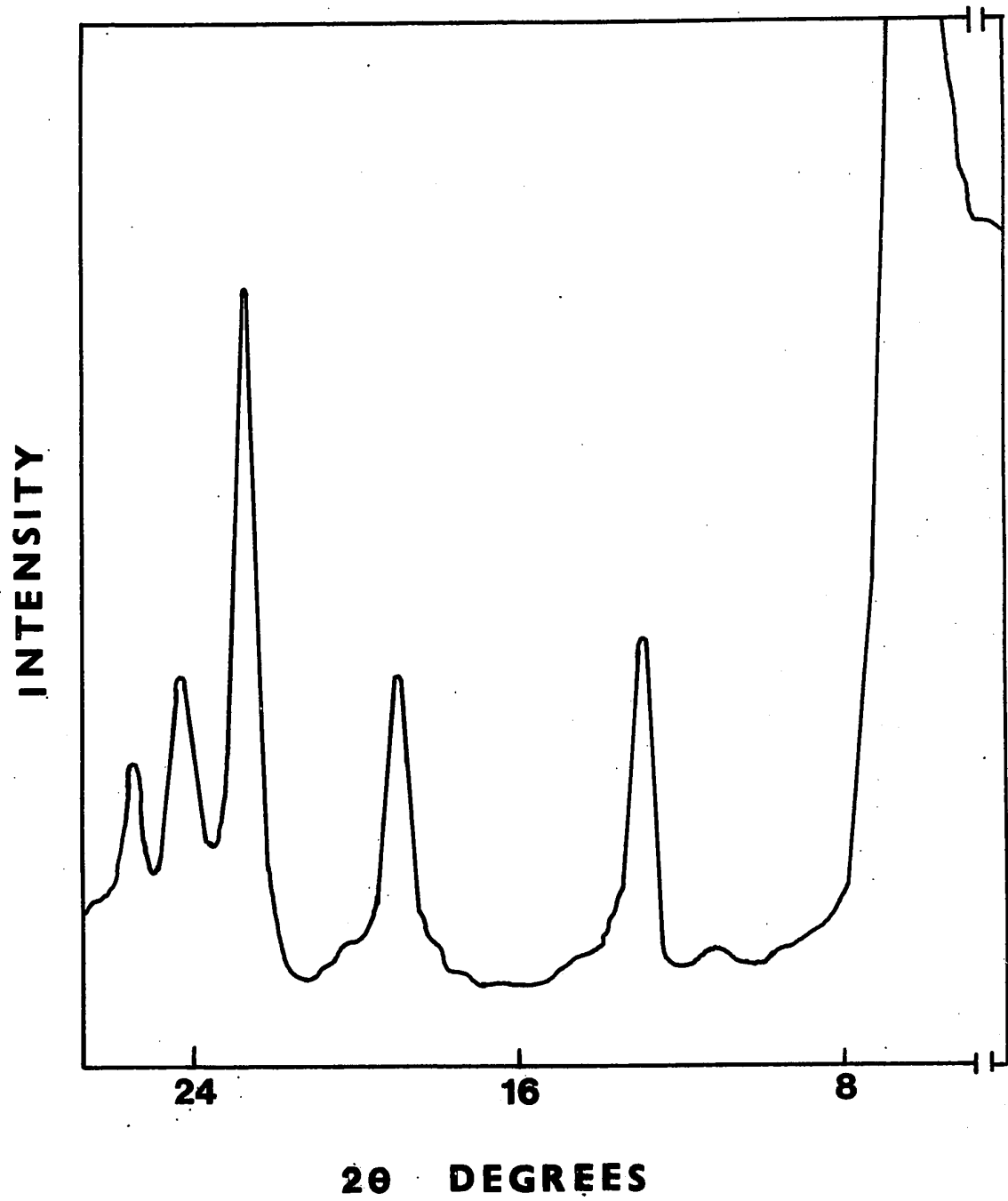


Figure 5. X-ray Diffractogram of Meprobamate Form I

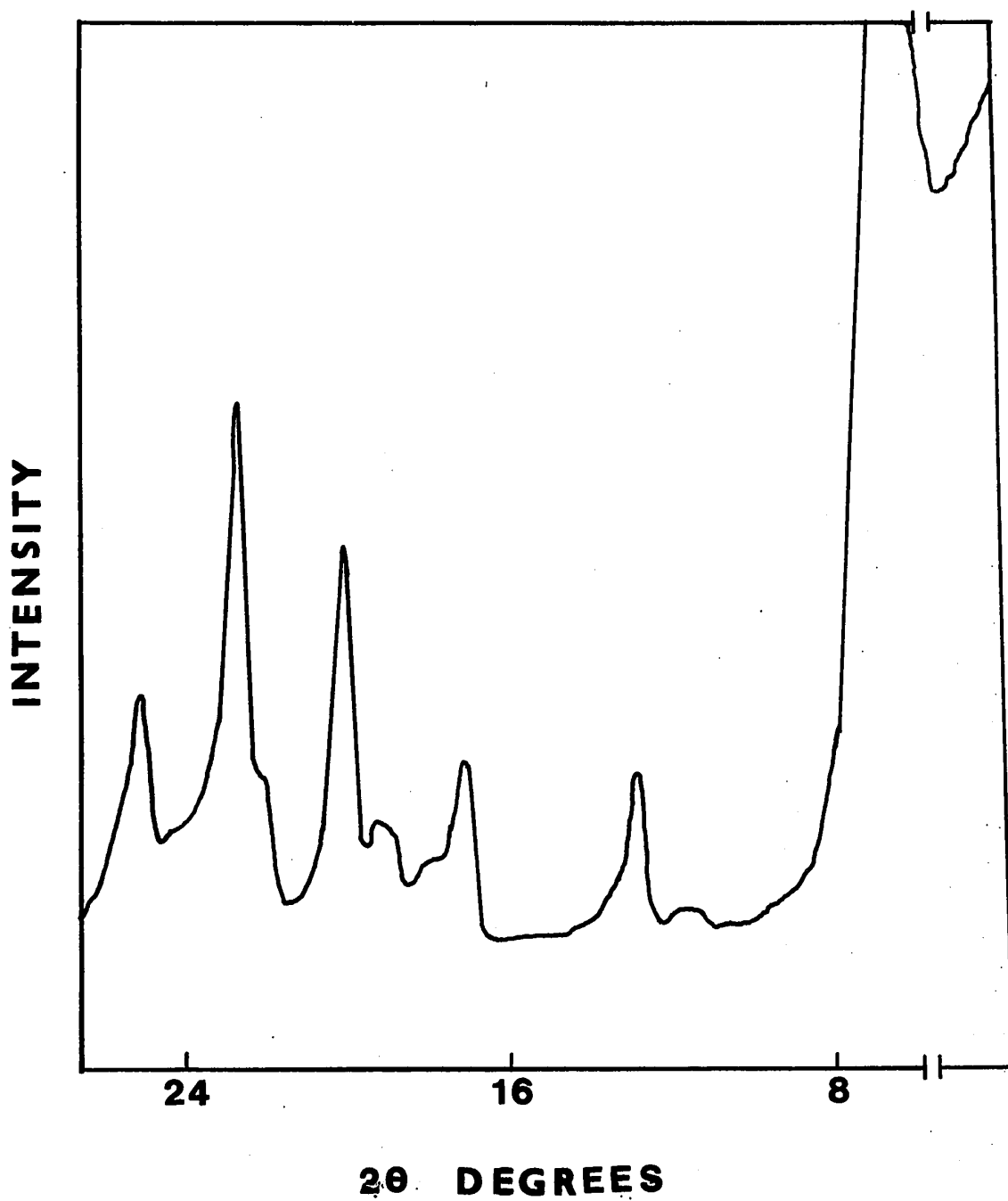


Figure 6. X-ray Diffractogram of Meprobamate Form II

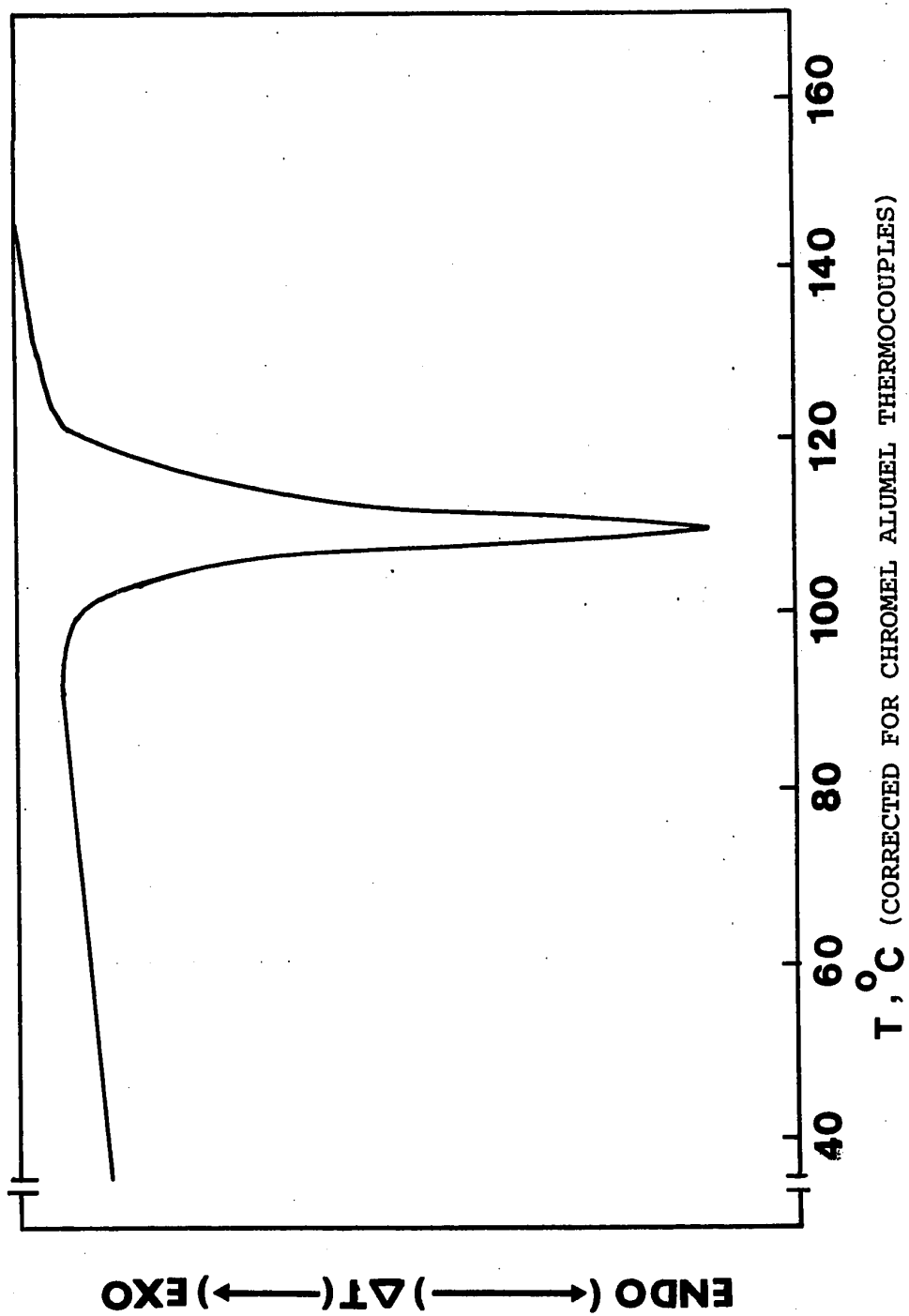


Figure 7. DTA Thermogram of Meprobanate Form I

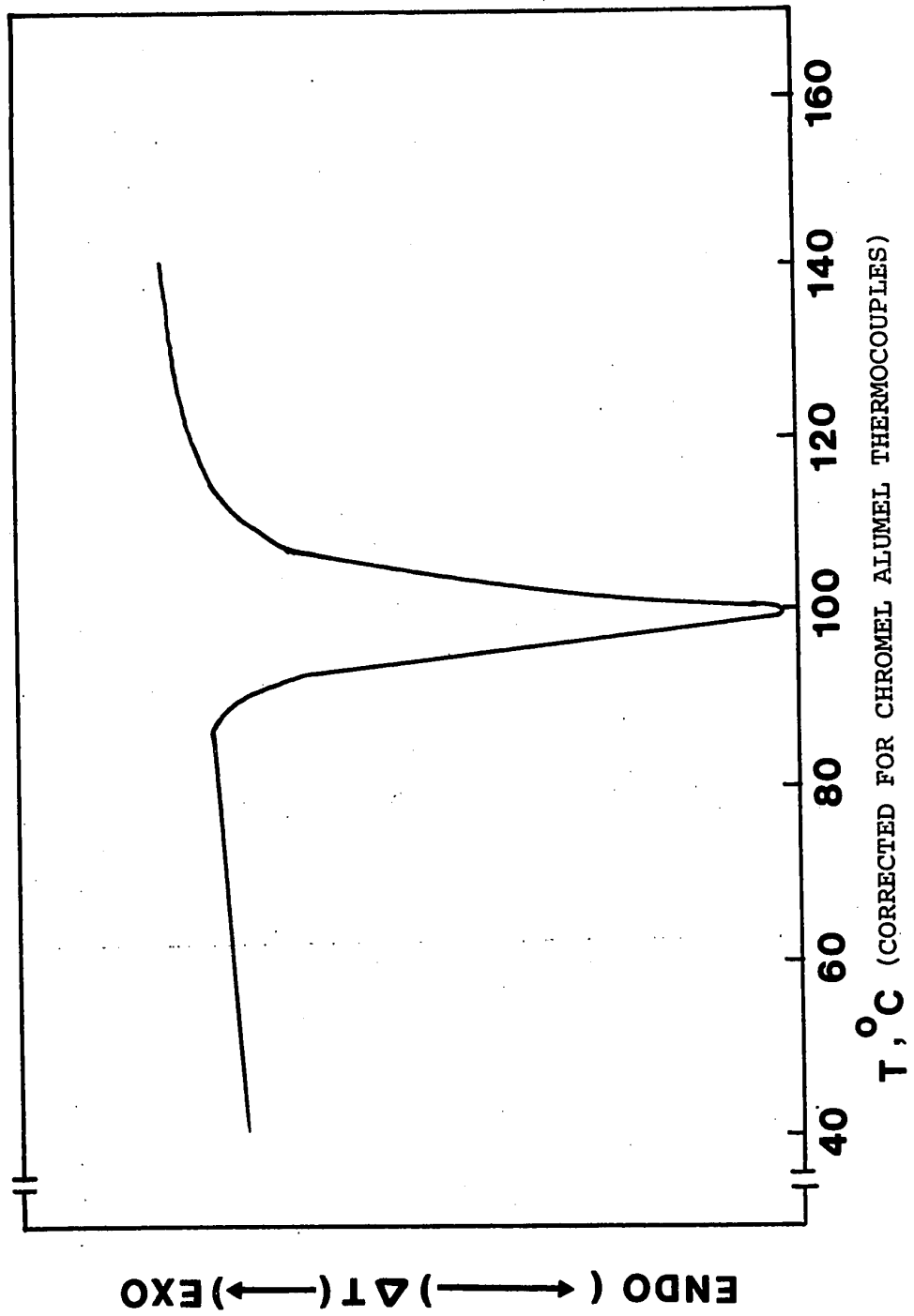


Figure 8. DTA Thermogram of Meprobamate Form II

3. Quantitative Measurements of Heats of Fusion

Calibration of the Calorimeter Cell:

Figure 9 shows the calibration curve for the differential thermal analyser calorimeter cell. The curve is plotted from the calibration coefficients computed for gallium, indium and tin by the following equation (236):

$$E = \frac{\Delta H M a}{A T_s \Delta T_s} \quad (\text{eq. 17})$$

where E = calibration coefficient, $\text{mcal}^\circ\text{C}^{-1} \text{min}^{-1}$;

ΔH = heat of fusion, mcal mg^{-1} ;

M = sample mass, mg;

a = heating rate, $^\circ\text{C min}^{-1}$, $10^\circ\text{C min}^{-1}$;

A = peak area, in^2 ;

T_s = X-axis sensitivity, $^\circ\text{C in}^{-1}$, 20°C in^{-1} (except for tin, 50°C in^{-1});

ΔT_s = Y-axis sensitivity, $^\circ\text{C in}^{-1}$, $0.5^\circ\text{C in}^{-1}$.

The values of fusion temperature and calibration coefficient of gallium, indium and tin are given in Table IV.

Table IV

Fusion Temperature and Calibration Coefficient
of Gallium, Indium and Tin

Material	Fusion Temperature ($^\circ\text{C}$)	Calibration Coefficient ^a ($\text{mcal } ^\circ\text{C}^{-1} \text{min}^{-1}$)
Gallium	30	48.0
Indium	156	58.6
Tin	233	68.4

a Mean of six runs

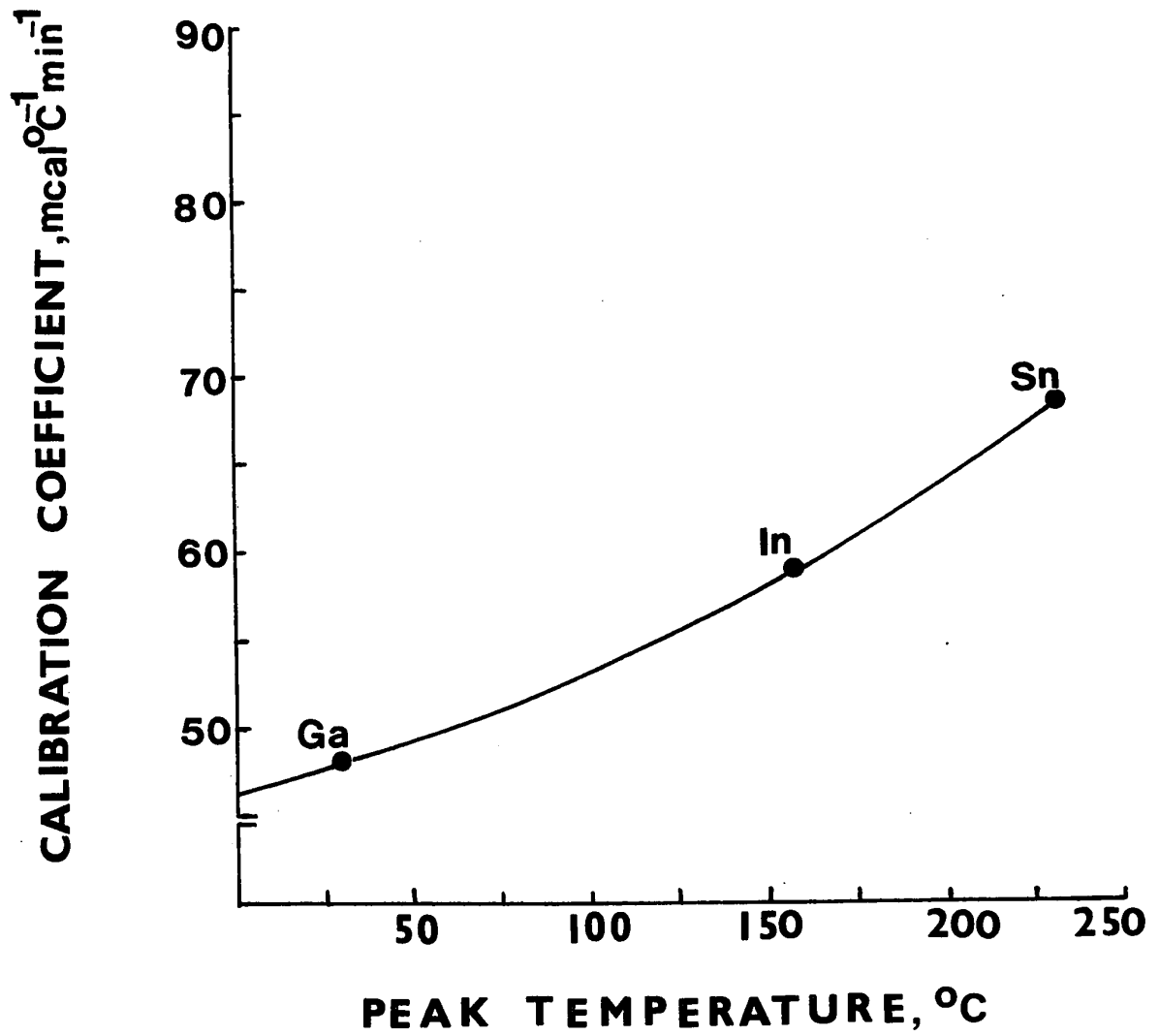


Figure 9. Calibration Curve for the DTA Calorimeter Cell

For calculation of the heats of fusion of sulfathiazole Form II and meprobamate Form I and Form II, the fusion temperatures were determined from the thermograms by extrapolating the fusion endotherms to the pre-fusion base line. The values of the calibration coefficient corresponding to each fusion temperature were obtained from Figure 9.

From the calibration coefficient thus obtained, the heats of fusion for sulfathiazole Form II and meprobamate Form I and Form II were computed by substituting the peak area obtained in the following equation (236).

$$\Delta H = \frac{EA\Delta T_s T_s}{Ma} \quad (\text{eq. 18})$$

where ΔH = heat of fusion, mcal mg^{-1} ;
 E = calibration coefficient, $\text{mcal } ^\circ\text{C}^{-1} \text{min}^{-1}$;
 A = peak area, in^2 ;
 ΔT_s = Y-axis sensitivity, $^\circ\text{C in}^{-1}$, $0.5^\circ\text{C in}^{-1}$;
 T_s = X-axis sensitivity, $^\circ\text{C in}^{-1}$, 20°C in^{-1} ;
 M = sample mass, mg ;
 a = heating rate, $^\circ\text{C in}^{-1}$, $10^\circ\text{C min}^{-1}$.

The results of the differential thermal analysis are given in Table V.

4. Gas-liquid Chromatographic Procedure

Figure 10 shows a typical gas chromatogram of an aqueous extract containing meprobamate and dibutylphthalate (internal standard). Good symmetrical peaks were obtained for both meprobamate and dibutylphthalate. The solvent was ether and eluted rapidly with very little tailing.

Table V

Differential Thermal Analysis Results

	Meprobamate Form I	Meprobamate Form II	Sulfathiazole Form II
Fusion Temp. (°C)	103	94	200
Calibration Co- efficient (mcal °C ⁻¹ min ⁻¹)	53.6	53.0	63.5
Heat of Fusion DTA (Kcal mole ⁻¹)	7.143±0.190	6.061±0.237	6.131±0.300
Heat of Fusion Lit. *(Kcal mole ⁻¹)	-	-	(5.970±0.230)

*Ref. (236)

The optimum conditions for gas-liquid chromatographic analysis were maintained so that a minimum time was required for eluting the drug, while maintaining the resolution and sensitivity. The injection port temperature was set so that at 230°C practically no breakdown of the meprobamate occurred and yet the temperature was high enough to elute the meprobamate and the internal standard in a reasonable time.

The retention time for meprobamate was 2.8 minutes and for dibutylphthalate was 4.5 minutes. The retention time for each drug was the average of three determinations. Sample injections could be made every seven minutes without any apparent effect on quantitation and peak separation.

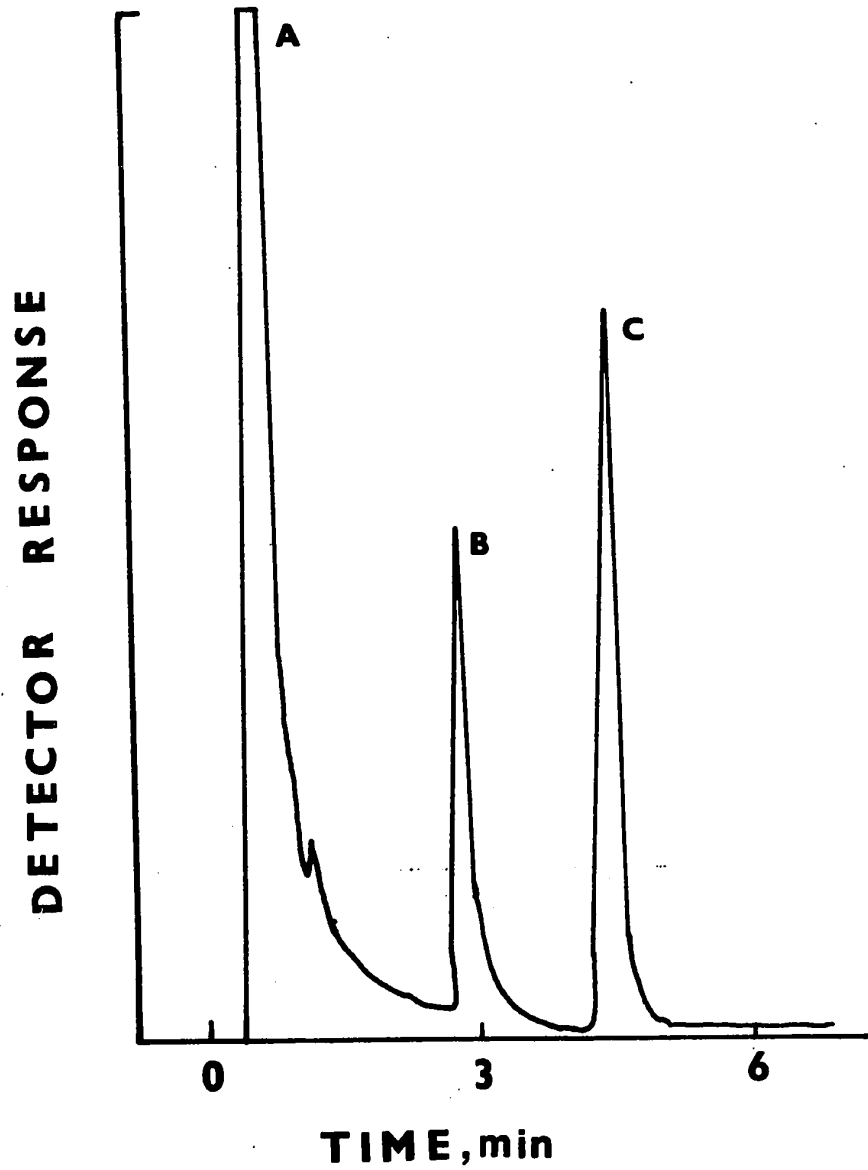


Figure 10. Typical Gas Chromatogram of an Aqueous Extract Containing Meprobamate
A = Solvent (ether); B = Meprobamate;
C = Dibutylphthalate (internal standard)

Extraction Procedure:

The extraction procedure for meprobamate from aqueous solutions was found to be very efficient giving a good recovery of the drug (Table VI).

Table VI
Recovery of Meprobamate from Aqueous Solutions

Meprobamate added (mcg ml ⁻¹)	Recovered (mcg ml ⁻¹)	% Recovery
100	98.0 ^a	98.0
200	199.1 ^b	99.5±2.2 ^c
400	384.3 ^a	96.0

a Mean of three runs

b Mean of eight runs

c ± standard deviation

The blank extraction did not give any peak corresponding to meprobamate.

No loss of meprobamate in distilled water was found, when meprobamate solutions were left at 25°C for one week and at 40°C for three days.

A calibration curve (Figure 11) was prepared for the solutions of meprobamate in distilled water from the values given in Table VII.

The curve is rectilinear over the range 50-400 mcg of meprobamate per ml of solution. This indicates that the relative response of the instrument was linear over the range of concentrations studied. The calibration curve prepared at later times did not show any significant deviation from the original curve.

Table VII

Relationship of the Concentration of Meprobamate
to Peak Area for Meprobamate/Peak Area
for Internal Standard

Concentration of Meprobamate (mcg ml ⁻¹)	Peak Area Meprobamate/ Peak Area of Internal Standard ^a
50	0.262
100	0.440
150	0.677
200	0.867
250	1.093
300	1.275
350	1.508
400	1.715

a Mean of three runs

Calculations of Meprobamate Concentration:

Since the exact volume of injection and the volume of solution after concentration was difficult to control because of the volatility of ether, an internal standard was used to determine the equivalent amount of original sample represented by the peak area.

Dibutylphthalate was found to be satisfactory internal standard, since it elutes shortly after the meprobamate. The concentration of meprobamate was calculated as follows:

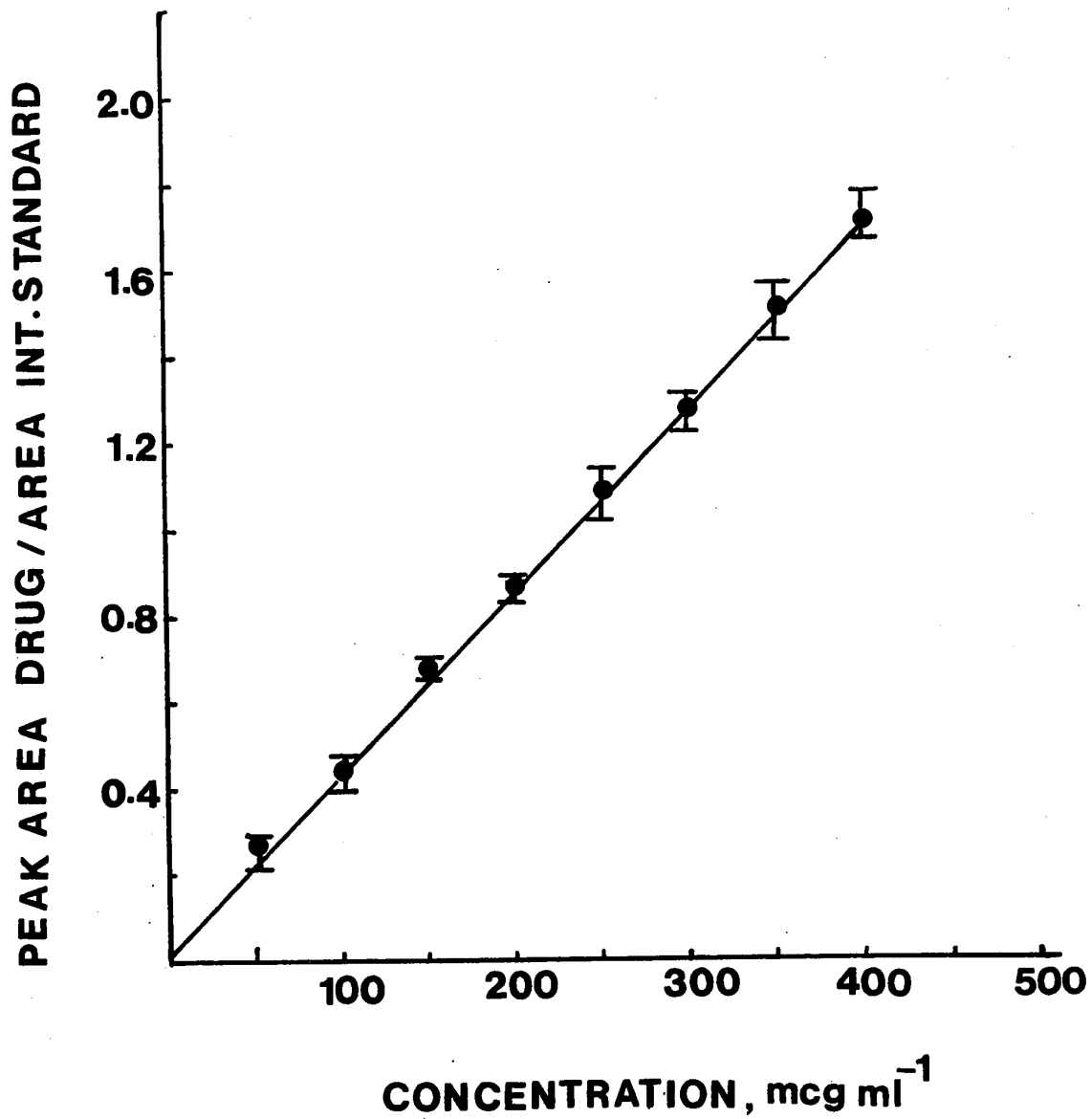


Figure 11. GLC Calibration Curve for Meprobamate in Distilled Water; Ranges indicated thus: I.

$$\text{mg meprobamate} = \frac{P_m}{P_d} \div K \quad (\text{eq. 19})$$

where P_m = peak area of meprobamate;

P_d = peak area of dibutylphthalate;

K = slope determined from the calibration curve

made with injections of meprobamate standard.

5. Solubility and Dissolution Rate Studies

The experimental data for the dissolution rates of meprobamate Form I and Form II, in distilled water, at 25°C are given in Table VIII and shown in Figure 12. The figure shows the concentration of each polymorph in solution as a function of time in the presence of an excess of the solid phase and under constant agitation. It is apparent from the data that Form II has a faster dissolution rate than Form I. The solution obtained at equilibrium from Form II has approximately twice the concentration of that from Form I. Figure 12 also shows that after the maximum concentration is reached, the concentration of Form II falls to that of Form I.

A graph of the data in Table IX for the dissolution of meprobamate Form II, in distilled water at 25°C, 30°C, 35°C and 40°C is shown in Figure 13.

The dissolution behavior of the two forms in distilled water suggests that the maximum values obtained were good approximations of the true solubilities of these materials.

The solubilities of the two forms measured over the temperature range 25°C to 40°C are shown in Table X.

Table IX

Dissolution Rates in Distilled Water
of Meprobamate Form II at 30°C, 35°C and 40°C

Time	Mean Concentration (mg ml ⁻¹) ^a		
	30°C	35°C	40°C
1 min	3.85	4.72	7.09
3 "	5.42	7.87	10.80
5 "	6.59	8.77	12.43
7.5 "	6.67	9.09	12.95
10 "	7.86	10.53	12.42
15 "	8.45	10.62	13.17
20 "	7.89	9.97	12.81
8 hr	6.48	-	8.89
28 "	5.19	5.47	7.30

a Mean of three runs

Table X

Solubilities in Distilled Water of Meprobamate
Form I and Form II at 25°C, 30°C, 35°C and 40°C

Temperature (°C)	Concentration (mg ml ⁻¹)	
	Form II	Form I
25	6.220	3.337
30	8.169	4.251
35	10.575	5.661
40	12.797	7.429

Steady State

Table VIII
Dissolution Rates in Distilled Water
of Meprobamate Form I and Form II at 25°C

Time	Mean Concentration (mg ml ⁻¹) ^a	
	Form I	Form II
1 min	0.75	3.10
3 "	1.57	3.77
5 "	2.88	5.16
7.5 "	2.45	4.90
10 "	2.66	4.90
15 "	3.10	5.10
20 "	3.25	5.31
30 "	3.25	6.12
60 "	-	6.32
2 hr	-	5.63
28 "	3.40	5.20
128 "	3.35	3.61
168 "	3.35	3.62

a Mean of three runs

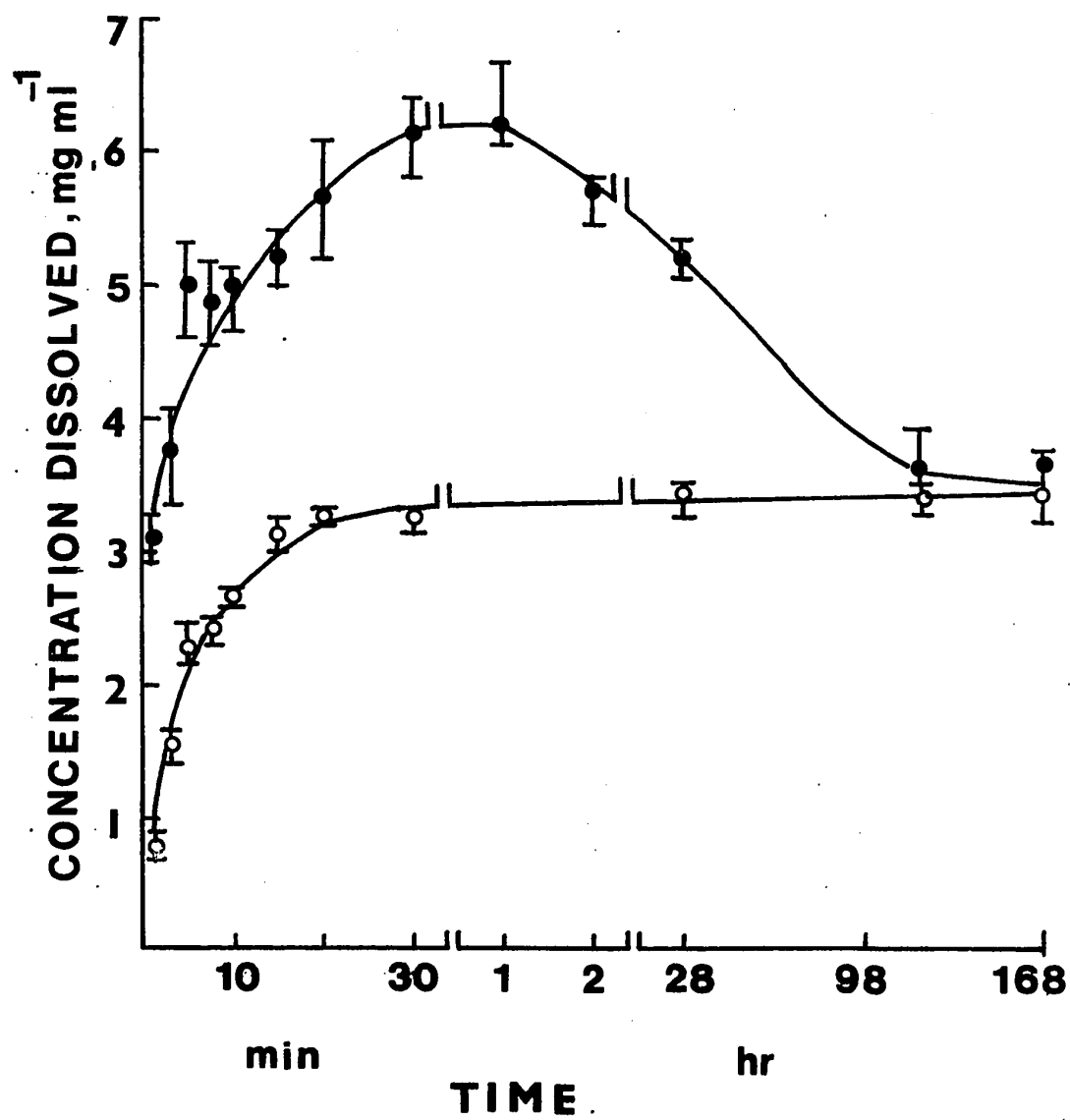


Figure 12. Dissolution Curves for Meprobamate Form I and Form II in Distilled Water at 25°C

Key: o, Form I; ●, Form II; Ranges indicated thus: I.

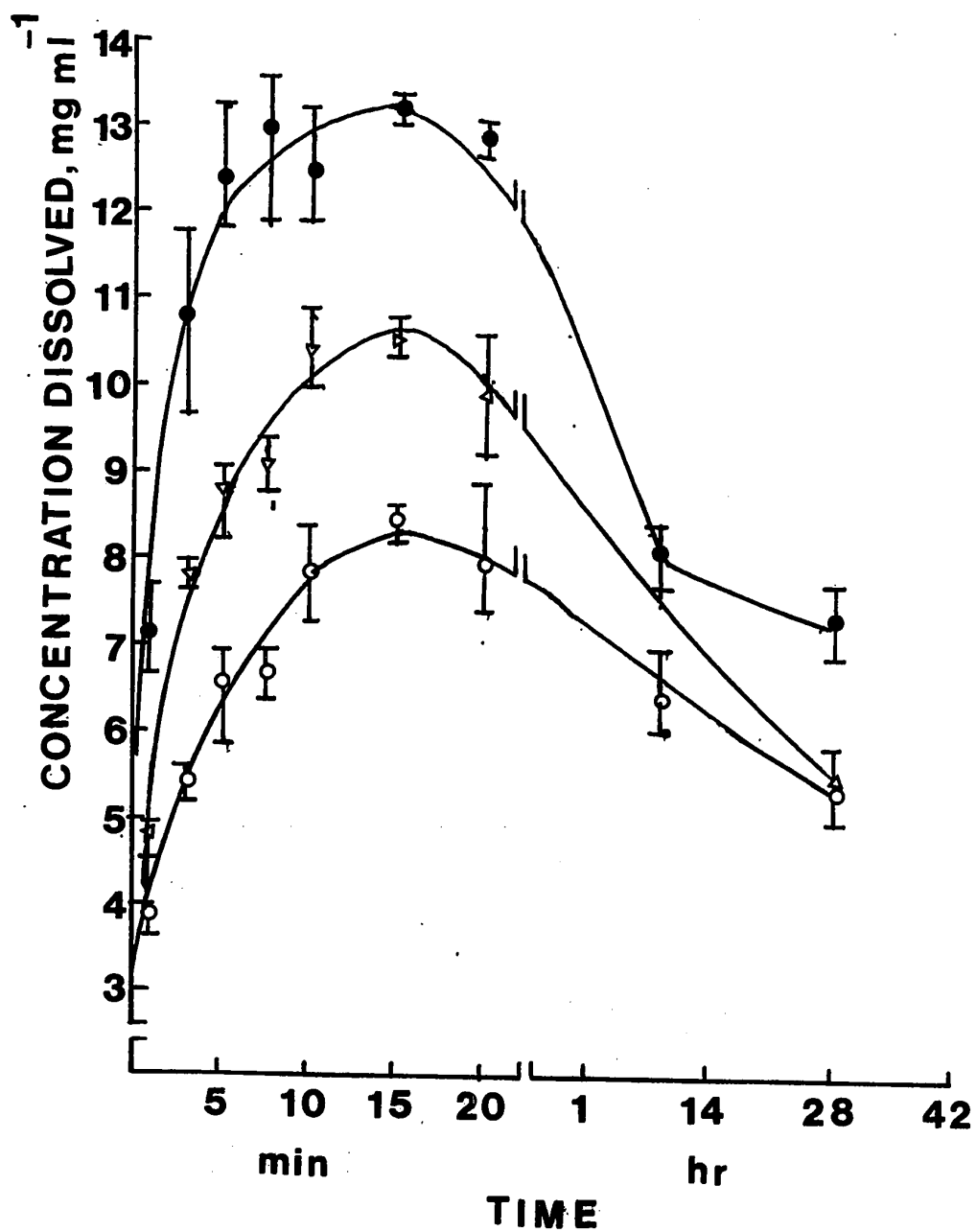


Figure 13. Dissolution Curves for Meprobamate Form II in Distilled Water

Key: ○, 30°C; △, 35°C; ●, 40°C.
 Ranges indicated thus: I.

The solubilities were then calculated in moles per liter of solution and these are shown in a van't Hoff-type plot in Figure 14. It is clear from the figure that a straight line relationship exists in the temperature range of 25°C to 40°C.

Confirmation of the Reversion of Form II to Form I:

The crystalline material obtained, when the solubility of Form II reached that of Form I, was found by the X-ray diffraction analysis to be Form I.

Calculations of the Thermodynamic Properties:

From the solubility measurements, it is possible to calculate the thermodynamic properties involved in the transformation of the metastable form to the stable one.

Heats of Solution:

The heats of solution for both the forms of meprobamate were calculated from the slopes of the lines in van't Hoff's plot (Figure 14). The regression lines gave slopes of -1975 and -2180 for the lines of Form II and Form I respectively. The slope of each line according to van't Hoff's equation is equal to $-\Delta H/2.303 R$. From this the ΔH is readily calculated by the following equation (279).

$$\Delta H = -2.303 R \times \text{slope} \quad (\text{eq. 20})$$

where ΔH = heat of solution;

R = gas constant (1.987 cal mole⁻¹ deg⁻¹).

From the slopes the heats of solution for both the forms were calculated. The values of heats of solution are

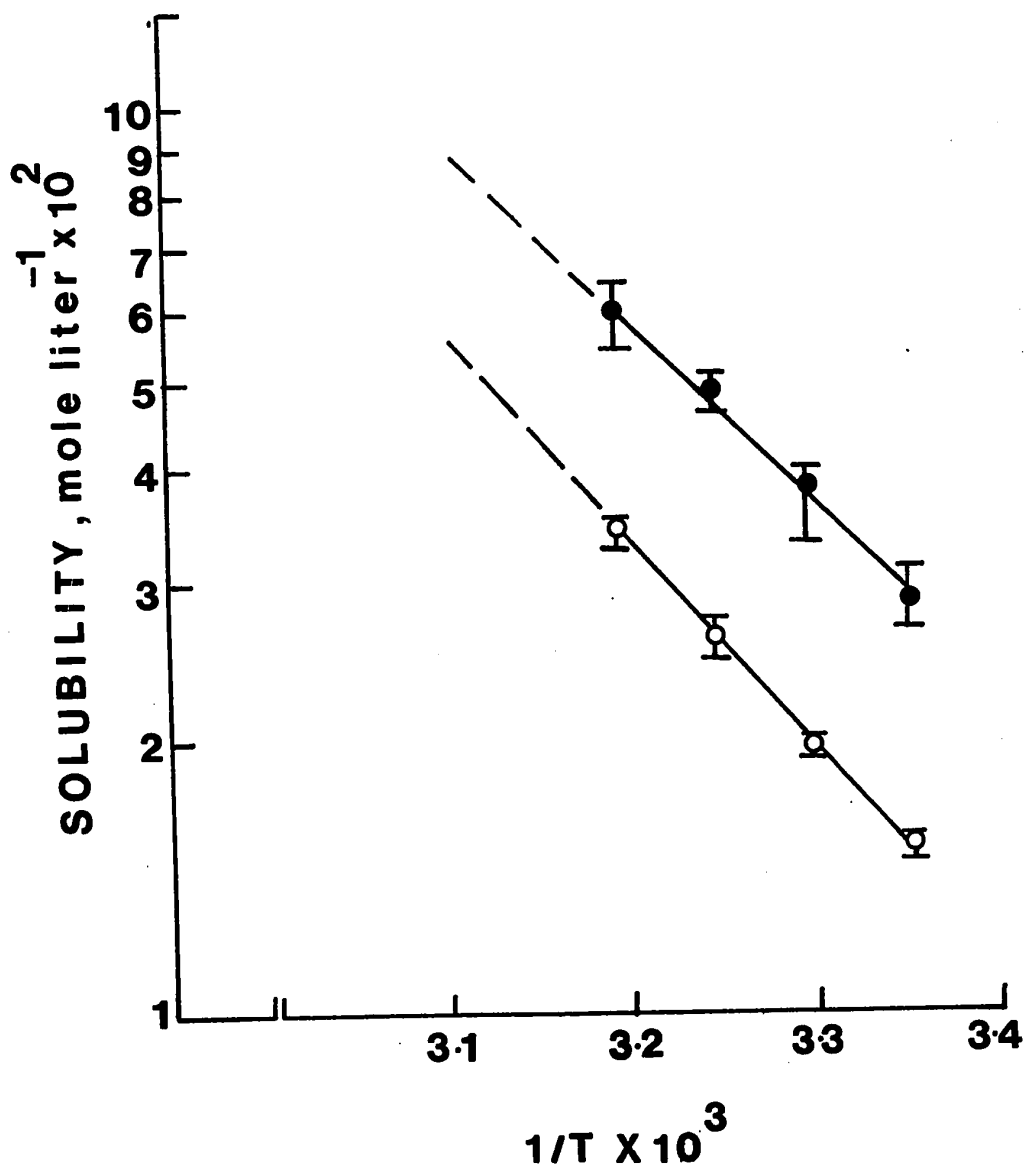


Figure 14. The van't Hoff Type Plot for Meprobamate Form I and Form II
Key: ○, Form I; ●, Form II.
Ranges indicated thus: I.

given in Table XI.

Free Energy Difference:

At constant temperature and pressure the free energy difference, ΔF_T , between the polymorphs I and II was calculated by the following equation (246):

$$\Delta F_T = RT \ln \frac{C_s \text{ Form I}}{C_s \text{ Form II}} \quad (\text{eq. 21})$$

where C_s = solubility of the polymorph at a particular temperature, T.

This equation relates the solubility, C_s , to the free energy differences involved in the conversion of the polymorph II to polymorph I at a particular temperature.

The Enthalpy Change:

The enthalpy change for the transition of Form II to Form I can be calculated by subtracting the heat of solution of Form I from that of Form II. The enthalpy change in the transition from Form II to Form I, that is $\Delta H_{II \rightarrow I}$, is $-939 \text{ cal mole}^{-1}$.

The Entropy Change:

The entropy change, ΔS_T , for the transition of Form II to Form I at a particular temperature, T, can be calculated by the following equation (246):

$$\Delta S_T = \frac{\Delta H_{II \rightarrow I} - \Delta F_T}{T} \quad (\text{eq. 22})$$

The value computed for the reversion of Form II to Form I at 25°C is given in Table XI.

The transition temperature for the reversion of Form II

Table XI

Thermodynamic Values Calculated for
Meproamate Form I and Form II

Form	Transition Temp. (°C) to Form I	Heat of Solution (Kcal mole ⁻¹)	ΔF_T (Cal mole ⁻¹)	ΔS_{298} (e.u.)	ΔS_{Trans} (e.u.)
I	-	9.975	-	-	-
II	186	9.036	-369	-1.91	-2.05

to Form I corresponds to the temperature at which the solubilities of the two forms are equal (246). The transition temperature is found by extrapolating the lines in the van't Hoff's plot and taking the temperature where both the lines meet. The transition temperature for this system is 186°C.

At the transition temperature the reversion of Form II to Form I, ΔF_T , is equal to zero and the entropy change, ΔS_{Trans} , can be calculated by the equation (246):

$$\Delta S_{Trans} = \frac{\Delta H_{II \rightarrow I}}{T} \quad (\text{eq. 23})$$

For meproamate ΔS_{Trans} was found to be -2.05 e.u. at 25°C.

6. Isergonic Relationship in Polymorphic Phase Reversion and Anhydrate to Hydrate Changes

Figure 15 shows the isergonic plot of the relation between enthalpy and entropy changes in polymorphic and hydrate transformations. This plot is constructed from the literature

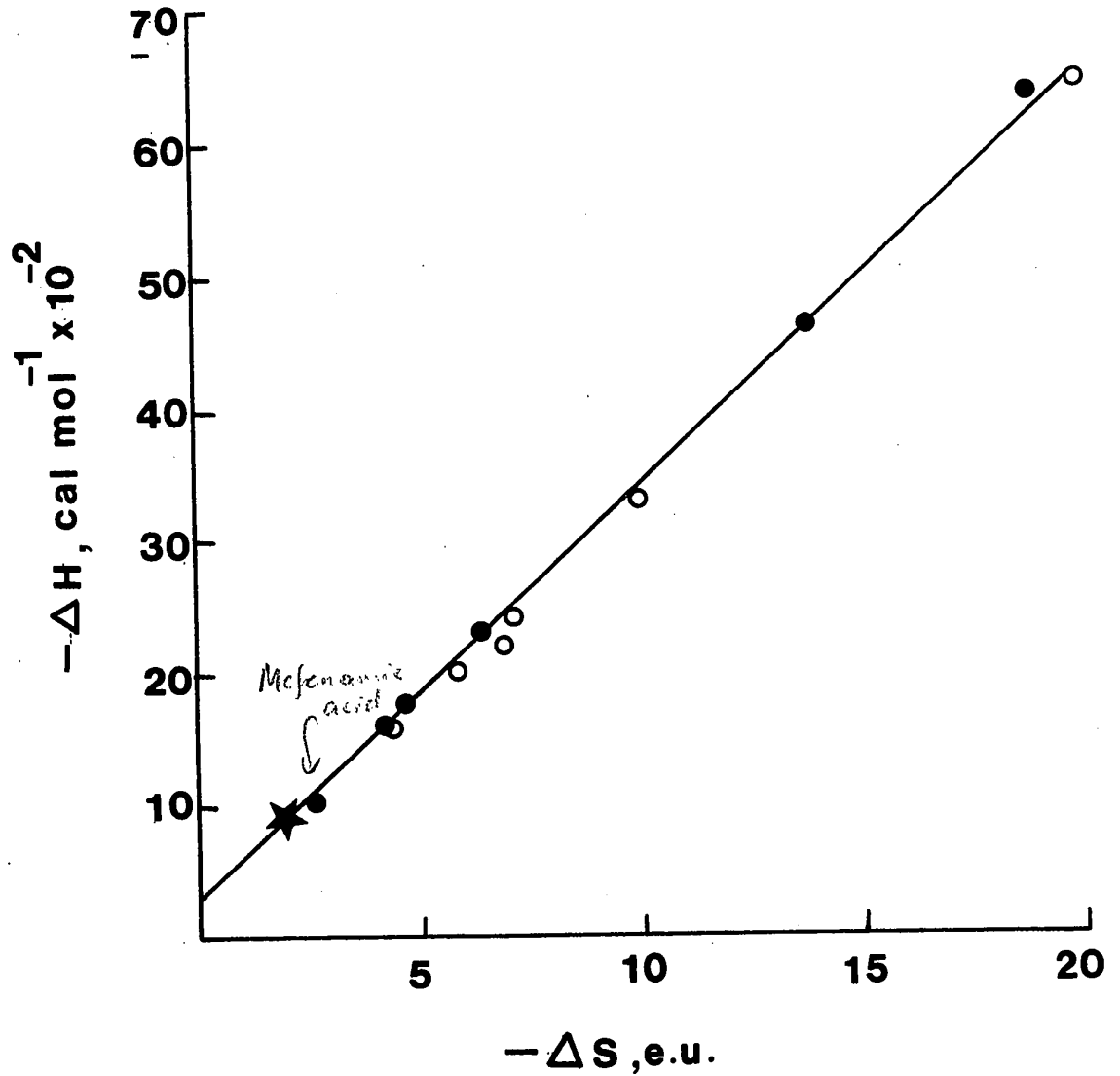


Figure 15. Isergonic Plot of the Relation Between Enthalpy and Entropy Changes in Polymorphic and Hydration Phase Transformations

Key: ●, polymorphic changes;
○, hydration changes; ★, this work.

values (261) of enthalpy and entropy changes for polymorphic phase reversion and for changes from the anhydrous to the hydrated form together with the value obtained for meprobamate and can be fitted in a straight line relationship: $-\Delta H = -203.941 - 316.619 \Delta S$, with a correlation coefficient of 0.997 with the theoretical correlation coefficient ($P' = 0.05$) of 0.55.

B. MULTICHANNEL COULTER COUNTER ASSEMBLY FOR DISSOLUTION RATE STUDIES

1. Size Distribution Measurements of Ragweed Pollen Grains and Latex Particles Using a Microscope

The results of the measurement of ragweed pollen grains are given in Table XII.

By plotting the cumulative number of oversize particles against the diameter, the median diameter of 19.06 μ was obtained.

The corresponding volume frequency distribution was calculated using the following equation:

$$V = \frac{\pi D^3}{6} \quad (\text{eq. 24})$$

where V = volume, μ^3 ; D = diameter, μ .

Table XII
Microscopic Measurement Data for Ragweed Pollen Grains

Diameter range (μ)	Number of Particles	Cumulative Number Oversize
14-14.9	3	400
15-15.9	12	397
16-16.9	29	385
17-17.9	47	356
18-18.9	93	309
19-19.9	100	216
20-20.9	57	116
21-21.9	31	59
22-22.9	20	28
23-23.9	6	8
24-24.5	2	2

The results of the volume frequency distribution are given in Table XIII.

Table XIII
Size Distribution of Ragweed Pollen Grains
with the Microscopic Method

Volume (μ^3)	Cumulative Number % Oversize	Probit Cumulative % Oversize
1437	100.00	
1768	99.25	7.43
2146	96.25	6.77
2574	89.00	6.23
3055	77.25	5.75
3593	54.00	5.10
4190	29.00	4.45
4851	14.75	3.96
5578	7.00	3.52
6373	2.00	2.95
7241	0.50	2.25

The volume frequency distribution for the latex particles was obtained using a similar method of calculation, and the median volume was found to be $3.604 \mu^3$. The results are given in Table XIV.

Table XIV
Size Distribution of Latex Particles
with the Microscopic Method

Volume (μ^3)	Cumulative Number % Oversize	Probit Cumulative % Oversize
1.437	100.00	
2.145	94.25	6.58
2.573	84.50	6.02
2.806	79.50	5.82
3.054	71.50	5.57
3.315	59.75	5.25
3.592	50.75	5.02
3.883	40.75	4.77
4.190	30.00	4.48
4.512	22.00	4.23
4.851	17.00	4.04
5.205	14.75	3.96
5.577	9.37	3.71
6.373	4.75	3.34

2. Size Distribution Measurements of Ragweed Pollen Grains and Latex Particles with the Coulter Counter Using the Conventional Method

Calibration of the Coulter Counter:

Table XV gives the counts of ragweed pollen grains with two pairs of threshold settings, using a 100 μ aperture tube and 500 μ l sample.

Table XV

Data for Calibration of the Coulter Counter
Using Ragweed Pollen Grains

Threshold Settings		Number of Particles	Average Number of Particles
t_L	t_U		
10	70	28832, 28845, 29501, 28982.	29040
49.5	70	14449, 14221, 14697, 14457.	14456

t_L = lower threshold setting;

t_U = upper threshold setting.

The particle counts obtained with a lower threshold setting of 49.5 are very close to half the total number of particles in the sample of suspension. The calibration constant, K, was then computed using the following equation:

$$K = \frac{V}{IA t_L} \quad (\text{eq. 25})$$

where K = calibration constant;

V = median volume, 3627 μ^3 ;

I = aperture current setting, 1;

A = amplification setting, 16;

t_L = lower threshold setting at the half count, 49.5.

The calibration constant, K, for the 100 μ aperture tube was calculated to be 4.58.

After the calibration constant, K, was determined, the particle volume was then calculated by the following equation:

$$V = K \cdot I \cdot A \cdot t_L \quad (\text{eq. 26})$$

Similarly, the calibration constant for the 50 μ aperture tube was determined using latex particles of median volume 3.604 μ^3 . The calibration constant, K, was calculated to be 0.452.

Size Analysis of Standard Materials:

Typical data for the size distribution of pollen grains are given in Table XVI, where

N = raw counts;

N' = final count after corrections for coincidence loss and background count;

V_L = volume corresponding to the lower threshold setting.

Correction for coincidence loss was made using the following equation (150):

$$N_c = P \left(\frac{N^0}{1000} \right)^2 \quad (\text{eq. 27})$$

where N_c = number of coincidence passages;

P = coincidence factor;

Table XVI

Coulter Counter Data and Number % Calculations

Sample—Ragweed pollen grains. Aperture diameter, 100 μ ; Electrolyte, aqueous solution of sodium chloride (0.9%); Manometer volume, 500 μ l; Dispersing agent, Isoterge; Calibration data, I = 1, A = 16, t_L = 49.5; Calibration constant, 4.58.

t_L	t_U	I	A	N	Average N	N'	V_L	$\Sigma N'$	Number % Oversize
28	70	4	16	5	4	5	8207	5	0.07
25	28	4	16	11	9	10	7328	15	0.20
43.5	50	2	16	28	31	30	6375	45	0.61
38	43.5	2	16	28	25	27	5569	72	0.98
33	38	2	16	80	78	79	4836	151	2.04
28.5	33	2	16	898	848	873	4177	1026	13.88
24.5	28.5	2	16	2740	2679	2710	3591	3754	50.80
21	24.5	2	16	2431	2378	2404	3078	6172	83.52
17.5	21	2	16	1002	989	996	2565	7170	97.02
15	17.5	2	16	119	131	125	2198	7295	98.71
12	15	2	16	50	43	46	1759	7341	99.34
20	24	1	16	23	25	24	1466	7365	99.66
16	20	1	16	15	19	17	1172	7382	99.89
12.5	16	1	16	8	7	8	916	7390	100.00

N° = observed count.

The coincidence factor, P , is derived by the following equation:

$$P = 2.5 \left(\frac{500}{V}\right) \left(\frac{D}{100}\right)^3 \quad (\text{eq. 28})$$

where D = aperture diameter, μ ;

V = sample volume, μl .

The true count is equal to $N_c + N^{\circ}$ and N' in Table XVI is equal to $N_c + N^{\circ}$ - background count.

The size distribution data for ragweed pollen grains and latex particles using the Coulter counter are given in Tables XVII and XVIII respectively.

3. Size Distribution Measurements of Ragweed Pollen Grains and Latex Particles Using the Multichannel Coulter Counter Assembly

Figure 16 shows the differential frequency distribution obtained for latex particles, during a 5 second counting period. The analyser was adjusted so that the channel number one corresponded to a particle volume of approximately zero. The channel number was thus proportional to particle volume. The total number of counts within a given channel is represented by a point on the differential frequency distribution curve.

Coincidence corrections were made as follows in two parts: some loss of counts by coincidence occurred at the multichannel analyser. This occurred when a second pulse arrives within the dead-time (about 18 micro seconds) of the

Table XVII
 Size Distribution of Ragweed Pollen Grains
 Using the Coulter Counter

Volume (μ^3)	Cumulative Number % Oversize ^a	Probit Cumulative % Oversize
916	100.00	
1172	99.88	8.06
1466	99.63	7.68
1759	99.28	7.45
2198	98.69	7.22
2565	97.07	6.90
3078	83.67	5.98
3591	50.81	5.02
4177	14.03	3.92
4836	2.09	2.97
5569	1.03	2.67
6375	0.66	2.54

a Mean of three runs

Table XVIII
Size Distribution of Latex Particles
Using the Coulter Counter

Volume (μ^3)	Cumulative Number % Oversize ^a	Probit Cumulative % Oversize
1.813	100.00	
2.266	99.20	7.41
2.719	97.26	6.92
3.172	79.60	5.83
3.626	49.25	4.98
4.079	24.79	4.32
4.532	13.73	3.91
5.212	6.75	3.51
5.665	2.80	2.90

a Mean of three runs

analyser. The percentage of counts lost in this way was read on the dead-time meter on the analyser, so that the recorded counts were corrected for the lost counts. For the latex particles the dead time was about 10% and the counts were corrected accordingly. Corrections for primary coincidence loss at the orifice were made, based upon the new total counts. For latex particles using a 50 μ orifice, the primary coincidence loss was about 3.5%.

The typical data for the size distribution of latex particles are illustrated in Table XIX. The data are taken from Figure 16 and include counts up to channel number 42, but exclude the doublets and triplets.

Since the background count was negligible, correction was not made in calculating the size distribution.

The cumulative counts were plotted against the channel number and are shown in Figure 17. The median volume is at channel number 27, and corresponds to $3.604 \mu^3$. The volume corresponding to each channel number was then calculated.

The results of the size distribution for latex particles as the number % of oversize particles are given in Table XX.

Similarly the size distribution was obtained with the ragweed pollen grains. For ragweed pollen grains the dead-time was about 3.5% and primary coincidence loss was less than 1%. The results of the size distribution of ragweed pollen grains are given in Table XXI.

Figure 18 shows the size distributions of latex particles using the three methods. Cumulative counts of oversize

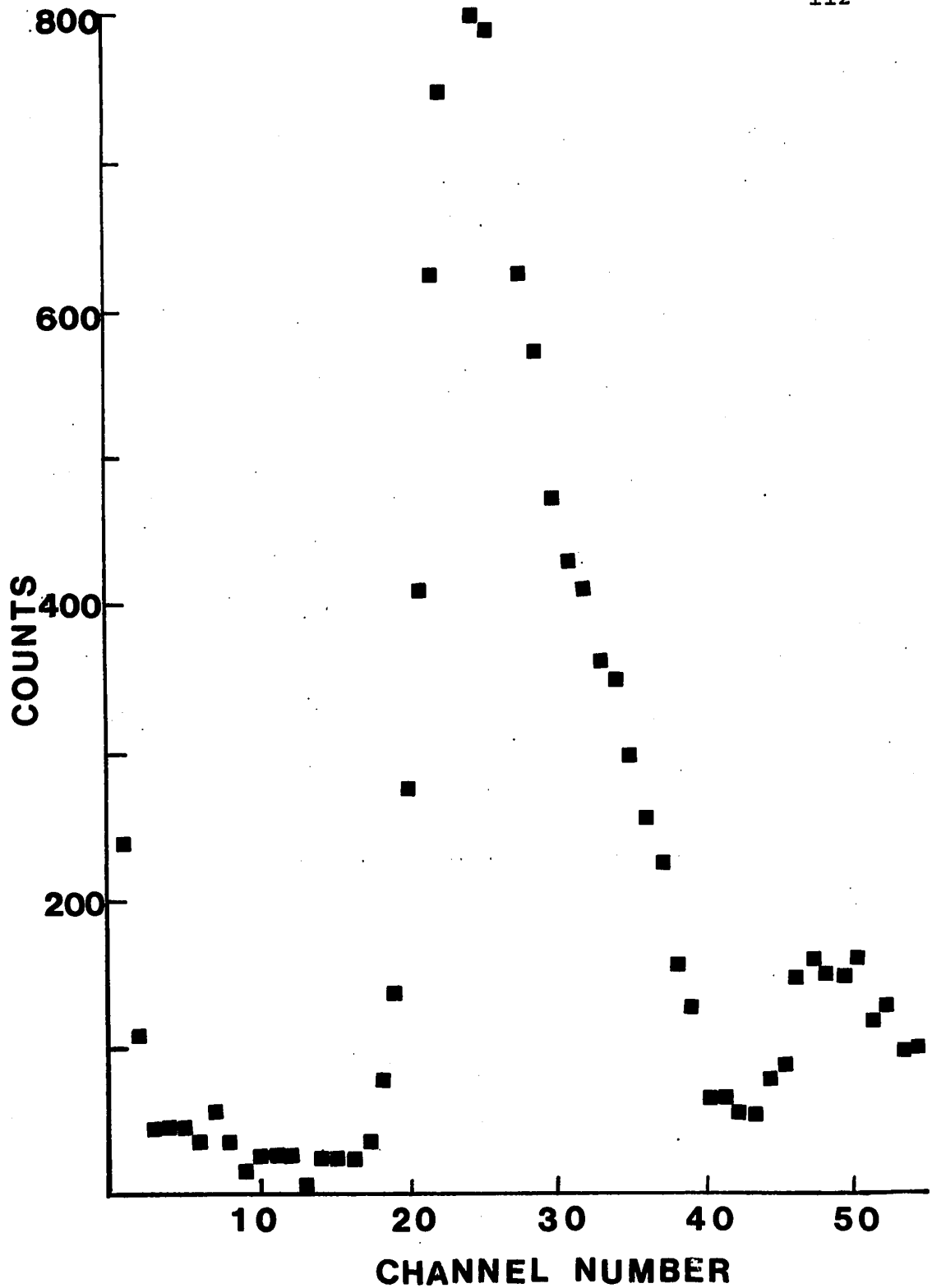


Figure 16. Differential Frequency Distribution Obtained for Latex Particles, Using the Multichannel Coulter Counter Assembly

Table XIX

Data for Size Distribution of Latex Particles
 Illustrating the Calibration of
 Multichannel Coulter Counter Assembly

Channel Number	N	N'	$\Sigma N'$	N''	$\Sigma N''$
42	50	55	55	57	57
41	60	66	121	68	125
40	60	66	187	68	193
39	120	132	319	137	330
38	150	165	484	171	501
37	225	245	729	254	755
36	255	281	1010	291	1046
35	295	325	1335	336	1382
34	350	385	1720	398	1780
33	360	396	2116	410	2190
32	410	451	2567	467	2657
31	430	463	3030	483	3140
30	470	517	3547	535	3675
29	570	627	4174	649	4324
28	620	682	4856	706	5030
27	670	737	5593	763	5793
26	785	863	6456	893	6686
25	795	875	7331	906	7592
24	850	935	8266	968	8560
23	745	819	9085	848	9408
22	620	682	9767	706	10114

continued

Table XIX - continued

Channel Number	N	N'	$\Sigma N'$	N''	$\Sigma N''$
21	410	451	10218	467	10581
20	275	303	10521	314	10895
19	135	149	10670	154	11049
18	70	77	10747	80	11129
17	30	33	10780	34	11163

N = raw count corresponding to the given channel number;

N' = count after correction for coincidence loss at multichannel analyser, 10%;

N'' = true count after correction for coincidence at multichannel analyser and primary coincidence.

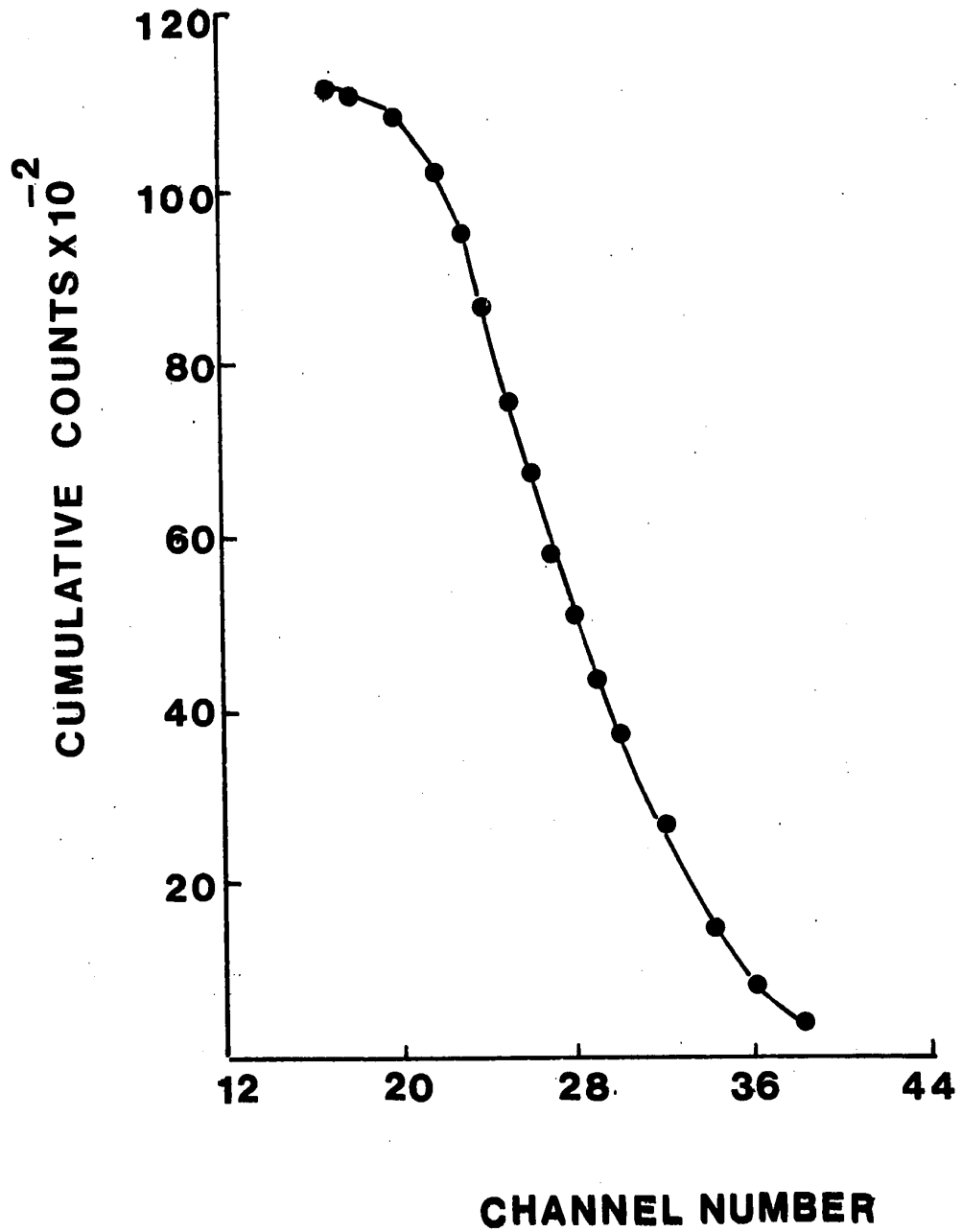


Figure 17. Plot of Cumulative Counts Obtained for Latex Particles Against the Channel Number

Table XX
 Size Distribution of Latex Particles
 Using Multichannel Coulter Counter Assembly

Volume (μ^3)	Cumulative Number % Oversize ^a	Probit Cumulative % Oversize
2.25	100.00	
2.78	95.50	6.69
3.05	85.19	6.04
3.18	77.16	5.74
3.31	68.30	5.48
3.44	59.88	5.25
3.58	51.90	5.05
3.71	44.90	4.87
3.84	38.61	4.71
3.98	32.88	4.56
4.11	28.10	4.42
4.24	23.87	4.29
4.37	19.88	4.15
4.50	16.26	4.01
4.64	13.02	3.87

a Mean of three runs

Table XXI
 Size Distribution of Ragweed Pollen Grains
 Using the Multichannel Coulter Counter Assembly

Volume (μ^3)	Cumulative Number % Oversize ^a	Probit Cumulative % Oversize
2176	100.00	
2499	99.37	7.49
2902	91.37	6.36
3143	79.88	5.84
3385	67.12	5.44
3546	55.60	5.14
3627	49.37	4.98
3708	43.26	4.83
3869	31.98	4.53
4030	21.62	4.21
4352	8.12	3.60

a Mean of three runs

particles were plotted against the particle volume using the probit transformation of the ordinate scale. The distributions for latex particles obtained from the Coulter counter methods are in agreement, showing that no loss of proportionality of pulses has occurred through the use of the interface circuit. The size distribution of latex particles based upon the microscopic measurement of a relatively small number of particles showed a fair agreement with these methods. The standard deviations of the diameter of the latex particles were found to be 0.13μ by the Coulter counter methods and 0.19μ by the microscopic method.

Figure 19 shows the size distributions of ragweed pollen grains using the three methods. Agreement is excellent between the size distributions obtained with the two Coulter counter methods. The distributions agree well with the microscopic method.

For the ragweed pollen grains the standard deviations of the particle diameters were found to be 1.01μ by the Coulter counter methods and 1.42μ by the microscopic method.

4. Size Distribution Measurements of Micronized Hydrocortisone Acetate and Griseofulvin

The size distributions of micronized hydrocortisone acetate using the Coulter counter in the conventional mode and the multichannel Coulter counter assembly are given in Tables XXII and XXIII respectively. The results are plotted in Figure 20.

Agreement between the two methods is good. The difference

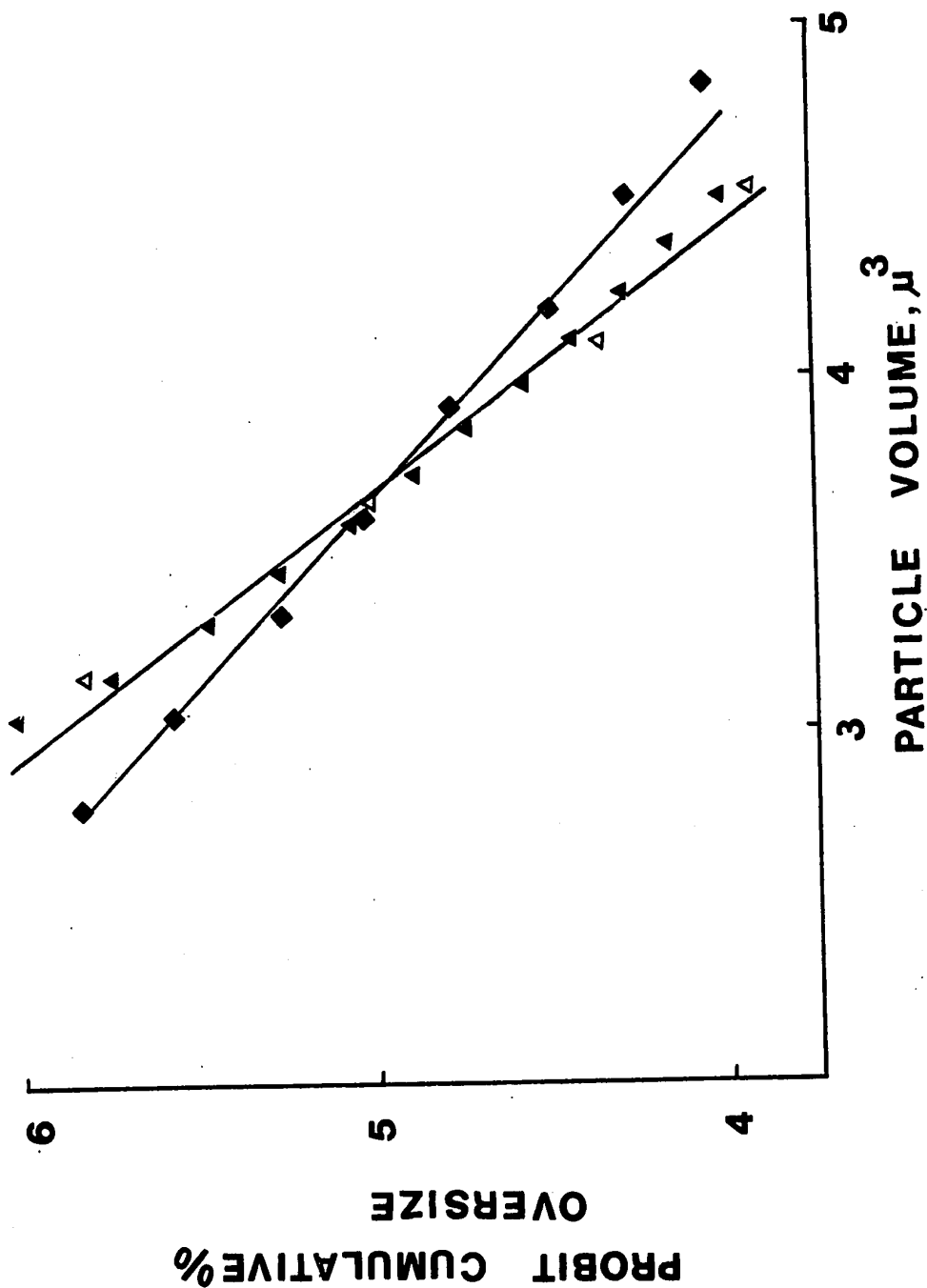


Figure 18. The Size Distributions of Latex Particles
 Key: \blacksquare , Microscopic Measurement; \triangle , Coulter Counter; \blacktriangle , Multichannel Coulter Counter Assembly.

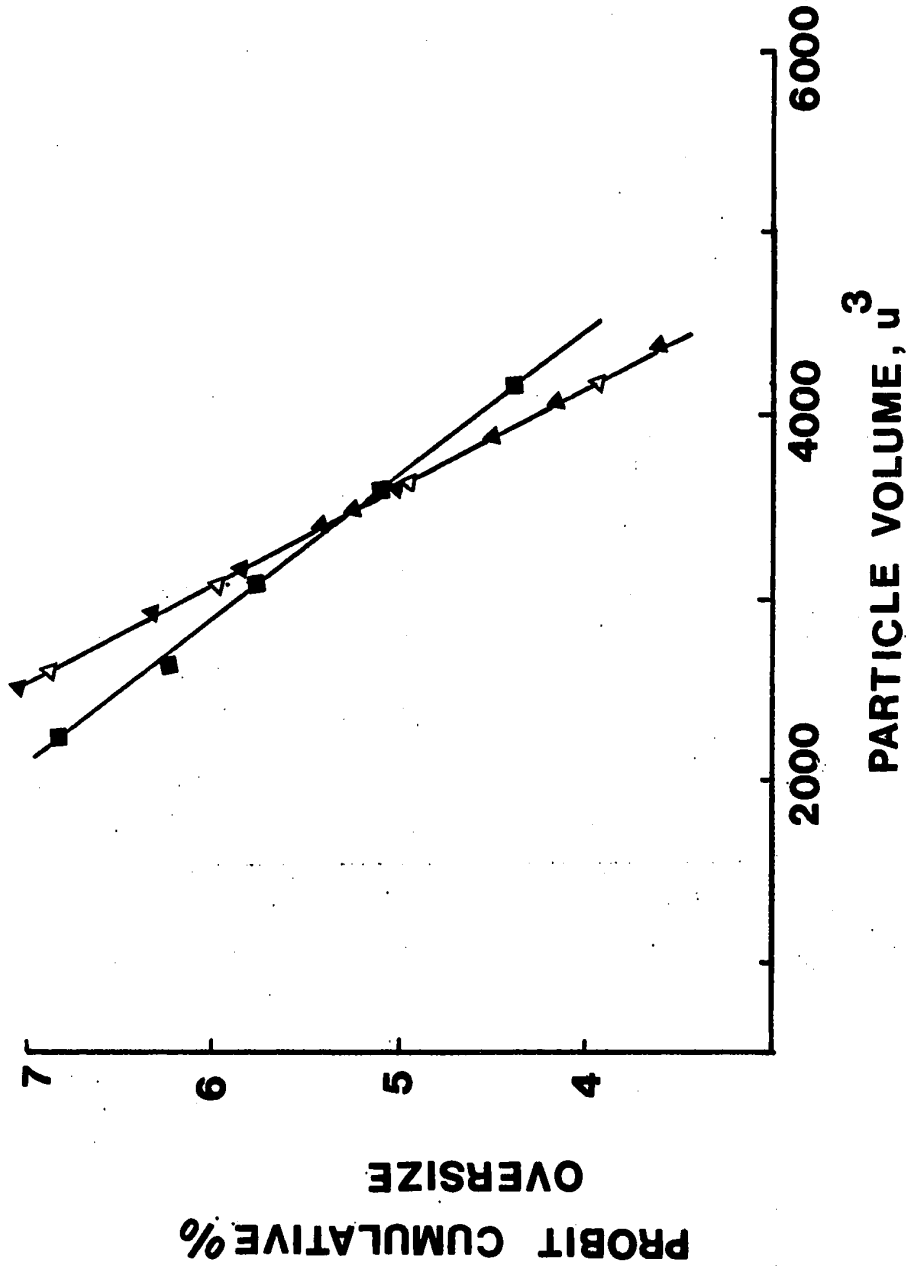


Figure 19. The Size Distributions of Ragweed Pollen Grains
 Key: ■, Microscopic Measurement; Δ, Coulter Counter; ▲, Multichannel Coulter Counter Assembly.

Table XXII
Size Distribution of Micronized Hydrocortisone
Acetate Using the Coulter Counter

Volume (μ^3)	Cumulative Number & Oversize ^a
1.70	100.00
3.39	95.92
4.52	89.13
5.65	83.39
6.78	77.12
9.04	66.07
11.13	56.32
13.50	48.52
15.82	41.72
18.12	36.78
20.38	32.51
22.65	28.11
45.30	7.99

^a Mean of three runs

Table XXIII
Size Distribution of Micronized Hydrocortisone
Acetate Using the Multichannel
Coulter Counter Assembly

Volume (μ^3)	Cumulative Number & Oversize ^a
3.93	100.00
4.50	91.77
5.45	84.62
6.06	78.81
7.57	68.09
9.09	59.89
10.60	52.04
12.12	46.19
15.14	36.65
18.17	28.66
21.20	22.45
24.23	17.15
27.26	12.72
30.28	8.73
34.83	3.46

a Mean of three runs

between the median volumes found by the two methods is about 5%, corresponding to a diameter difference of under 1.5%. In calculating the results, no attempt was made to estimate the 100% value for the number of particles in the sample, since the cumulative counts were still increasing steadily at successively lower particle sizes. The total count down to about 1.6 μ diameter was taken as the 100% value for both the methods.

Similar results were obtained using micronized griseofulvin. The results of the size distributions using the two Coulter counter methods are given in Tables XXIV and XXV, and plotted in Figure 21.

Table XXIV
Size Distribution of Micronized Griseofulvin
Using the Coulter Counter

Volume (μ^3)	Cumulative Number % Oversize ^a
2.26	100.00
3.39	87.38
4.52	75.64
5.65	65.98
6.78	57.26
9.04	42.70
11.13	30.86
13.50	21.60
15.82	14.60
18.12	9.28
36.24	2.13

^a Mean of three runs

Table XXV
Size Distribution of Micronized Griseofulvin
Using the Multichannel Coulter Counter Assembly

Volume (μ^3)	Cumulative Number % Oversize ^a
2.78	100.00
3.05	82.64
4.50	71.28
6.06	59.78
7.57	50.63
9.09	43.33
10.60	37.41
12.12	32.47
13.63	28.20
16.66	21.32
19.69	16.01
25.74	8.62

a Mean of three runs

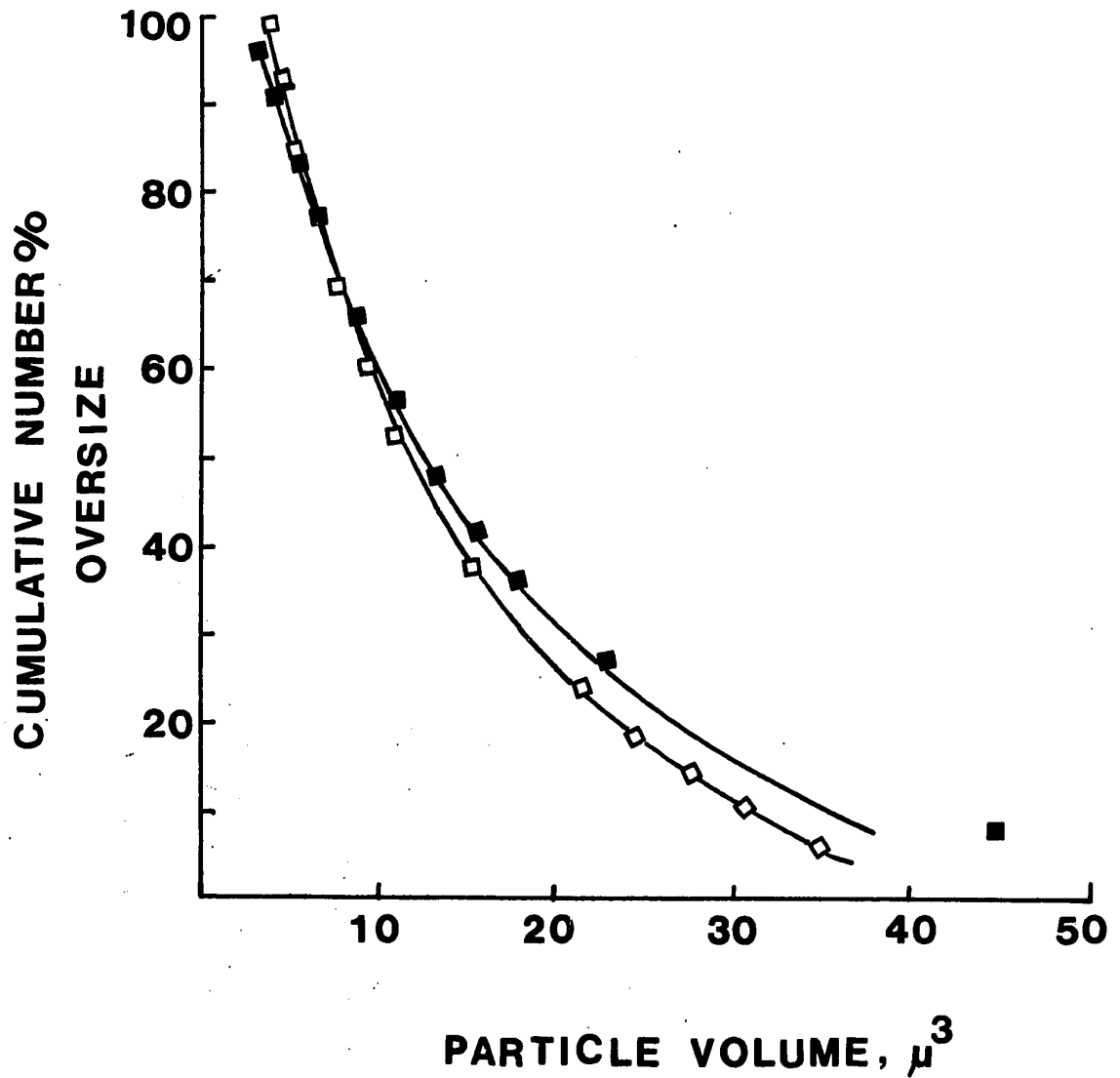


Figure 20. The Size Distributions of Micronized Hydrocortisone Acetate

Key: ■, Coulter Counter; □, Multi-channel Coulter Counter Assembly.

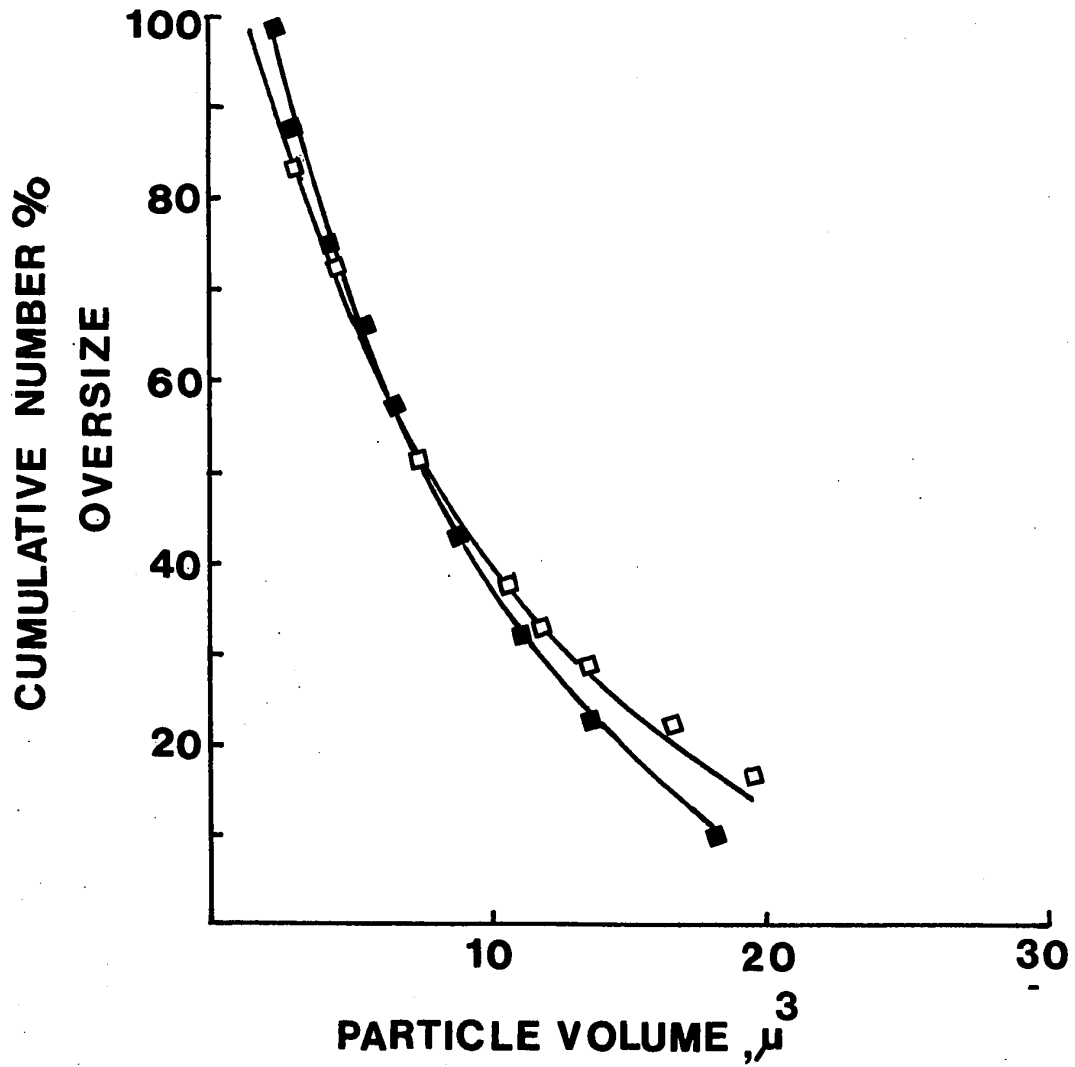


Figure 21. The Size Distributions of Micronized Griseofulvin

Key: ■ , Coulter Counter; □ , Multi-channel Coulter Counter Assembly.

5. Solubility Determination of Hydrocortisone Acetate and Griseofulvin

The results of the relationship of concentration of hydrocortisone acetate in solution to the absorbance at 246 nm and using 1 cm cell are shown in Table XXVI. The plot of absorbance against concentration gives a rectilinear curve over the range of 1 mcg to 16 mcg of hydrocortisone acetate per ml of the solution, as shown in Figure 22. This indicates that the Beer's law relationship is obeyed over this concentration range.

Table XXVI

Relationship of Concentration of Hydrocortisone Acetate to Absorbance at 246 nm

Concentration (mcg ml ⁻¹)	Absorbance ^a
1	0.038±0.001
2	0.078±0.002
4	0.155±0.000
8	0.318±0.003
12	0.476±0.002
16	0.632±0.003

a Mean of two determinations; ± ranges

The relationship of the concentration of griseofulvin to absorbance is given in Table XXVII and shown in Figure 23. The rectilinear curve over the range of 1 mcg to 12 mcg of griseofulvin per ml of solution indicates that the Beer's law

relationship is obeyed over this concentration range.

Table XXVII

Relationship of Concentration of
Griseofulvin to Absorbance at 292 nm

Concentration (mcg ml ⁻¹)	Absorbance ^a
1	0.078±0.003
2	0.157±0.002
4	0.315±0.001
6	0.475±0.000
8	0.630±0.004
12	0.940±0.005

a Mean of two determinations; ± ranges

The solubilities of hydrocortisone acetate and griseofulvin in water and electrolyte solutions are given in Table XXVIII.

Table XXVIII

Solubility of Hydrocortisone Acetate and Griseofulvin

Substance	Solvent	Solubility mcg ml ⁻¹
Hydro- cortisone Acetate	Water	10.0
	Aqueous sodium chloride solution (0.9%)	10.0
Griseofulvin	Water	8.2
	Aqueous sodium chloride solution (0.9%)	8.0
	0.05% solution of Tween 80 in normal saline	9.8
	0.1% solution of Tween 80 in normal saline	12.1

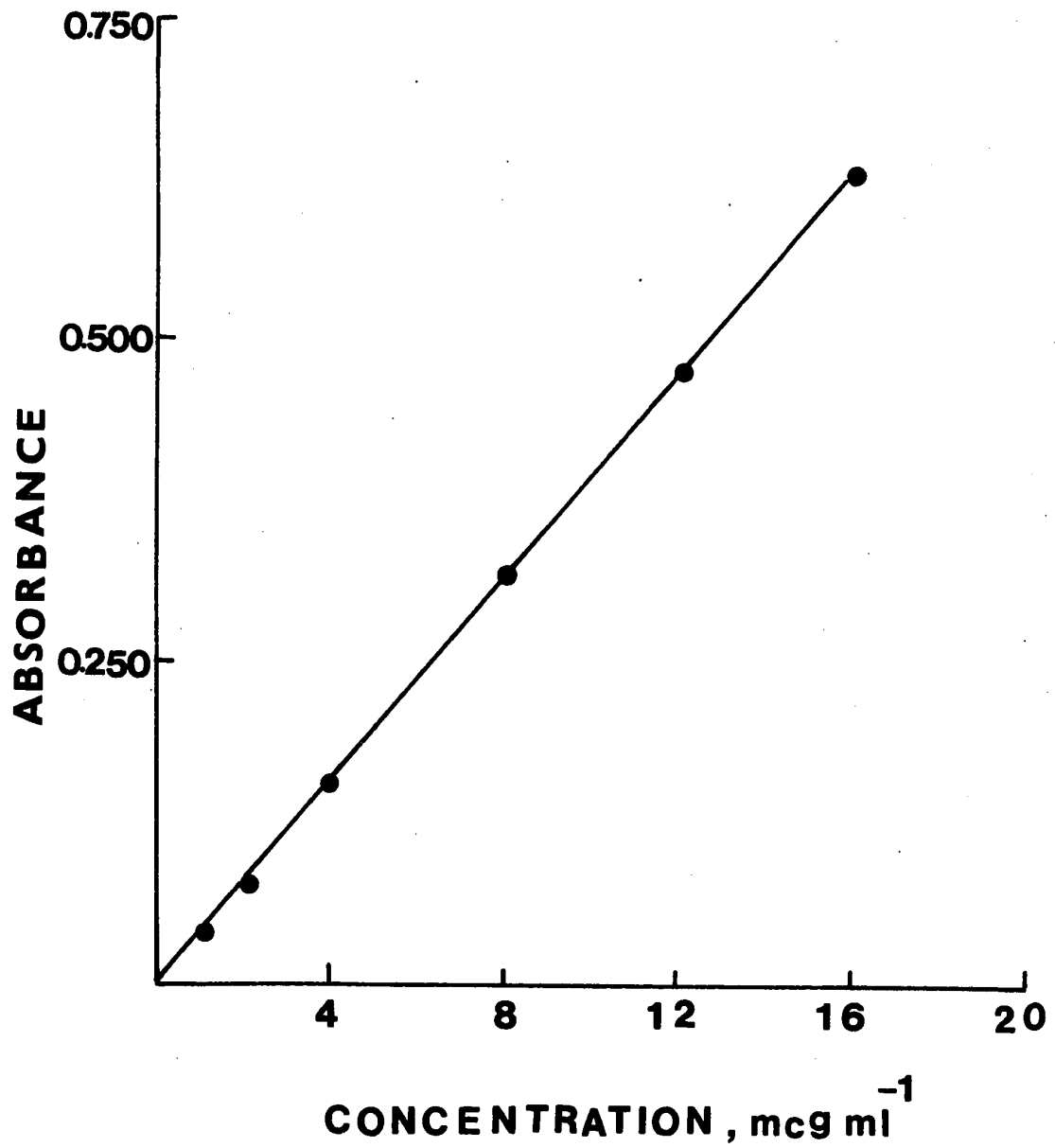


Figure 22. Relationship of Concentration of Hydrocortisone Acetate to Absorbance at 246 nm.

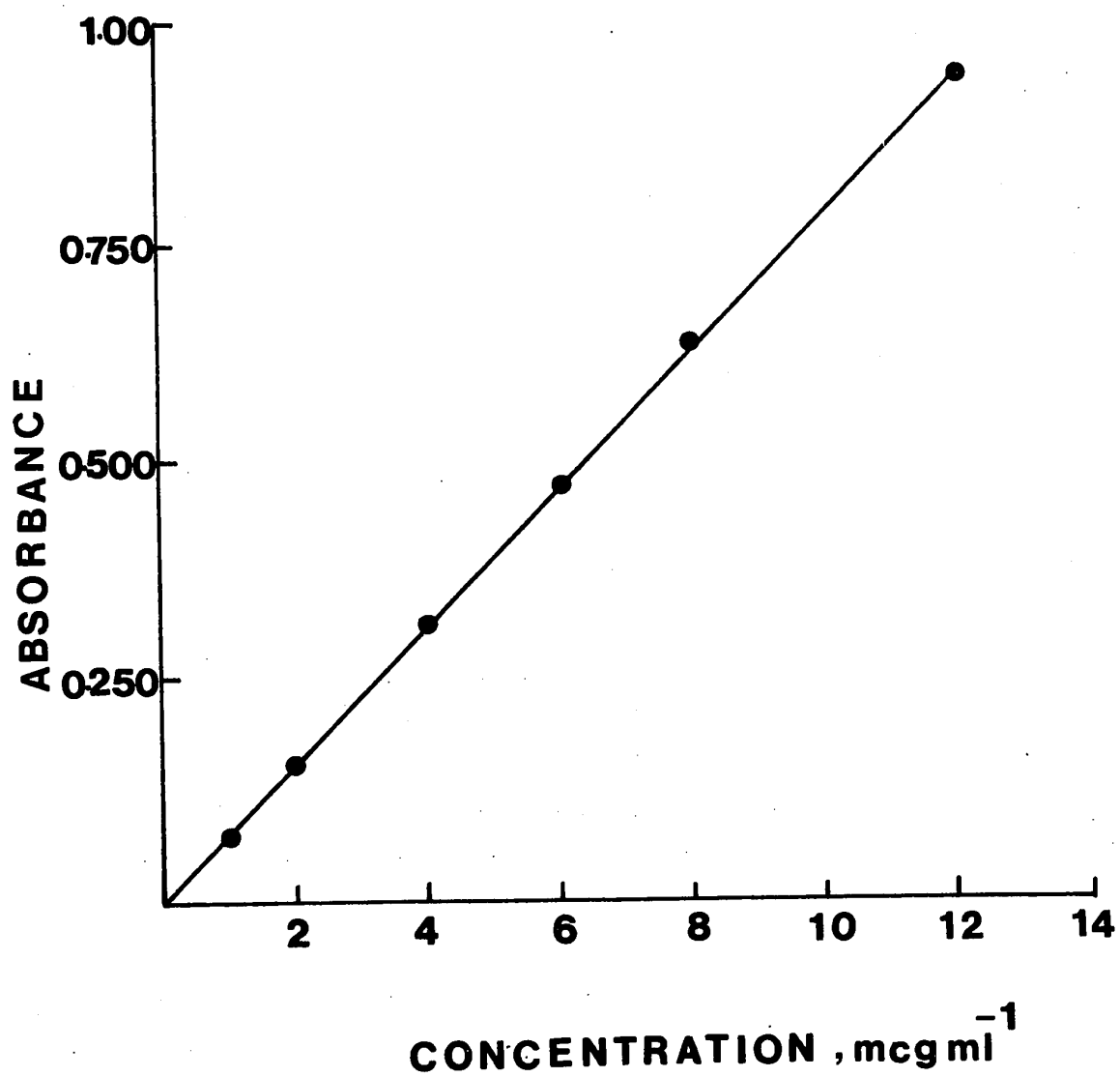


Figure 23. Relationship of Concentration of Griseofulvin to Absorbance at 292 nm

6. Dissolution Rate Studies

The results obtained for dissolution of micronized hydrocortisone acetate in 0.9% aqueous sodium chloride solution using multichannel Coulter counter assembly are given in Table XXIX. These results are obtained directly from the counts in each channel plotted by the X-Y recorder, after correction for background counts. Coincidence count losses were very low (<0.1%), making correction unnecessary. In Figures 24 and 25 cumulative counts are plotted against the particles radius and the square of the particle diameter respectively.

The results obtained for dissolution of micronized griseofulvin in 0.05% and 0.1% Tween 80 solution in normal saline are given in Tables XXX and XXXI respectively. These results are plotted in Figures 26 to 29 as the cumulative counts against the particles radius and the square of the particle diameter.

Table XXXII shows the results obtained for dissolution of micronized hydrocortisone acetate in normal saline based upon chemical analysis of the solution.

Table XXXIII shows the results obtained for dissolution of micronized griseofulvin in the dissolution media based upon chemical analysis of the solution.

Table XXIX

Multichannel Coulter Counter Assembly Data for
Dissolution of Micronized Hydrocortisone Acetate
in 0.9% Aqueous Sodium Chloride Solution

Dia- meter (μ)	(Dia- meter) ² (μ^2)	Radius (μ)	Cumulative Counts Oversize ^a			
			90	Time (seconds) 190	290	490
1.74	3.03	0.87	2508	2158	1954	1546
1.85	3.42	0.92	2219	1870	1680	1390
1.94	3.76	0.97	1969	1643	1484	1137
2.03	4.12	1.06	1565	1316	1179	871
2.25	5.06	1.12	1287	1061	950	695
2.49	6.20	1.24	899	716	617	437
2.54	6.45	1.27	796	653	560	382
2.69	7.24	1.34	609	485	421	287
2.82	7.95	1.41	431	344	299	197
3.02	9.12	1.51	192	146	133	81

a 25 seconds counting period

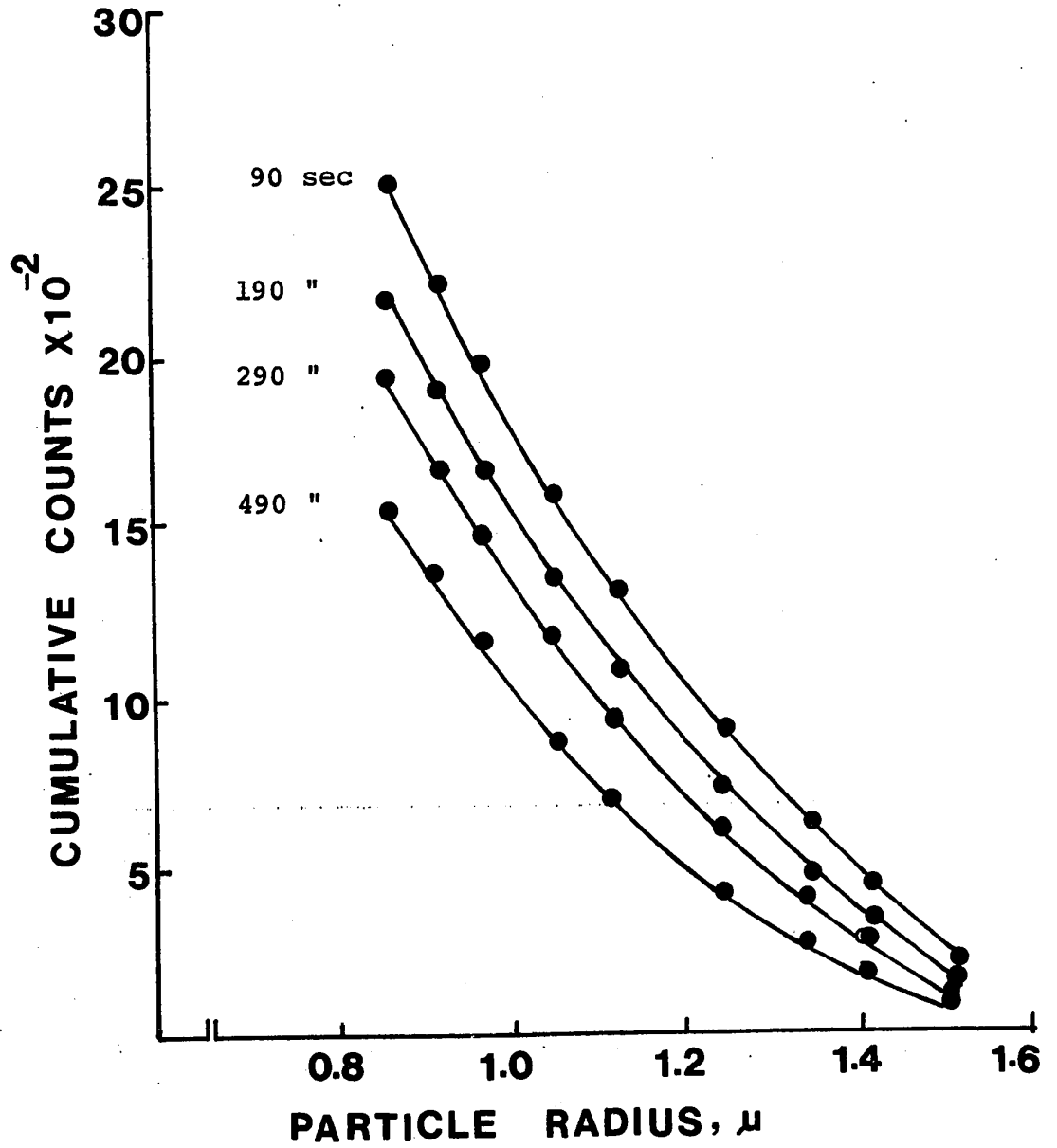


Figure 24. Plots of Cumulative Counts Against Particle Radius for Micronized Hydrocortisone Acetate in Normal Saline

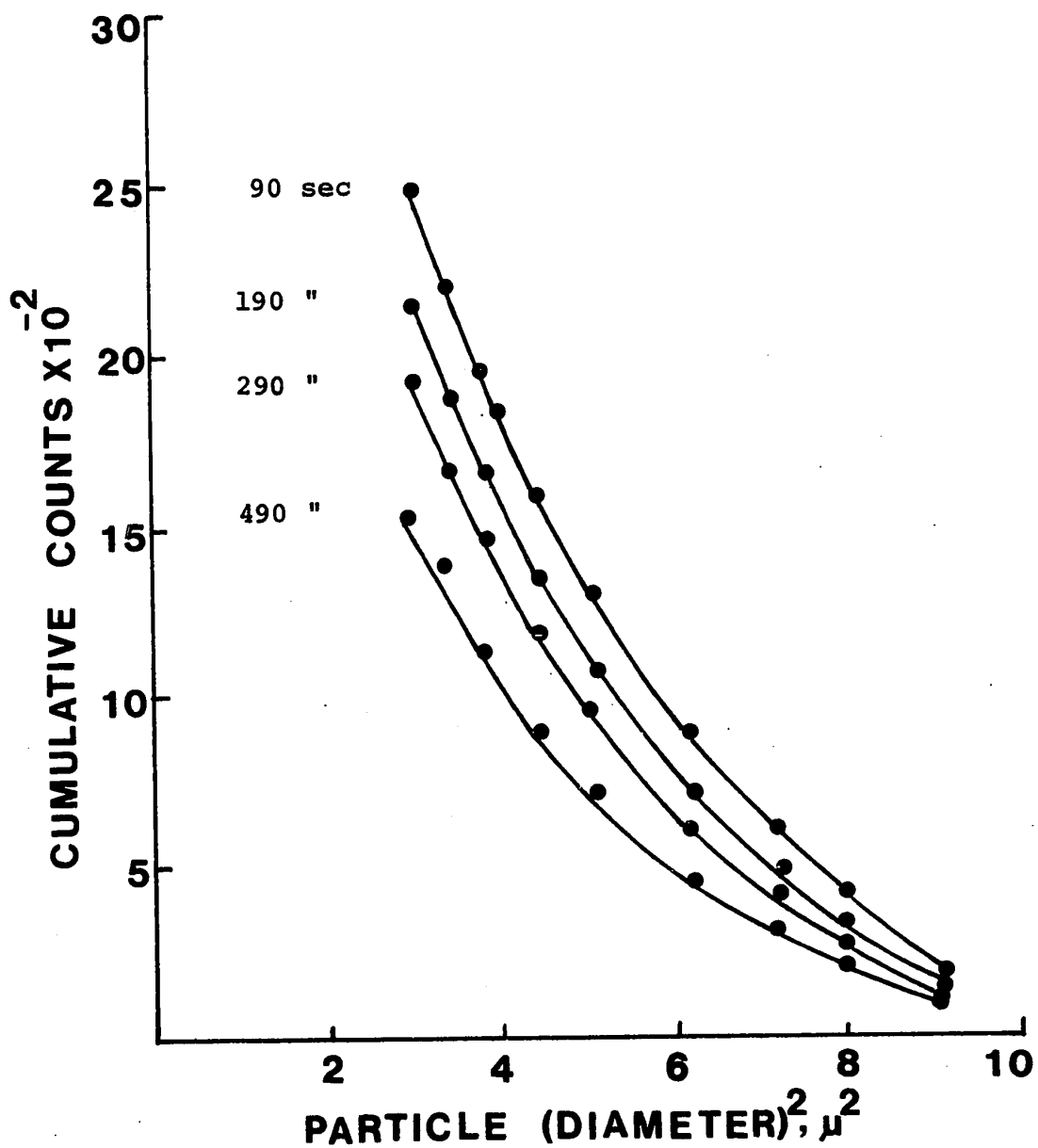


Figure 25. Plots of Cumulative Counts Against Particle (Diameter) 2 for Micronized Hydrocortisone Acetate in Normal Saline

Table XXX
 Multichannel Coulter Counter Assembly Data for
 Dissolution of Micronized Griseofulvin
 in 0.05% Tween 80 Solution in Normal Saline

Dia- meter (μ)	(Dia- meter) ² (μ^2)	Radius (μ)	Cumulative Counts Oversize ^a				
			30	120	240	420	600
1.74	3.03	0.87	2985	2252	1750	1226	797
1.85	3.42	0.92	2713	2051	1585	1089	715
2.03	4.12	1.02	2311	1706	1214	868	575
2.25	5.06	1.12	1807	1328	991	643	404
2.49	6.20	1.24	1272	916	691	416	253
2.69	7.24	1.34	862	622	452	275	160
2.82	7.95	1.41	628	432	318	187	105
2.94	8.64	1.47	333	223	180	102	52

a 20 seconds counting period

Table XXXI
 Multichannel Coulter Counter Assembly Data for
 Dissolution of Micronized Griseofulvin
 in 0.1% Tween 80 Solution in Normal Saline

Dia- meter (μ)	(Dia- meter) ² (μ^2)	Radius (μ)	Cumulative Counts Oversize ^a				
			Time (seconds)				
			30	120	240	420	600
1.74	3.03	0.87	3300	2601	2056	1375	897
1.85	3.42	0.92	3012	2376	1853	1223	806
2.03	4.12	1.02	2484	2022	1489	986	627
2.25	5.06	1.12	1903	1526	1112	748	450
2.49	6.20	1.24	1366	1065	771	528	304
2.69	7.24	1.34	934	716	518	346	202
2.82	7.95	1.41	657	479	345	239	137
2.94	8.64	1.47	339	263	188	138	61

a 20 seconds counting period

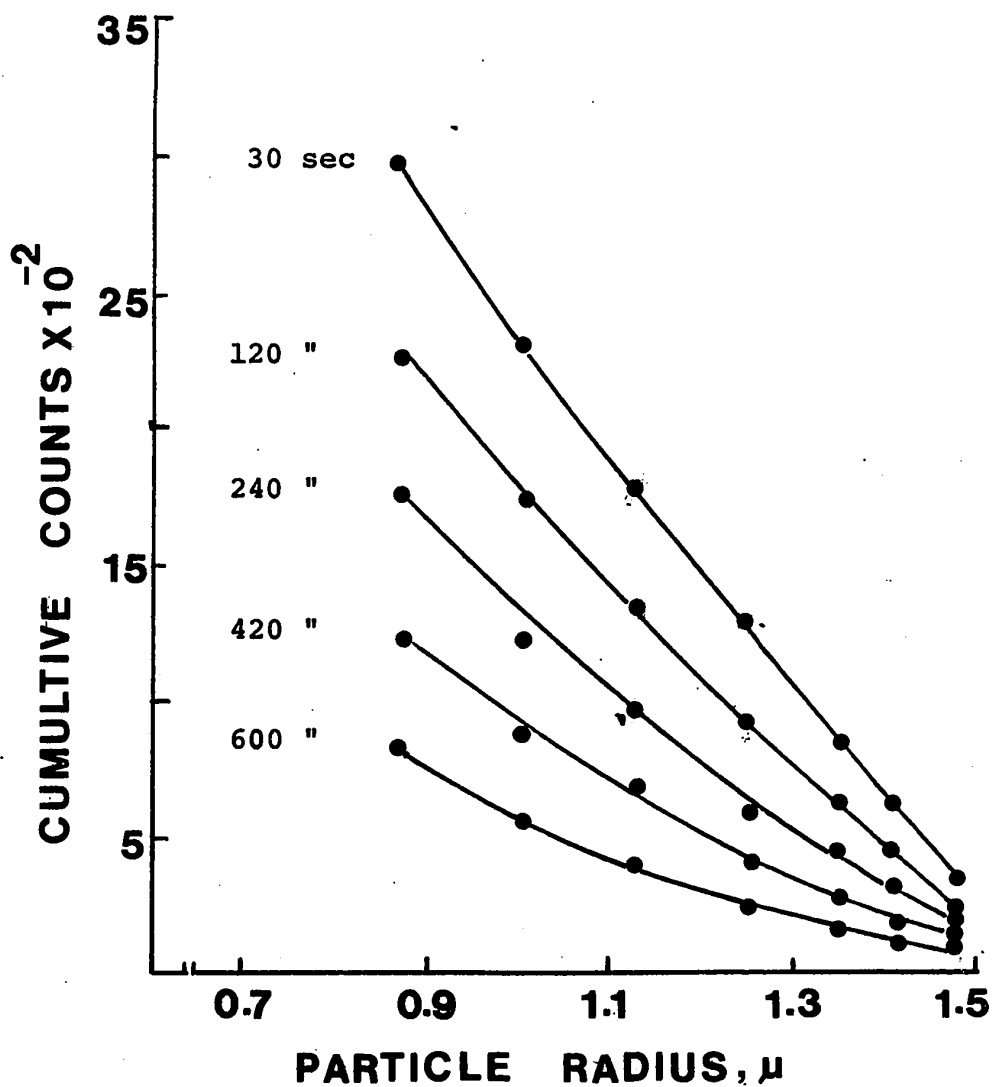


Figure 26. Plots of Cumulative Counts Against Particle Radius for Micronized Griseofulvin in 0.05% Tween 80 Solution in Normal Saline

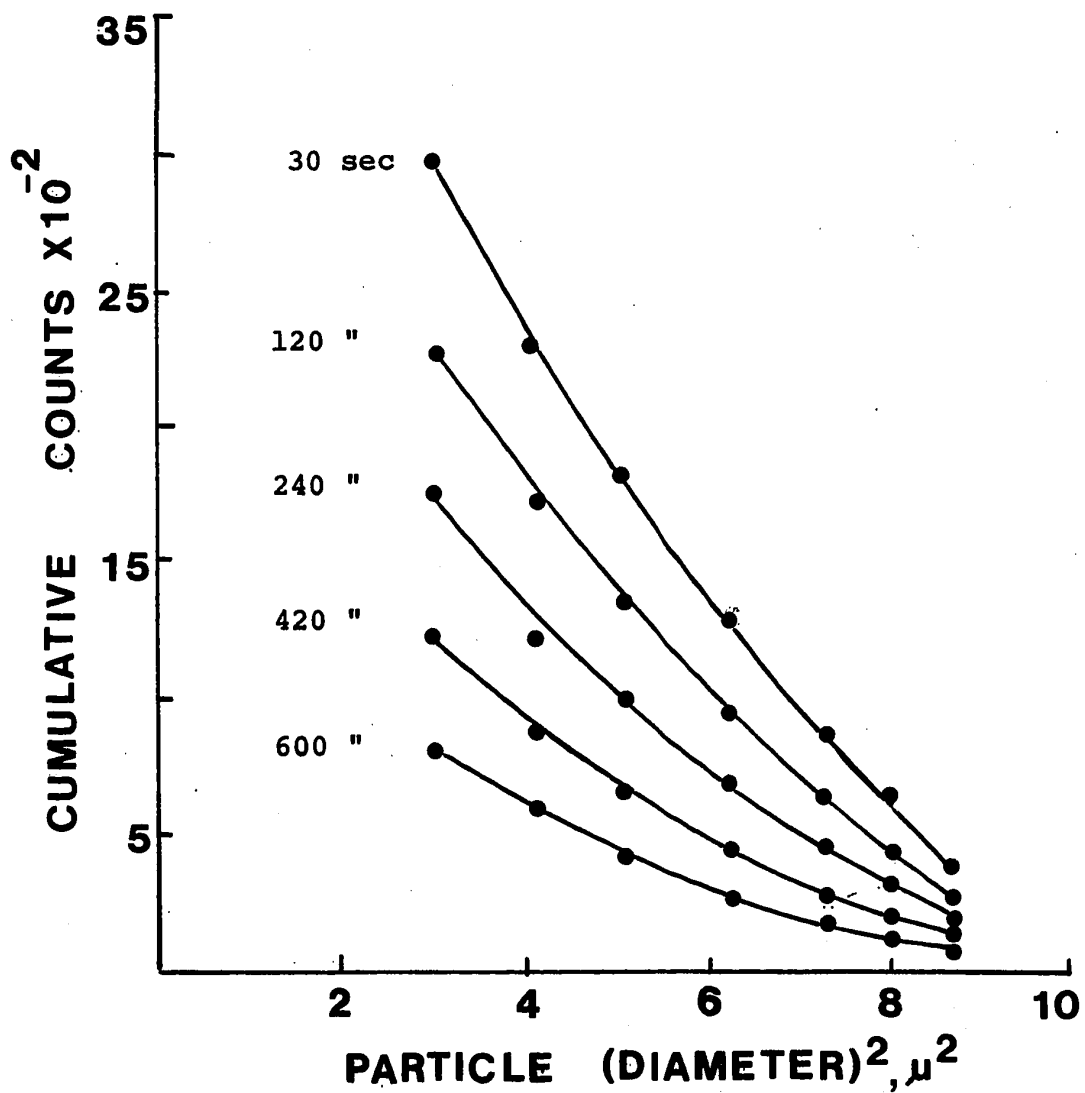


Figure 27. Plots of Cumulative Counts Against Particle (Diameter)² for Micronized Griseofulvin in 0.05% Tween 80 Solution in Normal Saline

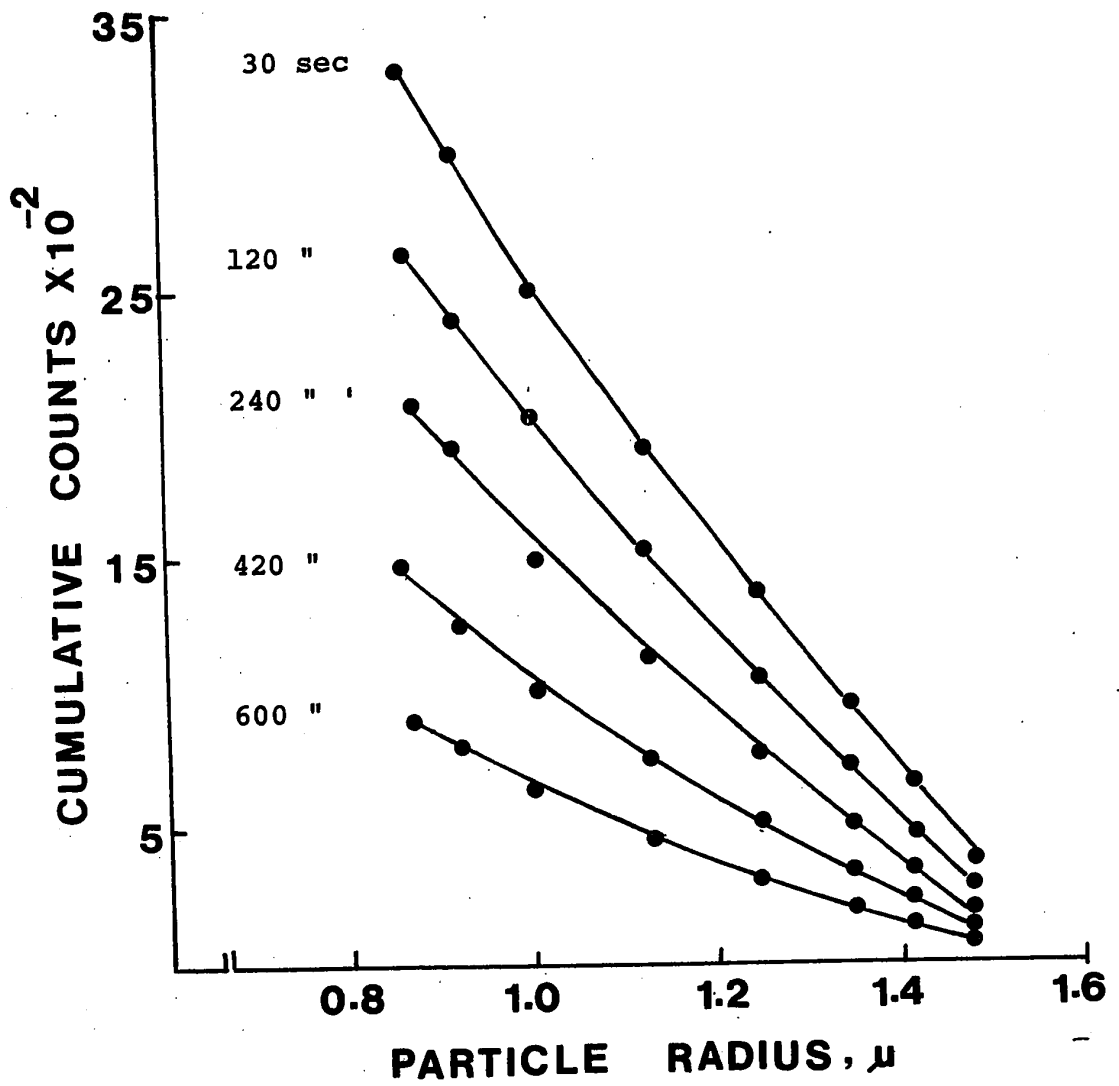


Figure 28. Plots of Cumulative Counts Against Particle Radius for Micronized Griseofulvin in 0.1% Tween 80 Solution in Normal Saline

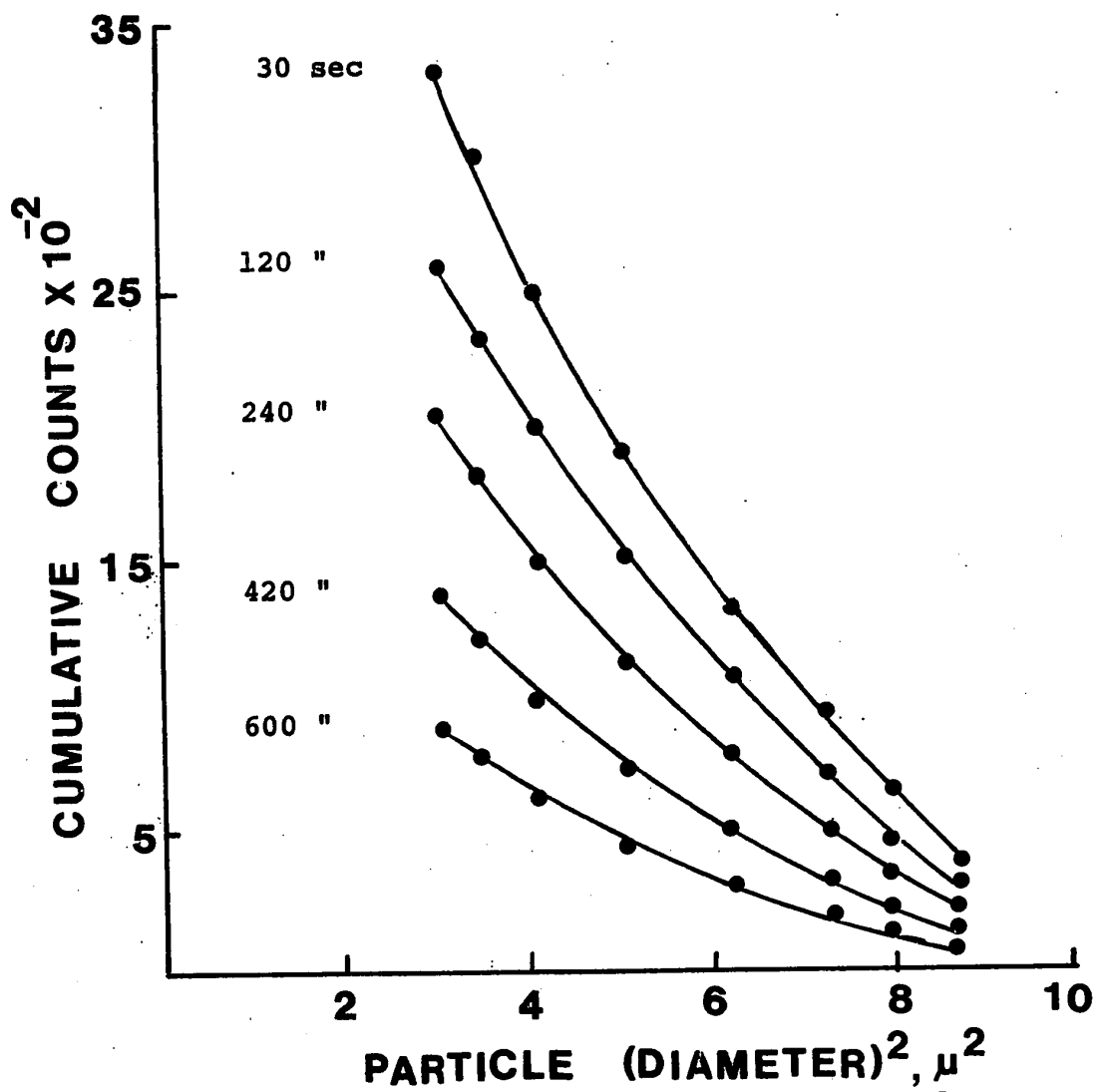


Figure 29. Plots of Cumulative Counts Against Particle (Diameter)² for Micronized Griseofulvin in 0.1% Tween 80 Solution in Normal Saline

Table XXXII

Dissolution of Micronized Hydrocortisone Acetate
by Chemical Method

Time (sec)	Amount Dissolved in 200 ml ^a (mcg)	
	A	B
90	80	
190	96	
290	108	
490	122	

a Mean of six runs

Table XXXIII

Dissolution of Micronized Griseofulvin
by Chemical Method

Time (sec)	Amount Dissolved in 200 ml ^{aa} (mcg)	
	A	B
30	42	40
120	78	88
240	114	118
420	134	152
600	144	176

aa Mean of two runs

A 0.05% Tween 80 solution in
normal saline

B 0.1% Tween 80 solution in
normal saline

CHAPTER V. DISCUSSION

A. PHYSICO-CHEMICAL STUDIES OF MEPROBAMATE

1. Preparation of Polymorphic Forms of Meprobamate

Meprobamate was found to exist in two different polymorphic forms. The Form II was obtained from Form I by crystallization from the super-cooled melt. Since Form II is generally more soluble and has a lower melting point than that of the Form I, super-cooling below the melting point of the Form II was considered necessary to crystallize Form II from the melt.

Because the meprobamate Form I was heated at 110°C during the preparation of Form II, decomposition could be expected. Elemental analysis of the Form II indicated, however, that no significant decomposition occurred during heating of Form I.

2. Characterization of the Polymorphic Forms

Melting Point Determination:

The melting point of meprobamate Form I, as determined by capillary tube method, hot stage microscope and the differential thermal analysis technique, was in the range of 102 - 106°C, as reported in the literature for meprobamate (280). The melting point range obtained for each of the polymorphic forms was almost the same using these three techniques. Thus, any of the three techniques could be used for melting point determinations. However, hot stage microscope and differential thermal analysis methods were used so that any polymorphic transitions could be observed. Transition from Form II to Form I was not observed when

Form II was heated to 30°C above the fusion temperature in the DTA calorimeter, nor when heated to 180°C on the hot stage microscope at which temperature it decomposed.

Infrared Spectroscopy:

The infrared spectrum of Form I was identical to that given in the literature for meprobamate (281). Meprobamate Form II spectrum showed an extra small peak at 1450 cm^{-1} , which however could not be used for identification purposes. Biles (282) has reported that a given phase can be identified more easily by the X-ray diffraction pattern than by the use of infrared spectroscopy.

X-ray Diffraction Pattern:

The powder method using the nickel filtered $\text{CuK}\alpha$ radiation provided a means of characterization of polymorphic forms of meprobamate. Distinct differences were evident from the powder diffraction recordings. These distinguishing features could be utilized for the identification and for analysis of the two forms in mixtures.

Differential Thermal Analysis:

Large differences in the fusion temperatures of meprobamate forms were observed using this technique. The DTA calorimetric technique was used for determination of the heats of fusion. Guillory (236) has reported some of the advantages in using DTA for determining heat of transition between the polymorphs. The heat of fusion of sulfathiazole Form II was determined, and found to be in agreement with the reported literature (236) value, confirming the cali-

bration of the calorimeter cell.

In the present investigation, repeated experiments failed to produce a polymorphic transition peak, when Form II was heated from room temperature to 30°C above the fusion temperature.

It was found from the experimental results that DTA calorimeter could be employed routinely with confidence for characterization of the polymorphic forms and in the determinations of the heats of fusion.

3. Analytical Procedure for Determination of Meprobamate Contents

The analysis of meprobamate has drawn considerable attention in recent years because of widespread use of this drug as a tranquillizer. The gas-liquid chromatography method has been shown to be very useful technique for the quantitative analysis of meprobamate in biological fluids. The method developed in this study was found to have a high degree of accuracy and percent recovery. With the conditions of the experiment, practically no breakdown of meprobamate in the gas chromatogram occurred, and good symmetrical peaks were obtained for meprobamate and for the internal standard. The sample injections could be made about every seven minutes without any apparent effect on quantitation, separation or background.

Peak areas relative to the internal standard were used to calculate the concentration of unknown samples. Peak height, though simple to estimate, did not give reproducible

results.

Dibutylphthalate was found to be a satisfactory internal standard, since it eluted shortly after the meprobamate and appeared as a symmetrical peak.

The relative response of the instrument was linear over the range of 50 - 400 mcg of meprobamate per ml of solution. This has been shown from the linear relationship between the peak areas ratios of meprobamate and internal standard.

The standard deviation of eight analyses of an aqueous solution containing 200 mcg of meprobamate per ml of solution was 2.2%, indicating a satisfactory precision of the gas-liquid chromatographic procedure.

4. Solubility and Dissolution Rate Studies

The characteristic dissolution behavior of Form II showed a peak concentration followed by a decrease with time. When the powder particles of Form II were added to water, transport of the solute from the surface of the dispersed particles took place. This resulted in a concentration higher than that of Form I and the initial dissolution of Form II was related to the solubility of Form II. When the bulk liquid became supersaturated, Form I started to crystallize out on the surface of the solid. Dissolution then proceeded from the mixture of two polymorphic forms and the concentration of Form II decreased gradually and finally the saturated concentration fell essentially to that of Form I.

Higuchi and co-workers (50) have shown that the

dissolution rate remains within 99% of the pure Form II from time $t = 0$ until $t = t'$, where t' is given by

$$t' = \frac{0.01\epsilon h^2 A_{II}}{\tau C_s^{II} D}$$

where ϵ = porosity of the Form I residue layer

h = thickness of the diffusion layer

A_{II} = amount of Form II per unit volume in the original mixture

τ = tortuosity of the Form I layer

C_s^{II} = solubility of the Form II

D = diffusion coefficient.

The concentration of Form II at the maximum point was about twice the solubility of Form I at the same temperature. When the dissolution reached equilibrium, the crystals formed were examined by X-ray diffraction and confirmed the complete transformation of Form II to Form I.

Thermodynamic Properties:

The thermodynamic properties calculated in Chapter IV are based on the assumption that Henry's law is obeyed.

It has been reported (283) that the internal energy of an organic crystal depends upon the packing density of the molecules and that the entropy of the crystal is affected by the symmetry of the molecule. The crystal of an organic compound with a closest packed arrangement of molecules has the minimum free energy. The small free energy difference and the low entropy value obtained for this compound can be ascribed to the small meprobamate molecules which are

symmetrical and are able to pack closely in the crystal lattice.

Higuchi (180) has reported that the in vivo availability of the drug is often directly related to the thermodynamic activity of the system and many workers (246, 256) subsequently confirmed this hypothesis experimentally.

Aguiar and co-workers (248) reported the effect of polymorphism on the absorption of chloramphenicol palmitate and observed a higher and faster absorption from the metastable form. Aguiar and Zelmer (246) calculated the thermodynamic data for polymorphs of chloramphenicol palmitate and mefenamic acid, and found a relatively larger free energy difference between the polymorphs A and B of chloramphenicol palmitate but only a small free energy difference between the polymorphs I and II of mefenamic acid. These workers correlated the free energy differences with the absorption rates of these drugs and concluded that the differences found in the absorption of chloramphenicol palmitate polymorphs A and B could be attributed to the relatively large free energy difference between the polymorphs. On the other hand no appreciable difference in the absorption of mefenamic acid polymorphs was observed and this was believed to be due to the smaller free energy difference.

Free energy differences, ΔF_T , between the polymorphs A and B for chloramphenicol palmitate, Forms I and II of mefenamic acid, anhydrous-trihydrate ampicillin system together with the values obtained for polymorphs of meprobamate

are given in Table XXXIV.

Table XXXIV

Free Energy Differences of Various Polymorphic Systems
and Anhydrous-Trihydrate Ampicillin System

System	ΔF_{298} cal mole ⁻¹	ΔF_{303} cal mole ⁻¹	Reference
Chloramphenicol palmitate Poly- morphs A and B	-	-744	246
Mefenamic acid polymorphs I and II	-	-251	246
Meproamate Forms I and II	-369	-402	This work
Anhydrous- trihydrate ampicillin	-430	-	256

The results of the present investigation suggest that a greater biological availability may exist with meproamate Form II than Form I. Further, the rate of absorption of a drug is often limited by its dissolution rate. A higher and faster absorption for chloramphenicol palmitate polymorph B and anhydrous ampicillin was attributed to their higher solubilities which were maintained for a long period of a minimum of 2 days for chloramphenicol palmitate polymorph B and 7 hours for anhydrous ampicillin. Although the mefenamic acid Form II initially had a greater solubility than Form I, the solubility decreased rapidly. Aguiar and Zelmer (246) found that at 30°C, the solubility of mefenamic acid Form II

in dodecyl alcohol decreased to Form I in 2.5 hours. Higuchi and co-workers (50) studied the effect of the solvent system on sulfathiazole polymorphs and reported that the reversion of sulfathiazole Form II to Form I must be more rapid in water than in organic solvents. The reversion of mefenamic acid Form II in water can therefore be expected to be less than 2.5 hours. This may be the reason why no appreciable difference in the absorption of mefenamic acid as Form I and Form II was observed.

Form II of meprobamate has a greater solubility than Form I in distilled water. The solubility of meprobamate Form II remains higher than that of Form I for about 28 hours at 30°C. Because of the slow reversion of meprobamate Form II to Form I a higher rate of in vivo availability may be obtained when Form II is used.

Since Form II was found to be stable at room temperature, formulations made using meprobamate Form II may be expected to remain stable for a minimum of one year.

It has been suggested that the difference in the dissolution rates of different crystalline forms may be due to the existence of the crystal defects. As meprobamate Form I was heated to 110°C in the preparation of Form II, small amounts of decomposition products may be formed and produce these crystal defects, thus giving a higher thermodynamic activity of Form II.

B. MULTICHANNEL COULTER COUNTER ASSEMBLY FOR DISSOLUTION RATE STUDIES

1. Dissolution Rate Studies of Micronized Hydrocortisone Acetate

Edmundson and Lees (43) suggested that the dissolution of a crystal is essentially an etching process, where a given surface recedes at a constant rate in conformity with the equation

$$d_t = d_o - k_2t \quad (\text{Equation 12; Chapter II})$$

If this is true, then the curves obtained when the cumulative counts were plotted against the radius of the particle, as shown in Figure 24, should all have the same shape but be displaced horizontally an equal distance during equal time intervals. With micronized hydrocortisone acetate, this did not appear to be the case.

From the curves shown in Figure 24, it can be seen that the rates of decrease of particle radius during the 90 seconds to 490 seconds period are 3.8×10^{-8} cm sec⁻¹ for particles of radius 1.3 to 1.6 μ and 6.0×10^{-8} cm sec⁻¹ for particles of radius 0.8 to 1.3 μ .

Edmundson and Lees (43) reported on the dissolution rate of recrystallized hydrocortisone acetate of about 15 to 30 μ diameter range in 1% aqueous sodium chloride solution, using the Coulter counter. They gave a value that corresponds to 2.3×10^{-8} cm sec⁻¹ radius loss. The results obtained in this study are in fair agreement with the reported results

of Edmundson and Lees and show that there is a higher rate of recession of the solid surface in the case of the smaller particles.

Higuchi (42) has given a derivation of an equation based upon the assumption that the rate of dissolution is controlled by diffusion of drug molecules across the boundary layer surrounding the particles.

According to the Higuchi equation

$$a^2 = a_0^2 - 2 \frac{D\Delta C}{p} t \quad (\text{Equation 10; Chapter II})$$

where a = radius of particle at time $t = t$

a_0 = radius of particle at time $t = 0$.

To test the application of this equation to the data obtained using the multichannel Coulter counter assembly, plots of cumulative counts against (diameter)² were constructed. If the equation is applicable, then these curves should be displaced along the abscissa with time but without changes in shape. This was found to be true with the materials studied. In the above equation, ΔC is the difference between the solute concentration at the surface of the particle, and the solute concentration in the bulk of the solution. If ΔC is constant then the horizontal displacement between these curves should be constant in equal time intervals, and this was found to be the case.

For hydrocortisone acetate the equation obtained was

$$a^2 = a_0^2 - 1.2 \times 10^{-11} \text{ cm}^2 \text{ sec}^{-1}.$$

Since the quantity of the solid used corresponded to about 10% of that required for saturation, so that the ΔC remained essentially constant and did not decrease by more than 10%, the uniform shape of the curves was expected.

All the factors in the Higuchi equation are known, or can be calculated. The diffusion coefficient, D , was estimated from the Stokes-Einstein equation

$$D = \frac{kT}{6\pi\eta s} \quad (\text{eq. 29})$$

where D = diffusion coefficient

k = Boltzmann constant, 1.38×10^{-16} ergs deg $^{-1}$ molecule $^{-1}$

T = absolute temperature, 298.2°K

η = viscosity of the solvent, ≈ 0.0091 poise

s = hydrodynamic radius of the hydrocortisone acetate molecule, 5.0×10^{-8} cm.

The value of " s " was calculated from the following equation:

$$\frac{4}{3}\pi s^3 \rho = \frac{M}{N} \quad (\text{eq. 30})$$

where M = molecular weight of hydrocortisone acetate, 404.51

N = Avogadro's number, 6.03×10^{23} mole $^{-1}$

ρ = density of hydrocortisone acetate, 1.289 (43).

The diffusion coefficient, D , was obtained to be 4.8×10^{-6} cm 2 sec $^{-1}$.

Substitution of this value into the Higuchi equation gave

$$a^2 = a_0^2 - 7.4 \times 10^{-11} \text{ cm}^2 \text{ sec}^{-1}$$

which is in fair agreement with the experimental value.

2. Dissolution Rate Studies of Micronized Griseofulvin

For micronized griseofulvin the rates of particle decrease were found from the Figures 26 and 28 and were calculated to vary between $6.0 \times 10^{-8} \text{ cm sec}^{-1}$, for particles of radius 1.3 to 1.6 μ , and $8.4 \times 10^{-8} \text{ cm sec}^{-1}$, for particles of radius 0.8 to 1.3 μ .

Using the equation for the diffusion controlled theory of dissolution the results for the micronized griseofulvin obtained from Figures 27 and 29 fit the equations

$$a^2 = a_0^2 - 1.9 \times 10^{-11} \text{ cm}^2 \text{ sec}^{-1}$$

for 0.05% Tween 80 solution in normal saline, and

$$a^2 = a_0^2 - 2.3 \times 10^{-11} \text{ cm}^2 \text{ sec}^{-1}$$

for 0.1% Tween 80 solution in normal saline.

The diffusion coefficient for micronized griseofulvin was calculated theoretically from the Stokes-Einstein equation. The value obtained gave the equations

$$a^2 = a_0^2 - 7.2 \times 10^{-11} \text{ cm}^2 \text{ sec}^{-1}$$

for 0.05% Tween 80 solution in normal saline, and

$$a^2 = a_0^2 - 8.8 \times 10^{-11} \text{ cm}^2 \text{ sec}^{-1}$$

for 0.1% Tween 80 solution in normal saline.

These results are in fair agreement with the experimental values.

For micronized griseofulvin essentially the same results were obtained for rate of dissolution in both the 0.05% and 0.1% Tween 80 solutions in normal saline. Because of the relatively large static charge and higher surface energies, micronized griseofulvin powder exists in the form of

agglomerates and wetting is essential to maintain the material in a uniform dispersion. The surfactant helped to wet the griseofulvin powder.

Agreement of the results with the Higuchi equation indicates that the rate-determining step in the dissolution of micronized hydrocortisone acetate and griseofulvin in the systems studied is the rate of diffusion of drug molecules across the boundary layer surrounding the particle.

Based upon the lower experimental value of the constant in the Higuchi equation it appears that the dissolution rates of materials studied were lower than the calculated theoretical values. In the case of micronized hydrocortisone acetate, this could be due to incomplete wetting of the powder. However, for micronized griseofulvin Tween 80 aided in wetting the powder so this was not the explanation in this case. The concentrations of Tween 80 in normal saline dissolution media were above the critical micelle concentration (285). The increase in the solubility of the drug in the presence of Tween 80 in the dissolution media was due to the micellar solubilization. Elworthy and Lipscomb (286) reported on the dissolution of griseofulvin in nonionic surfactants and suggested that the griseofulvin molecules were situated within the micelles, adjacent to the hydrocarbon region of the surfactant. Because of the lower activation energy in the presence of surface active agents transfer of griseofulvin molecules from the crystal to the solution is probably facilitated, thus giving a higher dissolution rate (287). If the

drug molecules are associated with the micelles of Tween 80, then a smaller diffusion coefficient can be expected (42), in accordance with our experimental results.

3. Limitations and Advantages of the Multichannel Coulter Counter Assembly

Calculations of Weight Percent Materials Dissolved

The weight of the materials, W_t , dissolved during the time intervals between particle counts was calculated from the following equation, in which the assumption is made that the particles are spherical.

$$W_t = \frac{\pi(d_2^3 - d_1^3) p \Delta N V_m}{6V_s} \quad (\text{eq. 31})$$

where d_2 = diameter of particles at time t_2 , μ

d_1 = diameter of particle at time t_1 , μ

p = density, gm cm^{-3} , 1.289 for micronized hydrocortisone acetate (43), and 1.440 for micronized griseofulvin (288)

ΔN = number of particles with the size range considered

V_m = volume of dissolution medium, 200 ml

V_s = sample volume, 0.25 ml for micronized hydrocortisone acetate and 0.20 ml for micronized griseofulvin.

The calculated weight of the materials dissolving during the time intervals between the particle counts was about 15% of that calculated from the results of the chemical analysis during the same time intervals. This was expected since particle counts were made over only a relatively narrow

range of sizes.

In dissolution rate studies, the aperture current and amplification settings were not altered and the complete size distributions could not be obtained. Using the constant aperture current and amplification settings, a lower and upper limit of about 1.6 μ and 3 μ respectively were obtained, which represented about 20% by weight of the material for micronized hydrocortisone acetate and about 55% by weight of the material for micronized griseofulvin. The contributions to the amount of drug in solution made by the particles outside of this range could not be estimated from the experimental results.

Evaluation of the Method

The experimental results show that the multichannel Coulter counter assembly is a useful apparatus for determination of particle size distributions. The method offers two main advantages over the Coulter counter used as a single channel instrument.

1. The speed of data acquisition is increased, permitting the use of the method for kinetic studies and for dynamic systems.
2. The error involved in setting the threshold is avoided. This is particularly important for materials with narrow size distributions.

The method, however, has the same general limitations as of the Coulter counter.

The lower limit of particle size observed using a 50 μ

aperture tube was about 1.6μ as compared to the suggested lower limit of 1μ . This may be due to the thermal effects or to background noise. Samyn and McGee (289) observed a loss of count in samples meeting the suggested size limits of Coulter counter, that is, 2% to 40% of the aperture diameter. They suggested that this was due to the presence of larger particles in the sample. It was reported that the 100μ aperture tube can accurately measure down to 2μ , the suggested lower limit, only if all the particles above 10μ are removed from the sample. This effect can be observed even when the size distribution is narrow (290).

The Coulter counter gives no information about particle shape and only measures the d_v , the diameter of an equivalent sphere (43). Further, if the particles are highly anisometric, the response of the Coulter counter may not be proportional to the particle volume. A diameter error of about 3% has been calculated theoretically for a system consisting of a non-conducting prolate spheroid with an axial ratio of 4.0 (291).

In kinetic studies, the multichannel Coulter counter assembly has the limitation that the lower and upper limits of particle size are kept constant because the aperture current and amplification settings are not altered during the dissolution study.

CHAPTER VI. SUMMARY

1. The existence of two polymorphic forms of meprobamate has been confirmed by melting point, infrared spectroscopy, X-ray diffraction and differential thermal analyser calorimetry.
2. A gas-liquid chromatographic method has been developed for the quantitative determination of meprobamate in water.
3. The solubility and the relative rates of dissolution in water of both the forms of meprobamate have been determined over a temperature range of 25 to 40°C. The Form II was found to be significantly more soluble than the Form I at all temperatures studied.
4. The thermodynamic values have been calculated for meprobamate Form I and Form II. It is suggested that a greater thermodynamic activity of Form II and its slow reversion to Form I may give a higher in vivo availability.
5. A multichannel analyser was assembled with the Coulter counter, and used for determinations of the size distributions. The size distributions obtained using the Coulter counter in conventional mode, and a microscope, agreed well with those obtained using this unit.
6. The multichannel Coulter counter was used to follow the change in particle size distributions of micronized hydrocortisone acetate and griseofulvin powders in electrolyte solutions in studies of dissolution rates.

BIBLIOGRAPHY

1. Noyes, A. and Whitney, W., J. Am. Chem. Soc., 19, 930 (1897).
2. Noyes, A. and Whitney, W., Z. Phys. Chem., 23, 689 (1897).
3. Bruner, M.L. and Tolloczko, S., Z. Phys. Chem., 35, 283 (1900).
4. Bruner, M.L. and Tolloczko, S., Z. Anorg. Chem., 28, 314 (1901).
5. Bruner, M.L. and Tolloczko, S., Z. Anorg. Chem., 35, 23 (1903).
6. Bruner, M.L. and Tolloczko, S., Z. Anorg. Chem., 56, 58 (1908); through Chem. Abstr., 2, 620 (1908).
7. Bruner, M.L. and Tolloczko, S., Bull. Internat. Acad. Cracovie., 672 (1907); through Chem. Abstr., 2, 1775 (1908).
8. Nernst, W., Z. Phys. Chem., 47, 52 (1904).
9. Brunner, E., Z. Phys. Chem., 47, 56 (1904).
10. Roller, P.S., J. Phys. Chem., 35, 1133 (1931).
11. Roller, P.S., J. Phys. Chem., 36, 1202 (1932).
12. Roller, P.S., J. Phys. Chem., 39, 221 (1935).
13. Van Name, R.G. and Hill, D.U., Am. J. Sci., 36, 543 (1913); through Chem. Abstr., 8, 602 (1914).
14. Van Name, R.G. and Hill, D.U., Am. J. Sci., 42, 307 (1916); through Chem. Abstr., 10, 2830 (1916).
15. King, C.V., J. Am. Chem. Soc., 57, 828 (1935).
16. Wilderman, M., Z. Phys. Chem., 66, 445 (1909); through Chem. Abstr., 3, 2081 (1909).

17. Zdanovskii, A.B., J. Phys. Chem. (U.S.S.R.), 20, 379 (1946); through Chem. Abstr., 40, 6960² (1946).
18. Zdanovskii, A.B., J. Phys. Chem. (U.S.S.R.), 20, 869 (1946); through Chem. Abstr., 41, 2306g (1947).
19. Zdanovskii, A.B., Zhur. Fiz. Khim., 25, 170 (1951); through Chem. Abstr., 48, 4291c (1954).
20. Higuchi, W.I., Parrott, E.L., Wurster, D.E. and Higuchi, T., J. Am. Pharm. Assoc., Sci. Ed., 47, 376 (1958).
21. King, C.V. and Brodie, S.S., J. Am. Chem. Soc., 59, 1375 (1937).
22. Hixson, A.W. and Baum, S.J., Ind. Eng. Chem., 36, 528 (1944).
23. Hixson, A.W. and Crowell, J.H., Ind. Eng. Chem., 23, 923 (1931).
24. Niebergall, P.J., Milosovich, G. and Goyan, J.E., J. Pharm. Sci., 52, 236 (1963).
25. Niebergall, P.J. and Goyan, J.E., J. Pharm. Sci., 52, 29 (1963).
26. Parrott, E.L., Wurster, D.E. and Higuchi, T., J. Am. Pharm. Assoc., Sci. Ed., 44, 269 (1955).
27. Goldberg, A.H., Gibaldi, M., Kanig, J.L. and Mayersohn, M., J. Pharm. Sci., 55, 581 (1966).
28. Goldberg, A.H., Gibaldi, M. and Kanig, J.L., J. Pharm. Sci., 55, 482 (1966).
29. Clements, J.A. and Stanski, D., Can. J. Pharm. Sci., 6, 9 (1971).

30. Danckwerts, P.V., *Ind. Eng. Chem.*, 43, 1460 (1951).
31. Fage, A. and Townend, H.C.H., *Proc. Roy. Soc. (London)*, 135A, 656 (1932); through *Chem. Abstr.*, 26, 3050 (1932).
32. Hanratty, T.J., *A.I.Ch.E.J.*, 2, 359 (1956).
33. Johnson, A.I. and Huang, C.J., *A.I.Ch.E.J.*, 2, 412 (1956).
34. Goyan, J.E., *J. Pharm. Sci.*, 54, 645 (1965).
35. Higuchi, W.I., *J. Pharm. Sci.*, 56, 315 (1967).
36. Wurster, D.E. and Taylor, P.W., *J. Pharm. Sci.*, 54, 169 (1965).
37. Wagner, J.G., *J. Pharm. Sci.*, 50, 359 (1961).
38. Wurster, D.E. and Taylor, P.W., Jr., *J. Pharm. Sci.*, 54, 670 (1965).
39. Higuchi, W.I. and Hiestand, E.N., *J. Pharm. Sci.*, 52, 67 (1963).
40. Fick, A., *Phil. Mag.*, 10, 3 (1855).
41. Higuchi, W.I., Rowe, E.L. and Hiestand, E.N., *J. Pharm. Sci.*, 52, 162 (1963).
42. Higuchi, W.I., *J. Pharm. Sci.*, 53, 405 (1964).
43. Edmundson, I.C. and Lees, K.A., *J. Pharm. Pharmacol.*, 17, 193 (1965).
44. Levy, G. and Procknal, J.A., *J. Pharm. Sci.*, 51, 294 (1962).
45. Morozowich, W., Chulski, T., Hamlin, W.E., Jones, P.M., Northam, J.I., Purmalis, A. and Wagner, J.G., *J. Pharm. Sci.*, 51, 993 (1962).

46. Higuchi, W.I., Mir, N.A., Parker, A.P. and Hamlin, W.E., J. Pharm. Sci., 54, 8 (1965).
47. Higuchi, W.I. and Hamlin, W.E., J. Pharm. Sci., 52, 575 (1963).
48. Higuchi, W.I., Gray, J.A., Hefferren, J.J. and Patel, P.R., J. Dental Res., 44, 330 (1965).
49. Higuchi, W.I., Patel, P.R. and Hefferren, J.J., J. Pharm. Sci., 54, 587 (1965).
50. Higuchi, W.I., Bernardo, P.D. and Mehta, S.C., J. Pharm. Sci., 56, 200 (1967).
51. Hamlin, W.E., Nelson, E., Ballard, B.E. and Wagner, J.G., J. Pharm. Sci., 51, 432 (1962).
52. Levy, G. and Procknal, J.A., J. Pharm. Sci., 53, 656 (1964).
53. Higuchi, W.I., Mir, N.A. and Desai, S.J., J. Pharm. Sci., 54, 1405 (1965).
54. Alexander, G.B., J. Phys. Chem., 61, 1563 (1957).
55. Wurster, D.E. and Seitz, J.A., J. Pharm. Sci., 49, 335 (1960).
56. "Remington's Pharmaceutical Sciences", 14th Ed., Hoover, J.E. and Osol, A., Mack Publishing Co., Pennsylvania, 1970, p. 320.
57. Atkinson, R.M., Bedford, C., Child, K.J. and Tomich, E.G., Antibiot. Chemother., 12, 232 (1962).
58. Kraml, M., Dubuc, J. and Gaudry, R., Antibiot. Chemother., 12, 239 (1962).

59. Duncan, W.A.M., MacDonald, G. and Thornton, M.J.,
J. Pharm. Pharmacol., 14, 217 (1962).
60. Mavel, J.R., Schlichting, D.A., Danton, C., Levy,
E.J. and Cahn, M.M., J. Invest. Dermatol., 42,
197 (1964).
61. Ullah, I. and Cadwallader, W.E., J. Pharm. Sci.,
60, 230 (1971).
62. Nelson, E., J. Am. Pharm. Assoc., Sci. Ed., 48, 96.
(1959).
63. Goldberg, A.H., Gibaldi, M. and Kanig, J.L., J.
Pharm. Sci., 54, 1145 (1965).
64. Chiou, W.N. and Niazi, S., J. Pharm. Sci., 60, 1333
(1971).
65. Goldberg, A.H., Gibaldi, M. and Kanig, J.L., J.
Pharm. Sci., 55, 487 (1966).
66. Sekiguchi, K. and Obi, N., Chem. Pharm. Bull., 9,
866 (1961).
67. Mayersohn, M. and Gibaldi, M., J. Pharm. Sci., 55,
1323 (1966).
68. Gibaldi, M., Feldman, S. and Bates, T.R., J. Pharm.
Sci., 57, 708 (1968).
69. Levy, G., Am. J. Pharm., 135, 78 (1963).
70. Dare, J.G., Australas. J. Pharm., 45, 558 (1964).
71. Fincher, J.H., J. Pharm. Sci., 57, 1825 (1968).
72. Dunning, W.G. and Kilpatrick, M., J. Phys. Chem., 42,
215 (1938).

73. King, C.V. and Braverman, M.M., J. Am. Chem. Soc., 54, 1744 (1932).
74. Johnson, R.S. and McDonald, H.J., J. Am. Chem. Soc., 72, 666 (1950).
75. Levy, G., J. Pharm. Sci., 52, 1039 (1963).
76. Hixson, A.W. and Baum, S.J., Ind. Eng. Chem., 33, 478 (1941).
77. Hixson, A.W. and Baum, S.J., Ind. Eng. Chem., 34, 120 (1942).
78. Garner, F.H. and Hoffman, J.M., A.I.Ch.E.J., 7, 148 (1961).
79. Levy, G., J. Mond. Pharm., 10, 237 (1967).
80. Levy, G., Leonards, J.R. and Procknal, J.A., J. Pharm. Sci., 54, 1719 (1965).
81. Abramson, M.B. and King, C.V., J. Am. Chem. Soc., 61, 2290 (1939).
82. Colburn, A.P., Trans. Inst. Chem. Engrs. (London), 29, 174 (1933).
83. Arnold, J.H., J. Am. Chem. Soc., 52, 3937 (1930).
84. Hamlin, W.E., Northam, J.I. and Wagner, J.G., J. Pharm. Sci., 54, 1651 (1965).
85. Nelson, E., J. Am. Pharm. Assoc., Sci. Ed., 47, 297 (1958).
86. O'Reilly, R.A., Nelson, E. and Levy, G., J. Pharm. Sci., 55, 435 (1966).
87. Bates, T.R., Gibaldi, M. and Kanig, J.L., Nature, 210, 1331 (1966).

88. Wurster, D.E. and Polli, G.P., *J. Pharm. Sci.*, 50, 403 (1961).
89. Singh, P., Desai, S.J., Flanagan, D.R., Simonelli, A.P. and Higuchi, W.I., *J. Pharm. Sci.*, 57, 959 (1968).
90. Riddiford, A.C., *J. Phys. Chem.*, 56, 745 (1952).
91. Cook, D., *Med. Serv. J. (Can.)*, 23, 323 (1967).
92. Hersey, J.A., *Mfg. Chemist and Aerosol News*, 40, 32 (1969).
93. Klein, L., *Bull. Biol. Pharmns.*, 273 (1932).
94. Elliott, G.H., *Pharm. J.*, 131, 514 (1933).
95. Nelson, E., *J. Am. Pharm. Assoc., Sci. Ed.*, 47, 300 (1958).
96. Wagner, C., *J. Phys. Chem.*, 53, 1030 (1949).
97. Gibaldi, M., Feldman, S., Wynn, R. and Weiner, N.D., *J. Pharm. Sci.*, 57, 787 (1968).
98. Jouhar, A.J., Garnett, E.S. and Wallington, J.S., *J. Pharm. Sci.*, 57, 617 (1968).
99. Cook, D., *Can. J. Pharm. Sci.*, 2, 91 (1967).
100. Cook, D., Chang, H.S. and Mainville, C.A., *Can. J. Pharm. Sci.*, 1, 69 (1966).
101. Levy, G. and Sahli, B.A., *J. Pharm. Sci.*, 51, 58 (1962).
102. Levich, V.G., "Physiochemical Hydrodynamics", Prentice-Hall, Inc., Englewood Cliffs, N.J., 1962, p. 69.
103. Gregory, D.P. and Riddiford, A.G., *J. Chem. Soc. (London)*, 3756 (1956).

104. Levy, G. and Tanski, W., Jr., J. Pharm. Sci., 53, 679 (1964).
105. Wood, J.H., Syarto, J.E. and Letterman, H., J. Pharm. Sci., 54, 1068 (1965).
106. Paikoff, M. and Drumm, G., J. Pharm. Sci., 54, 1693 (1965).
107. Nogami, H., Nagai, T. and Ito, K., Chem. Pharm. Bull., 14, 351 (1966).
108. Nogami, H., Nagai, T. and Suzuki, A., Chem. Pharm. Bull., 14, 329 (1966).
109. Nogami, H., Nagai, T. and Suzuki, A., Chem. Pharm. Bull., 14, 339 (1966).
110. Simonelli, A.P., Mehta, S.C. and Higuchi, W.I., J. Pharm. Sci., 58, 538 (1969).
111. Desai, S.J., Simonelli, A.P. and Higuchi, W.I., J. Pharm. Sci., 54, 1459 (1965).
112. Lapidus, H. and Lordi, N.G., J. Pharm. Sci., 55, 840 (1966).
113. Souder, J.C. and Ellenbogen, W.C., Drug Standards, 26, 77 (1958).
114. Shenoy, K.G., Chapman, D.E. and Cambell, J.A., Drug Standards, 27, 77 (1959).
115. Krueger, E.O. and Vliet, E.B., J. Pharm. Sci., 51, 181 (1962).
116. Rosen, E. and Swintosky, J.V., J. Pharm. Pharmacol., 12, 237T (1960).
117. Rosen, E., J. Pharm. Sci., 52, 98 (1963).

118. Montgomery, K.O., Flemming, C.V., Weinswig, M.H., Parke, R.F. and Swartz, H.A., J. Pharm. Sci., 53, 340 (1964).
119. "National Formulary", 12th Ed., (2nd Suppl.), Mack Publishing Co., Easton, Pa., 1967, p. 15.
120. Ferrari, A. and Khoury, A.J., Ann. N.Y. Acad. Sci., 153, 660 (1968).
121. Gibaldi, M. and Weintraub, H., J. Pharm. Sci., 59, 725 (1970).
122. Nelson, E., J. Am. Pharm. Assoc., Sci. Ed., 46, 607 (1957).
123. Levy, G. and Hayes, B.A., New Eng. J. Med., 21, 1053 (1960).
124. Mitchell, A.G. and Saville, D.J., J. Pharm. Pharmacol., 19, 729 (1967).
125. Levy, G., J. Pharm. Sci., 50, 388 (1961).
126. Levy, G., Can. Med. Assoc. J., 90, 978 (1964).
127. Levy, G., Antkowiak, J.M., Procknal, J.A. and White, D.C., J. Pharm. Sci., 52, 1047 (1963).
128. Flanagan, T.H., Broad, R.D., Rubinstein, M.H. and Longworth, A.R., J. Pharm. Pharmacol., 21, 129S (1969).
129. Brudney, N., Stewart, D.J. and Eustace, B.T., Can. Med. Assoc. J., 90, 980 (1964).
130. Lu, F.C., Rice, W.B. and Mainville, C.W., Can. Med. Assoc. J., 92, 1166 (1965).
131. Campagna, F.A., Cureton, G., Mirigian, R.A. and Nelson, E., J. Pharm. Sci., 52, 605 (1963).

132. Gershberg, S. and Stoll, F.D., J. Am. Pharm. Assoc., Sci. Ed., 35, 284 (1946).
133. Broadhead, J.F., Mitchell, A.G. and O'Reilly, W.J., Australas J. Pharm., 47, S92 (1966).
134. "British Pharmacopeia, 1963", The Pharmaceutical Press, London, 1963, p. 1157.
135. Vliet, E.B., Drug Standards, 27, 97 (1959).
136. Levy, G. and Gumtow, R.H., J. Pharm. Sci., 52, 1139 (1963).
137. Middleton, E.J., Davies, J.M. and Morrison, A.B., J. Pharm. Sci., 53, 1378 (1964).
138. Cambell, D.J. and Theivagt, J.G., Drug Standards, 26, 73 (1958).
139. Walters, V., J. Pharm. Pharmacol., 20, 228S (1968).
140. Caleswick, B., Katchen, B. and Black, J., J. Pharm. Sci., 54, 1277 (1965).
141. Engel, G.B., Australas, J. Pharm., 47, S22 (1966).
142. Jacob, J.T. and Plein, E.M., J. Pharm. Sci., 57, 798 (1968).
143. "National Formulary", 13th Ed., Mack Publishing Co., Easton, Pa., 1970, p. 802.
144. Searl, R.O. and Pernarowski, M., Can. Med. Assoc. J., 96, 1513 (1967).
145. "The United States Pharmacopeia", 18th Revision, Mack Publishing Co., Easton, Pa., 1970, p. 934.
146. Middleton, E.J., Chang, H.S. and Cook, D., Can. J. Pharm. Sci., 3, 97 (1968).

147. Goldberg, A.H., Gibaldi, M., Kanig, J.L. and Shanker, J., J. Pharm. Sci., 54, 1722 (1965).
 148. Coulter, W.H., Proc. Natl. Electron Conf., 12, 1034 (1956).
 149. Petro, A.J., J. Phys. Chem., 64, 1508 (1960).
 150. Thornton, M.J., J. Pharm. Pharmacol., 15, 742 (1963).
 151. Mathews, B.A. and Rhodes, C.T., J. Pharm. Sci., 56, 838 (1967).
 152. Schrag, K.R. and Corn, M., Am. Ind. Hyg. Assoc. J., 446 (1970).
 153. Cartmel, R. and Gerrard, H.N., Pharm. J., 383 (1963).
 154. Wood, W.M. and Lines, R.W., J. Soc. Cosmetic Chemists, 17, 197 (1966).
 155. Higuchi, W.I. and Saad, H.Y., J. Pharm. Sci., 54, 74 (1965).
 156. Saad, H.Y. and Higuchi, W.I., J. Pharm. Sci., 54, 1303 (1965).
 157. Piccolo, J. and Tawashi, R., J. Pharm. Sci., 60, 59 (1971).
 158. Wurster, D.E. and Polli, G.P., J. Pharm. Sci., 53, 311 (1964).
 159. Marlowe, E. and Shangraw, R.F., J. Pharm. Sci., 56, 498 (1967).
 160. Patel, N.K. and Foss, N.E., J. Pharm. Sci., 53, 94 (1964).
 161. Macdonald, H., Pisano, F., Burger, J., Dornbush, A. and Pelcak, E., Drug. Infor. Bull., 3, 76 (1969).
-

162. Tawashi, R., *Science*, 160, 76 (1968).
163. Piccolo, J. and Tawashi, R., *J. Pharm. Sci.*, 59, 56 (1970).
164. Myers, E.L., *Drug Cosmetic Ind.*, 87, 622 (1960).
165. Baun, D.G. and Walker, G.C., *J. Pharm. Sci.*, 58, 611 (1969).
166. Richter, A., Myhre, B. and Khanna, S.C., *J. Pharm. Pharmacol.*, 21, 409 (1969).
167. Pernarowski, M., Woo, W. and Searl, R.O., *J. Pharm. Sci.*, 57, 1419 (1968).
168. Schroeter, L.C. and Wagner, J.G., *J. Pharm. Sci.*, 51, 957 (1962).
169. Schroeter, L.C. and Hamlin, W.E., *J. Pharm. Sci.*, 52, 811 (1963).
170. Barzilay, R.B. and Hersey, J.A., *J. Pharm. Pharmacol.*, 20, 232S (1968).
171. Tingstad, J.E. and Riegelman, S., *J. Pharm. Sci.*, 59, 692 (1970).
172. Ullah, I. and Cadwallader, D.E., *J. Pharm. Sci.*, 59, 979 (1970).
173. McClintock, W.J., Swarbrick, J., Christian, J.E. and Banker, G.C., *J. Pharm. Sci.*, 54, 1782 (1965).
174. Langenbucher, F., *J. Pharm. Sci.*, 58, 1265 (1969).
175. Ganderton, D., Hadgraft, J.W., Rispin, W.T. and Thompson, A.G., *Pharm. Acta. Helv.*, 42, 152 (1967).
176. Lerk, C.F. and Zuurman, K., *J. Pharm. Pharmacol.*, 22, 319 (1970).

177. Verma, A.R. and Krishna, P., "Polymorphism and Polytypism in Crystals", John Wiley & Sons, Inc., New York, 1966, p. 7.
178. Mitscherlich, E., Ann. Chim. Phys., 19, 350 (1822).
179. Frederick, K.J., J. Pharm. Sci., 50, 531 (1961).
180. Higuchi, T., J. Am. Pharm. Assoc., Sci. Ed., 47, 657 (1958).
181. Mesley, R.J. and Johnson, C.A., J. Pharm. Pharmacol., 17, 329 (1965).
182. Mesley, R.J., Spectrochim. Acta, 22, 889 (1966).
183. Mesley, R.J. and Clements, R.L., Flaherty, B. and Goodhead, K., J. Pharm. Pharmacol., 20, 329 (1968).
184. Mesley, R.J. and Clements, R.L., J. Pharm. Pharmacol., 20, 341 (1968).
185. Mesley, R.J. and Houghton, E.E., J. Pharm. Pharmacol., 19, 295 (1967).
186. Brandstätter-Kuhnert, M., Junger, E. and Kofler, A., Microchem. J., 9, 105 (1965).
187. Brandstätter-Kuhnert, M. and Grimm, H., Mikrochim. Acta., 115 (1968).
188. Brandstätter-Kuhnert, M. and Grimm, H., Mikrochim. Acta., 127 (1968).
189. Brandstätter-Kuhnert, M., Hoffman, R. and Senn, M., Microchem. J., 7, 357 (1963).
190. Brandstätter-Kuhnert, M., Z. Phys. Chem., A191, 227 (1942); through Chem. Abstr. 37, 6534³ (1943).

191. Brandstätter-Kuhnert, M. and Aepkers, M., *Mikrochim. Acta.*, 1055 (1962).
192. Brandstätter-Kuhnert, M. and Aepkers, M., *Mikroskopie*, 16, 189 (1961).
193. Huang, T-Y., *Acta. Pharm. Int.*, 2, 43 (1951); through *Chem. Abstr.*, 46, 4172c (1952).
194. Huang, T-Y., *Acta. Pharm. Int.*, 2, 95 (1951); through *Chem. Abstr.*, 46, 7284c (1952).
195. Cleverly, B. and Williams, P.P., *Tetrahedron*, 7, 277 (1959).
196. Garratt, D.C. and Marshall, P.G., *J. Pharm. Pharmacol.*, 6, 950 (1954).
197. Callow, R.K. and Kennard, O., *J. Pharm. Pharmacol.*, 13, 723 (1961).
198. Smakula, E., Gori, A. and Wotiz, H.H., *Spectrochim. Acta.*, 9, 346 (1957).
199. Pheasant, R., *J. Am. Chem. Soc.*, 72, 4303 (1950).
200. Röpke, H. and Neudert, W., *Z. Anal. Chem.*, 170, 78 (1959).
201. Higuchi, W.I., Lau, P.K., Higuchi, T. and Shell, J.W., *J. Pharm. Sci.*, 52, 150 (1963).
202. Dickson, D.H.W., Page, J.E. and Rogers, D., *J. Chem. Soc.*, 443 (1955).
203. Roberts, G., *Anal. Chem.*, 29, 911 (1957).
204. Shell, J.W., *Anal. Chem.*, 27, 1665 (1955).
205. Brandstätter-Kuhnert, M., *Pure Appl. Chem.*, 10, 133 (1965).

206. Maron, S.H. and Prutton, C.F., "Principles of Physical Chemistry", 4th Ed., The MacMillan Co., New York, 1965, p. 70.
207. Trivedi, J., Shell, J.W. and Biles, J.A., J. Am. Pharm. Assoc., Sci. Ed., 48, 583 (1959).
208. Biles, J.A., J. Am. Pharm. Assoc., Sci. Ed., 44, 74 (1955).
209. Shell, J.W., Witt, N.F. and Poe, C.F., Mikrochim. Acta., 31 (1960).
210. Castle, R.N., Witt, N.F. and Poe, C.F., J. Am. Chem. Soc., 71, 228 (1949).
211. Castle, R.N., Witt, N.F., J. Am. Chem. Soc., 68, 64 (1946).
212. Biles, J.A., Witt, N.F. and Poe, C.F., J. Am. Pharm. Assoc., Sci. Ed., 42, 53 (1953).
213. Biles, J.A., Witt, N.F. and Poe, C.F., Mikrochim. Acta., 38, 591 (1951).
214. Reffner, J. and McCrone, W.C., Anal. Chem., 31, 1119 (1959).
215. Rose, H.A., Anal. Chem., 27, 469 (1955).
216. Rose, H.A. and Van Camp, A., Anal. Chem., 28, 1054 (1956).
217. Rose, H.A., Anal. Chem., 32, 1371 (1960).
218. Rose, H.A., Anal. Chem., 26, 1245 (1954).
219. Van Camp, A., Anal. Chem., 30, 1883 (1958).
220. Rose, H.A., Anal. Chem., 27, 1841 (1955).
221. Rose, H.A., Anal. Chem., 26, 938 (1954).

222. Castle, R.N., *Mikrochim. Acta.*, 38, 92 (1951).
223. Biles, J.A., *Mikrochim. Acta.*, 39, 69 (1952).
224. Kofler, A., *Mikrochim. Acta.*, 904 (1960).
225. Brandstätter-Kuhnert, M. and Kofler, A., *Mikrochim. Acta.*, 847 (1959).
226. Kendall, D.N., *Anal. Chem.*, 25, 382 (1953).
227. Ebert, A.A. and Gottlieb, H.B., *J. Am. Chem. Soc.*, 74, 2806 (1952).
228. Lin, H.O. and Guillory, J.K., *J. Pharm. Sci.*, 59, 972 (1970).
229. Ravin, L.J., Shami, E.G. and Rattie, E., *J. Pharm. Sci.*, 59, 1290 (1970).
230. French, W.N. and Morrison, J.C., *J. Pharm. Sci.*, 54, 1133 (1965).
231. Chapman, J.H., Page, J.E., Parker, A.C., Rogers, D., Sharp, C.J. and Staniforth, S.E., *J. Pharm. Pharmacol.*, 20, 418 (1968).
232. Huang, T-Y., *Acta. Pharm. Int.*, 2, 173 (1951); through *Chem. Abstr.*, 48, 10298g (1954).
233. Smothers, W.J. and Chiang, Y., "Handbook of Thermal Differential Analysis", Chemical Publishing Co., New York, 1966.
234. Wendlandt, W.W., "Thermal Methods of Analysis", Interscience, New York, 1964, p. 132.
235. Shenouda, L.S., *J. Pharm. Sci.*, 59, 785 (1970).
236. Guillory, J.K., *J. Pharm. Sci.*, 56, 72 (1967).
237. Verma, M.C.P., *J. Appl. Chem.*, 8, 117 (1958).

238. Sakurai, T. and Yabe, M., *J. Phys. Soc. Japan*, 13, 5 (1958); through *Chem. Abstr.*, 52, 6909c (1958).
239. Guillory, J.K., Hwang, S.C. and Lach, J.L., *J. Pharm. Sci.*, 58, 301 (1969).
240. Murphy, C.B., *Anal. Chem.*, 36, 347R (1964).
241. Ravin, L.J., and Higuchi, T., *J. Am. Pharm. Assoc., Sci. Ed.*, 46, 732 (1957).
242. Borka, L., *Acta Pharm. Hung.*, 40, 150 (1970); through *International Pharm. Abstr.*, 8, 1505 (1971).
243. Rudman, R. and Post, B., *Mol. Cryst.*, 3, 325 (1968).
244. Conklin, J.D. and Hailey, F.J., *Clin. Pharmacol. Therap.*, 10, 534 (1969).
245. Aguiar, A.J., Wheeler, L.M., Fusari, S. and Zelmer, J.E., *J. Pharm. Sci.*, 57, 1844 (1968).
246. Aguiar, A.J. and Zelmer, J.E., *J. Pharm. Sci.*, 58, 983 (1969).
247. Poole, J.W., Owen, G., Silverio, J., Freyhof, J.N. and Rosenman, S.B., *Curr. Therap. Res.*, 10, 292 (1968).
248. Aguiar, A.J., Krc, J, Jr., Kinkel, A.W. and Samyn, J.C., *J. Pharm. Sci.*, 56, 847 (1967).
249. McCrone, W.C., Jr., "Fusion Methods in Chemical Microscopy", Interscience Publishers, Inc., New York, N.Y., 1957, p. 132.
250. Milosovich, G., *J. Pharm. Sci.*, 53, 484 (1964).
251. Gross, N., *Z. Krist.*, 57, 145 (1922).
252. Taylor, H.S. and Henderson, W.N., *J. Am. Chem. Soc.*, 37, 1688 (1915).

253. Hill, A.E., J. Am. Chem. Soc., 59, 2243 (1937).
254. Eriksson, S.O., Svensk. Farm. Tidskr., 65, 353 (1961);
through Chem. Abstr., 55, 21486f (1961).
255. Shefter, E. and Higuchi, T., J. Pharm. Sci., 52, 781
(1963).
256. Poole, J.W. and Bahal, C.K., J. Pharm. Sci., 57, 1945
(1968).
257. Poole, J.W. and Bahal, C.K., J. Pharm. Sci., 59, 1265
(1970).
258. Nogami, H., Nagai, T. and Yotsuyanagi, T., Chem.
Pharm. Bull., 17, 499 (1969).
259. Nogami, H., Nagai, T., Fukuoka, E. and Yotsuyanagi, T.,
Chem. Pharm. Bull., 17, 23 (1969).
260. Mitchell, A.G. and Saville, D.J., J. Pharm. Pharmacol.,
21, 28 (1969).
261. Griffiths, R.V. and Mitchell, A.G., J. Pharm. Sci.,
60, 267 (1971).
262. Higuchi, T., J. Soc. Cosmetic Chemists, 11, 85 (1960).
263. Ballard, B.E. and Nelson, E., J. Pharmacol., Expt.
Therap., 135, 120 (1962).
264. Ballard, B.E. and Biles, J.A., Steroids, 4, 273
(1964); through Chem. Abstr., 61, 16384e (1964).
265. Anderson, C.M., Australas J. Pharm., 47, S44 (1966).
266. Haleblan, J. and Biles, J.A., Paper presented to
A.Ph.A. Academy of Pharmaceutical Sciences, Las Vegas
Meeting, April 1967.
267. Tawashi, R., J. Pharm. Pharmacol., 21, 701 (1969).

268. Mullins, J.D. and Macek, T.J., *J. Pharm. Sci.*, 49, 245 (1960).
269. "The United States Dispensatory", 25th ed., Osol, A. and Farrar, G.E., J.B. Lippincott Co., Philadelphia, 1955, p. 1960.
270. Glazko, A.J., Edgerton, W.H., Dill, W.A. and Lenz, W.R., *Antibiot. Chemotherap.*, 2, 234 (1952).
271. Hoffman, A.J. and Ludwig, B.J., *J. Am. Pharm. Assoc., Sci. Ed.*, 48, 740 (1959).
272. Walkenstein, S.S., Knebel, C.M., Macmullen, J.A. and Seifter, J., *J. Pharmacol. Exptl. Therap.*, 123, 254 (1958).
273. Olesen, O.V., *J. Pharmacol. et Toxicol.*, 24, 183 (1966).
274. Kazyak, L. and Knoblock, E.C., *Anal. Chem.*, 35, 1448 (1963).
275. Goldbaum, L.R. and Domanski, T.J., *J. Forensic Sci.*, 11, 233 (1966).
276. Skinner, R.F., *J. Forensic Sci.*, 12, 230 (1967).
277. Ho, N.F.H. and Higuchi, W.I., *J. Pharm. Sci.*, 56, 248 (1967).
278. Hill, V.G. and Roy, R., *J. Am. Ceram. Soc.*, 41, 532 (1958).
279. Patel, N.K. and Popli, S.D., *Am. J. Pharm. Edu.*, 33, 220 (1969).
280. *British Pharmaceutical Codex, 1968*, The Pharmaceutical Press, London, 1968, p. 472.

281. Clarke, E.G.C., "Isolation and Identification of Drugs", The Pharmaceutical Press, London, 1969, p. 744.
282. Biles, J.A., J. Pharm. Sci., 52, 1066 (1963).
283. Kitaigorodskii, A.I., "Organic Chemical Crystallography", Academy of Sciences Press, Moscow, U.S.S.R., 1955, p. VIII.
284. Mitchell, A.G., Milaire, B.L., Saville, D.J., and Griffiths, R.V., J. Pharm. Pharmacol., 23, 534 (1971).
285. Sheth, P.B., Solubilization and Stabilization Using Surfactants, Ph.D. Thesis, The University of Iowa, 1967, p. 61.
286. Elworthy, P.H., and Lipscomb, F.J., J. Pharm. Pharmacol., 20, 817 (1968).
287. Elworthy, P.H., and Lipscomb, F.J., J. Pharm. Pharmacol., 20, 923 (1968).
288. Mathews, B.A., and Rhodes, C.T., J. Pharm. Pharmacol., 20, 204S (1968).
289. Samyn, J.C., and McGee, J.P., J. Pharm. Sci., 54, 1794 (1965).
290. Edmundson, I.C., Nature, 212, 1450 (1966).
291. Kubitschek, H.E., Research, 13, 128 (1960).